Numerical Simulation of Fluid Flow in Fractured Reservoirs

Chensong Zhang

NCMIS & LSEC, Chinese Academy of Sciences
University of Chinese Academy of Sciences

University of Science & Technology of China — Dec 12, 2019

== version-2019.12.10-release ==

Outline

- Introduction to petroleum reservoir simulation
- Modelling fractured petroleum reservoirs
- Multiscale hybrid-mixed method for DFM
- Benchmark problems and numerical results
- Solution methods for field-scale simulation
- Decoupling, preconditioning, and iterative solvers
- Development of petroleum reservoir simulator
- Fluid-rock interaction in carbonate formation
- Managing uncertainty and improve reliability
- Gridding techniques for reservoir simulation
- Conclusions and on-going work

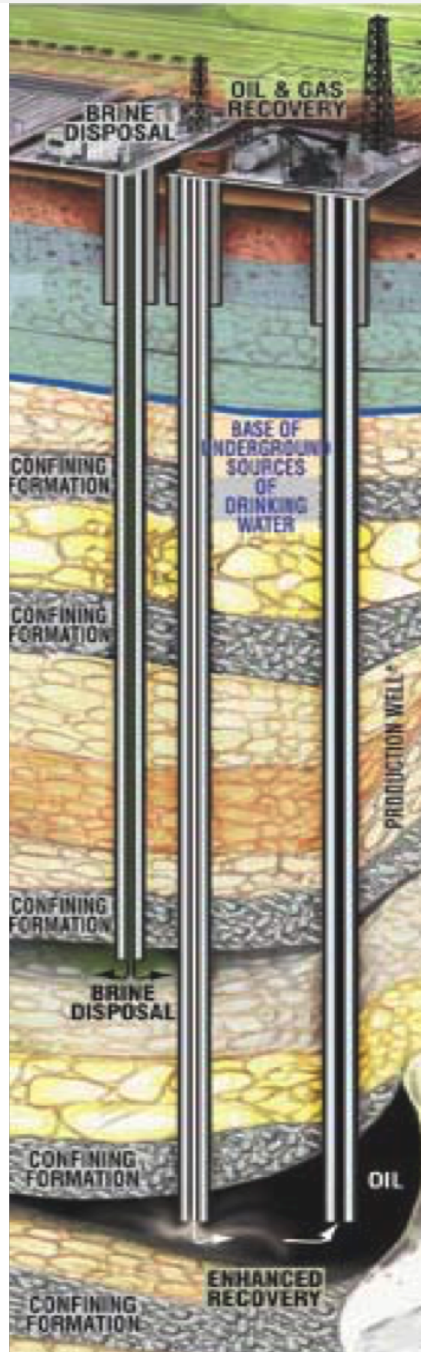

Introduction to petroleum reservoir simulation

1 Enhanced Oil Recovery and Simulation

2 Multiscale and Heterogenous Problem

3 Models of Interest

4 Oil-Water Two-Phase Model

5 Phase Behavior: Black Oil

6 Classical Black Oil Model

7 Phase Behavior: Compositional

8 General Compositional Model

9 Equations of State

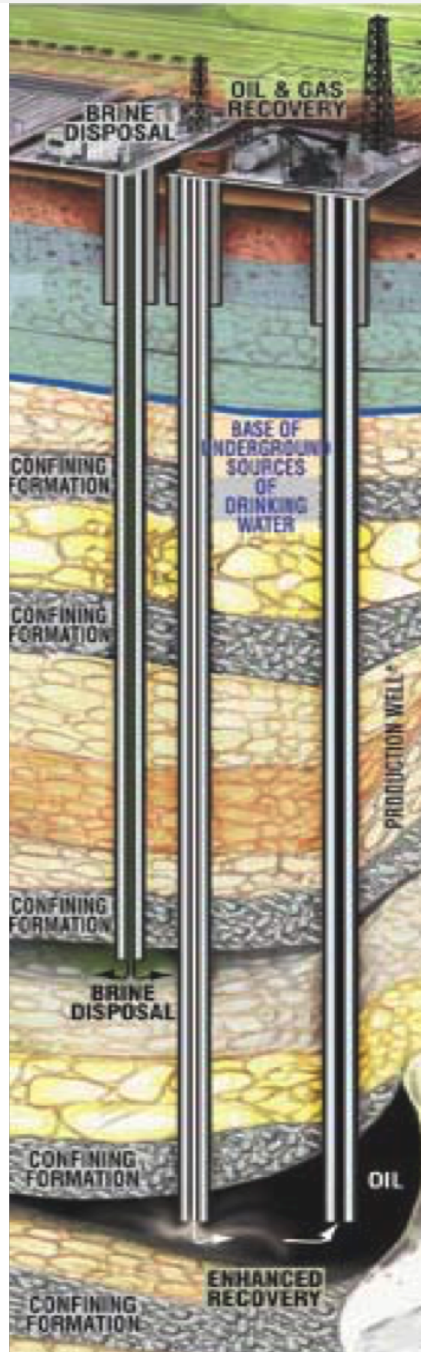

Enhanced Oil Recovery and Simulation

China outer-dependency for crude oil is 72.3% (data: end of year 2018)!

Peak oil theory, Hubbert 1956

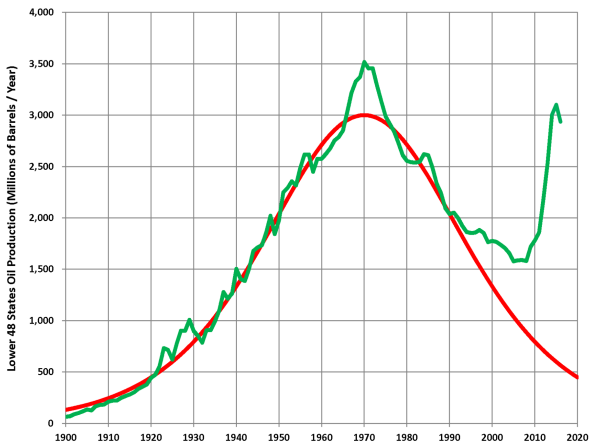

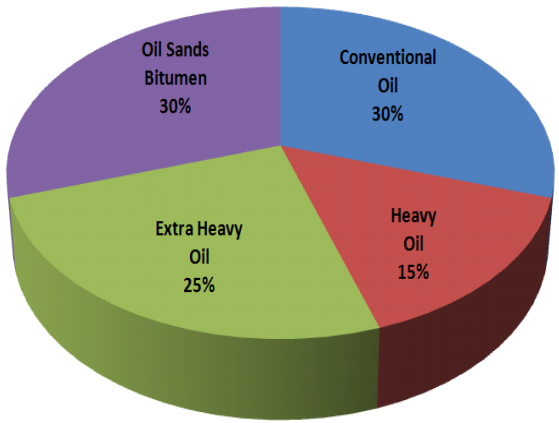

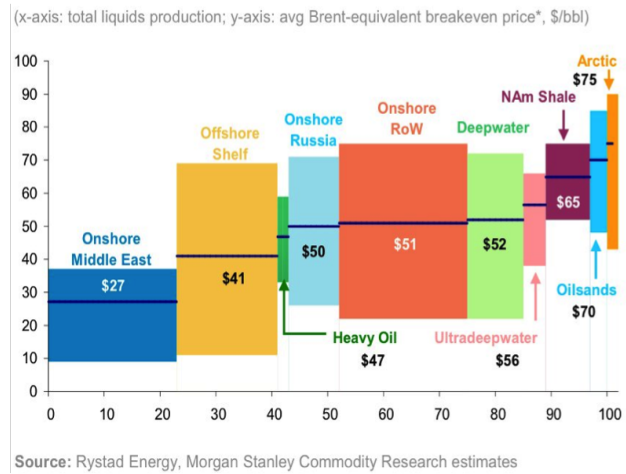

EOR techniques: improve recovery factor 20%–40% $\Longrightarrow$ 30%–60%

- Achieve miscibility and reduce residual oil saturation e.g. gas injection

☞ Chemical injection: polymer, surfactant, microbial, ... $\Longrightarrow$ Compositional models

☞ Unconventional oil/gas: fractures, vugs, ... $\Longrightarrow$ Fracture models

- Thermal injection: steam, fire, ... $\Longrightarrow$ Energy equation

Reduce wall cost required; improve accuracy/realism; decision making under uncertainty!

Multiscale and Heterogenous Problem

Traditionally, geomodeling of subsurface flows mainly focus on the larger scales, driven by the available measurement and by computation limitations

- Typical scales: field, single-well, lab, ...
- Sometimes important to zoom in, e.g.
  - Highly heterogenous reservoirs
  - IOR / EOR processes
  - Unconventional oil / gas reservoirs
  - ☞ Fluid-rock interactions
  - CO_2 sequestration
- Questions:
  - Which scales to focus on?
  - What scales to model/upscale?
  - Which heterogeneities matter most?

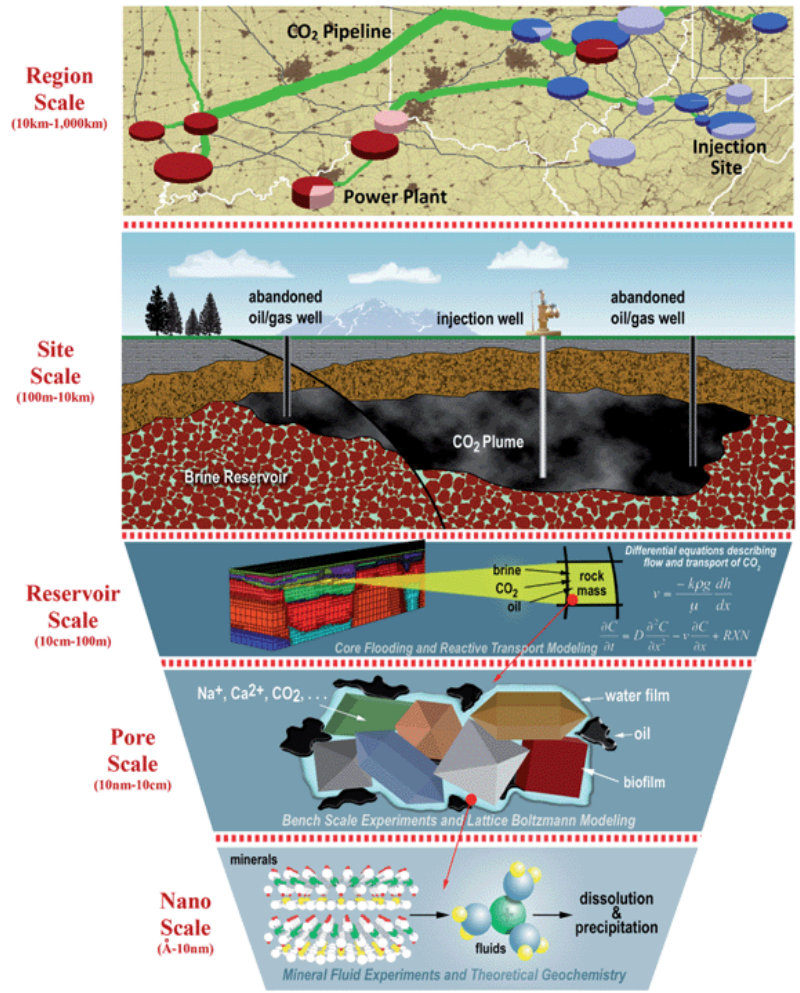

Models of Interest

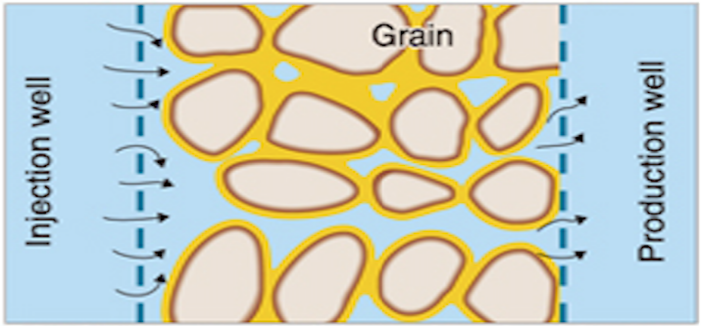

Immiscible displacement, water flooding

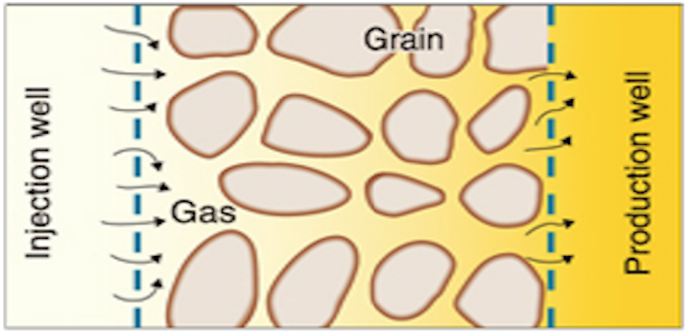

Miscible displacement, gas flooding

- ✓ Two-phase flow model: WO, OG
- ✓ Black oil model (three-phase flow) / volatile oil model
- ✓ General isothermal compositional model
- ✓ Chemical flooding: polymer, foam, surfactant, alkaline, ...
- ✓ Multiscale fracture models
  - Hybrid models: DPDP, DFM, ...
  - Single-domain Darcy-Stokes coupling
  - Carbonate fractured-cavity reservoirs
- ✎ Flow-geomechanic coupling (Biot)
- ✎ Non-isothermal flow: energy conservation

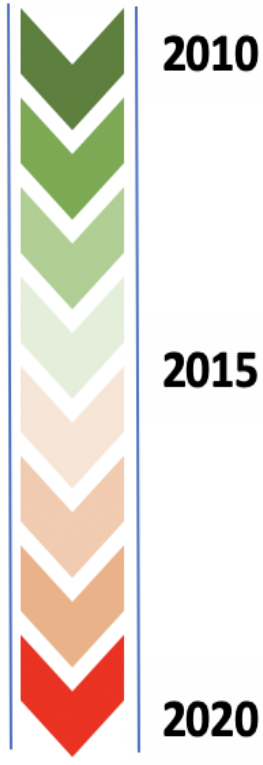

Oil-Water Two-Phase Model

In order to introduce IMPES/IMPEC, we give a simplified model

1. Mass conservation (assuming incompressibility):

$$\frac{\partial}{\partial t}\left(\phi\rho_w S_w\right) = -\nabla\cdot\left(\rho_w \mathbf{u}_w\right) + Q_W$$
$$\frac{\partial}{\partial t}\left(\phi\rho_o S_o\right) = -\nabla\cdot\left(\rho_o \mathbf{u}_o\right) + Q_O$$

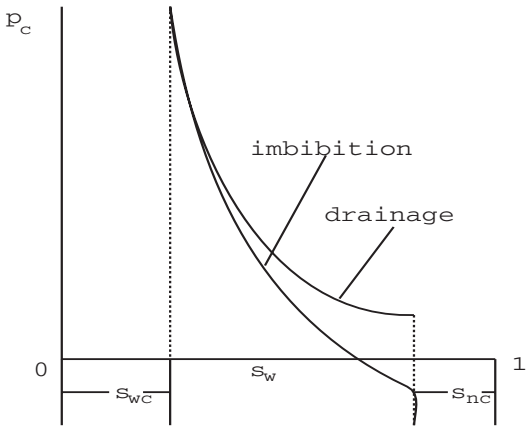

2. Darcy's law and constitutive equations:

$$\mathbf{u}_\alpha = -\frac{k k_{r\alpha}}{\mu_\alpha}(\nabla P_\alpha - \rho_\alpha \mathfrak{g}\nabla z), \quad \alpha = o, w$$
$$S_o + S_w = 1$$
$$P_o - P_w = 0 \quad \text{(for simplicity)}$$

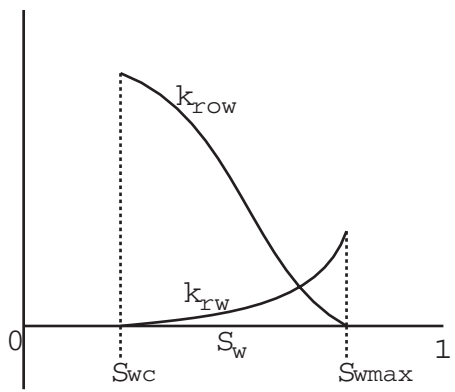

3. Well constraints + B.C. + I.C.

Phase Behavior: Black Oil

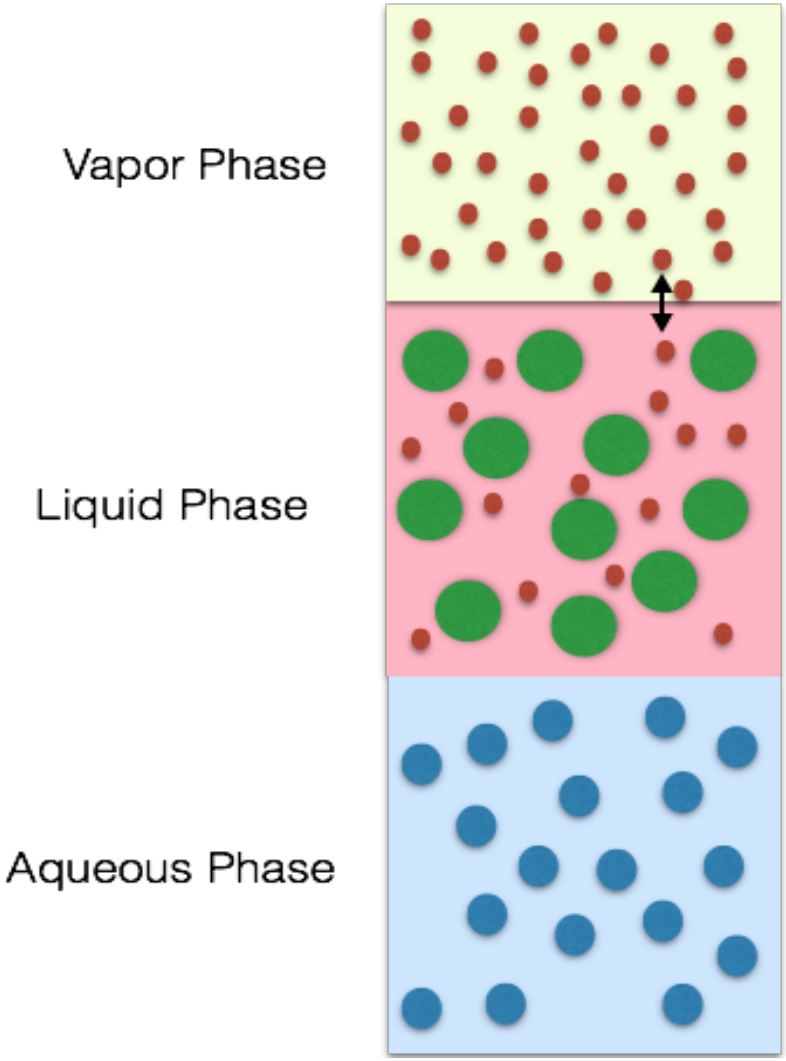

Black oil model

- The black oil model is based on simple interpolation of PVT properties as a function of pressure
- Water is modeled explicitly together with two hydrocarbon components, an oil phase and a gas phase
- At standard pressure and temperature, hydrocarbon components are divided into a gas component and an oil component in a stock tank
- No mass transfer occurs between the water phase and the oil/gas phases

[Chen, Huan, Ma 2006]

Classical Black Oil Model

1. Mass conservation (saturated & under-saturated):

$$\frac{\partial}{\partial t}\Big(\phi\rho_w S_w\Big) = -\nabla\cdot\Big(\rho_w \mathbf{u}_w\Big) + Q_W$$
$$\frac{\partial}{\partial t}\Big(\phi\rho_{oO} S_o\Big) = -\nabla\cdot\Big(\rho_{oO} \mathbf{u}_o\Big) + Q_O$$
$$\frac{\partial}{\partial t}\Big(\phi\rho_g S_g + \phi\rho_{oG} S_o\Big) = -\nabla\cdot\Big(\rho_g \mathbf{u}_g + \rho_{oG}\mathbf{u}_o\Big) + Q_G$$

2. Darcy's law and other constitutive equations:

$$\mathbf{u}_j = -\frac{\kappa\kappa_{rj}}{\mu_j}(\nabla P_j - \rho_j \mathfrak{g}\nabla z), \quad j = o, g, w$$
$$P_o - P_w = P_{cow}, \quad P_g - P_o = P_{cgo}$$
$$S_o + S_g + S_w = 1$$

3. Well constraints + B.C. + I.C.

PDE properties of the black oil model [Trangenstein, Bell 1986]

Phase Behavior: Compositional

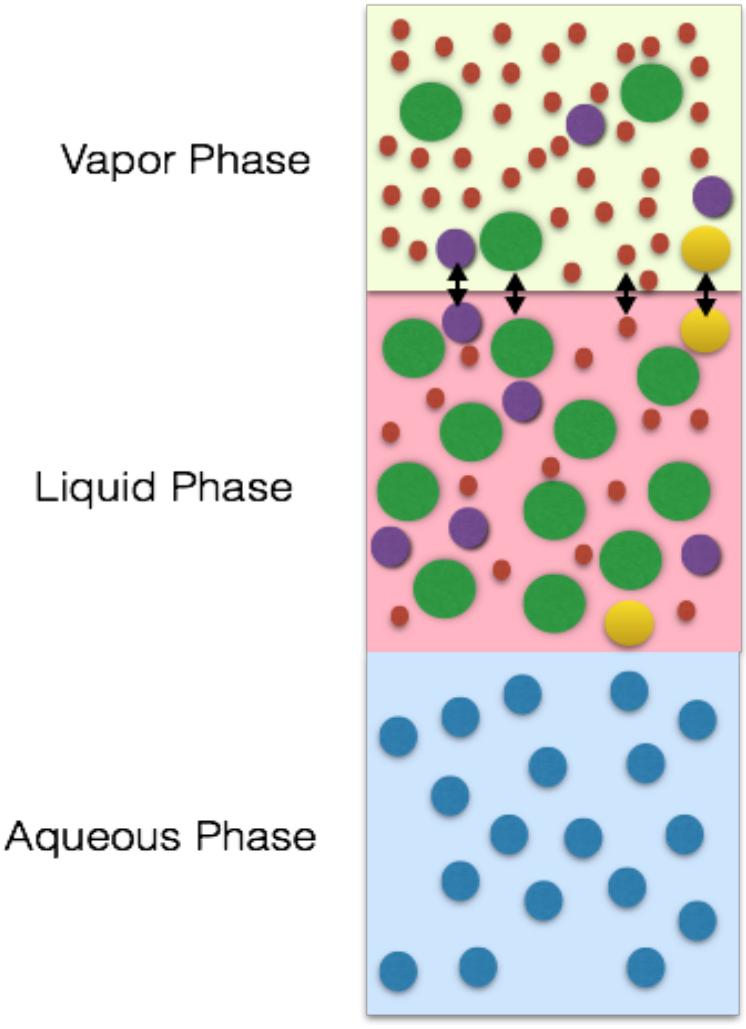

EOS compositional fluid

- In reservoirs containing light oil, the hydrocarbon composition affects fluid properties a lot
- A compositional model is based on a thermodynamically-consistent model such as an equation of state (EOS)
- Each hydrocarbon component is handled separately
- More unknowns than the black oil model: ξ_j is the molar density of phase j; x_{ij} is the molar fraction of comp i in phase j; N_i is the overall molar density of comp i

[Chen, Huan, Ma 2006]

General Compositional Model

$$\frac{\partial}{\partial t}\left(\phi \sum_{j=1}^{n_p} x_{ij}\xi_j S_j\right) + \nabla \cdot \mathbf{F}_i - \sum_{j=1}^{n_p} S_j r_{ij} = Q_i, \qquad i = 1 : n_c$$

$$\mathbf{F}_i = \sum_{j=1}^{n_p} \left(x_{ij}\xi_j \mathbf{u}_j - S_j \mathbf{D}_j \nabla(\xi_j x_{ij})\right), \qquad i = 1 : n_c$$

$$\mathbf{u}_j = -\frac{\kappa \kappa_{rj}}{\mu_j}(\nabla P_j - \gamma_j \nabla z), \qquad j = 1 : n_p$$

$$P_1 - P_j = P_{c1j}, \qquad j = 2 : n_p$$

$$\sum_{j=1}^{n_p} S_j = 1,$$

$$\sum_{i=1}^{n_c} x_{ij} = 1, \qquad j = 1 : n_p$$

$$f_{ij} = f_{i1}, \qquad i = 1 : n_c,\ j = 2 : n_p$$

[Collins, Nghiem, Li, Grabenstetter 1992; Qiao, Li, Johns, Xu 2014, 2015; ...]

Equations of State

How to find distribution of chemical components among phases?

Peng–Robinson EOS: [Peng, Robinson 1976]

$$p_j := \frac{RT}{V_j - b_j} - \frac{a_j}{V_j(V_j + b_j) + b_j(V_j - b_j)}, \quad j = o, g$$

where T is temperature, V_j is molar volume of phase j, and R is ideal gas constant

Change of variables:

$$A_j := \frac{a_j p_j}{R^2 T^2}, \quad B_j := \frac{b_j p_j}{RT}, \quad Z_j := \frac{p_j V_j}{RT}$$

$$Z_j^3 - (1 - B_j)Z_j^2 + (A_j - 2B_j - 3B_j^2)Z_j - (A_j B_j - B_j^2 - B_j^3) = 0$$

Fugacity:

$$f_{ij} := p_j x_{ij} \varphi_{ij}(Z_j), \quad i = 1, \ldots, n_c, \quad j = o, g \quad (\varphi_{ij} : \text{ fugacity coefficient})$$

Van der Waals / Redlich–Kwong / Redlich–Kwong–Soave EOS:

$$p_j := \frac{RT}{V_j - b_j} - \frac{a_j}{V_j(V_j + b_j)}, \quad j = o, g$$

Modelling fractured petroleum reservoirs

10 Fractured Oil/Gas Reservoirs

11 Challenges in Fractured Reservoir Simulation

12 Modeling Natural and Hydraulic Fractures

13 Darcy–Darcy Model for Fractured Reservoir

14 Darcy–Stokes/NS Model for Fractured Reservoir

15 Continuum Models

16 Discrete Fracture Model

17 Gridding for DFM Is Challenging

18 Embedded Discrete Fracture Model

19 Permeability Thickening of Wormlike Micellar Fluid

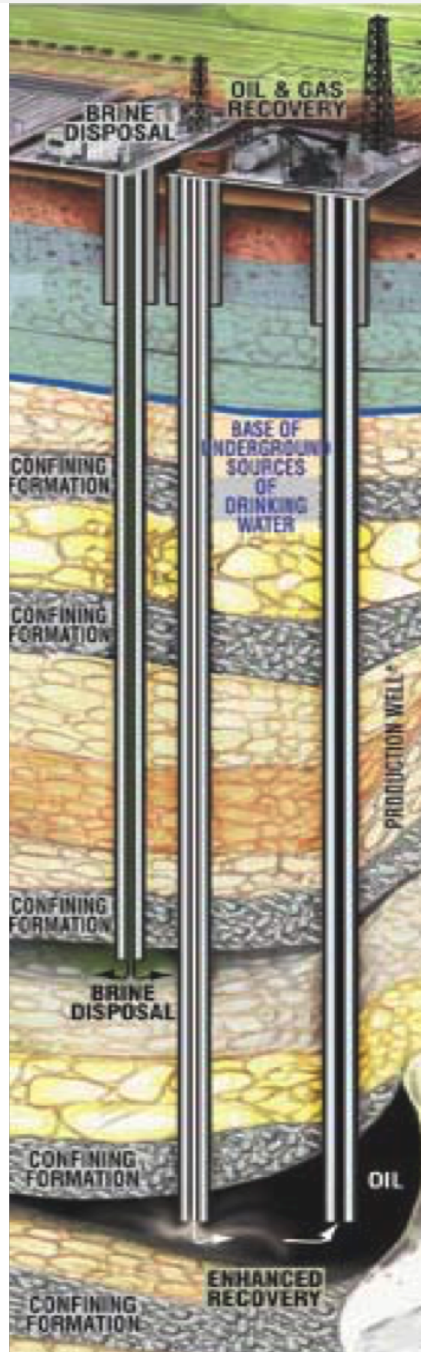

Fractured Oil/Gas Reservoirs

World Energy Outlook, International Energy Agency, 2006

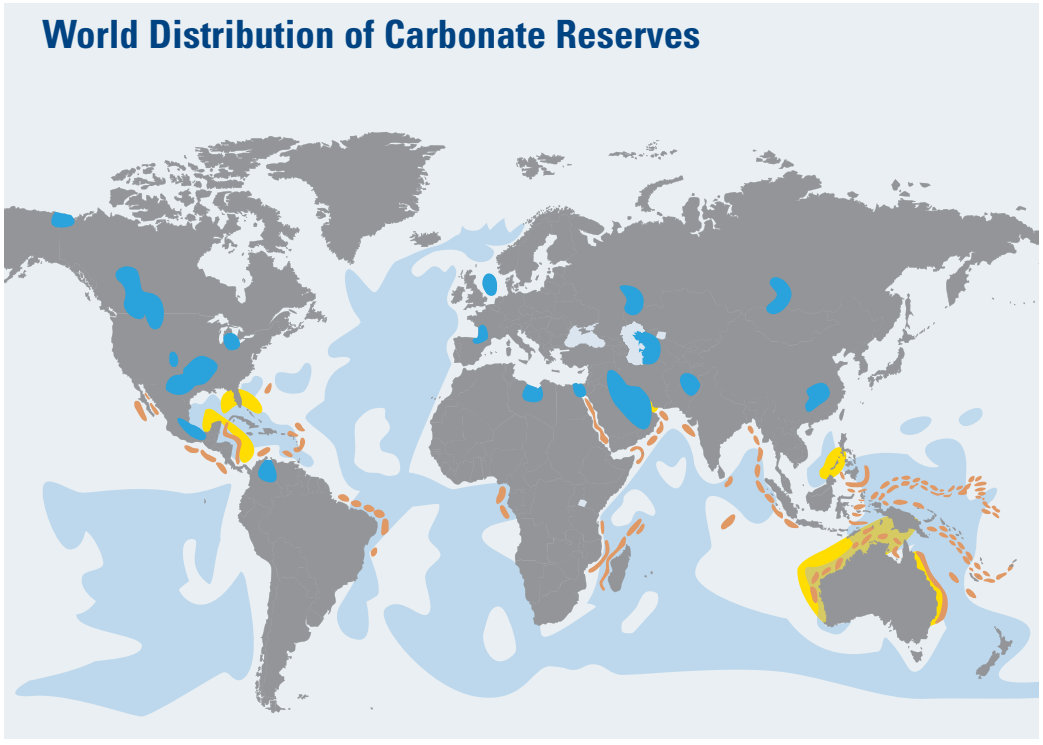

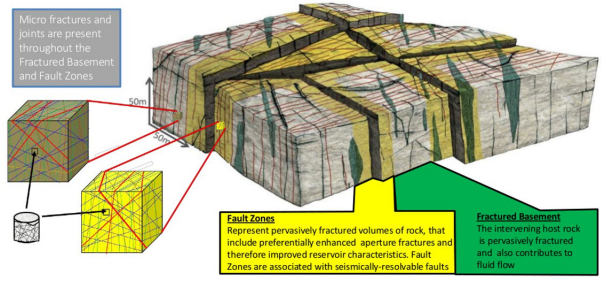

- Fractures are the most abundant visible features in the upper crust—More than 60% of oil and 40% of gas reserves are held in carbonates (fractured)

☞ Chemically active compared with sandstones

☞ Heterogeneity (porosity and wettability) at all scales (pores, grains, textures)

☞ Multiscale: range of scale from micro cracks to mile long features

Challenges in Fractured Reservoir Simulation

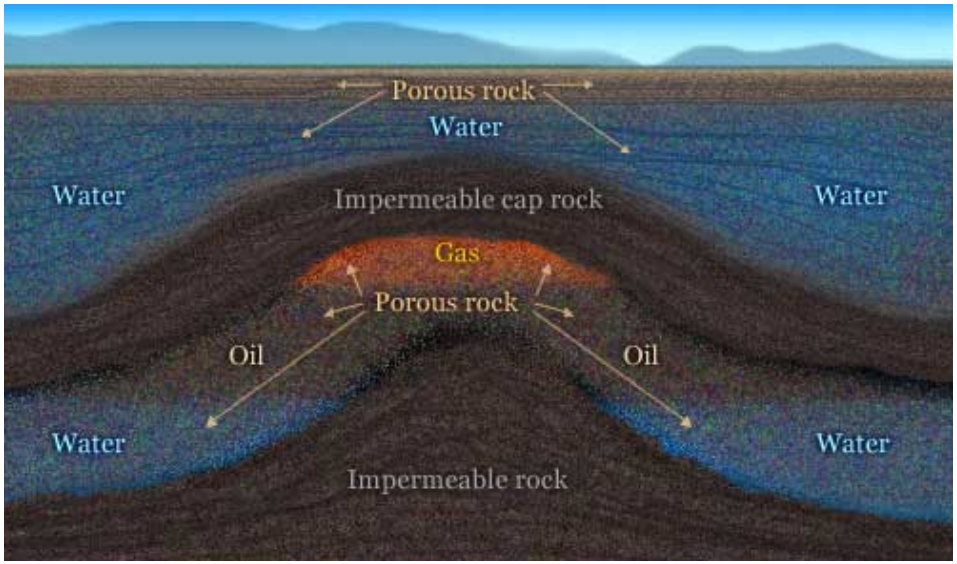

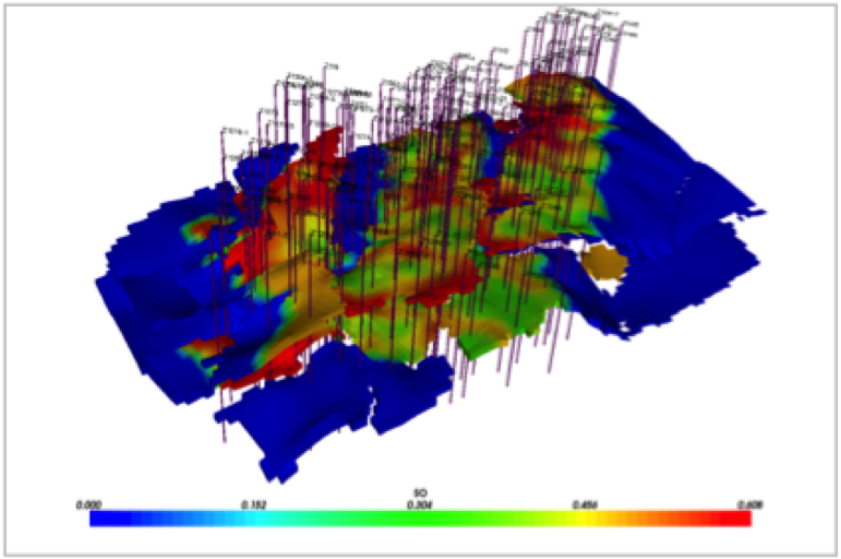

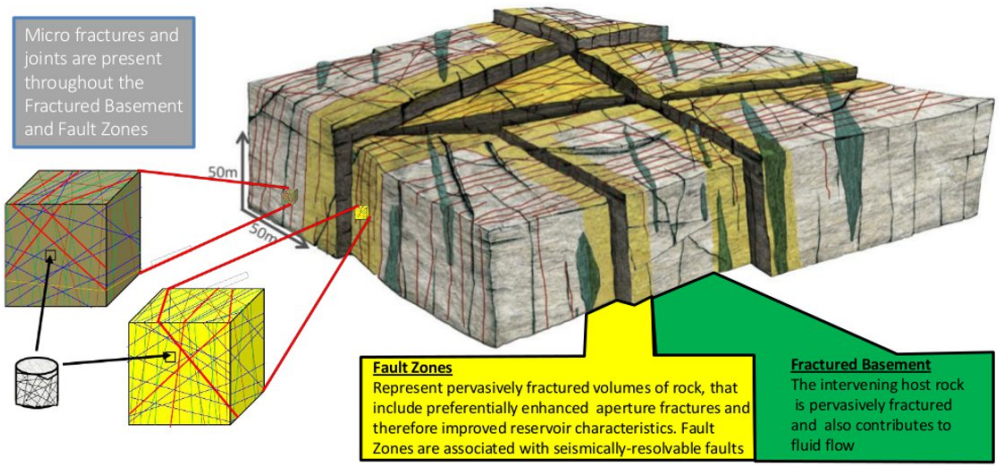

http://www.geoexpro.com/articles/2017/01/hiding-in-the-basement

Modeling Natural and Hydraulic Fractures

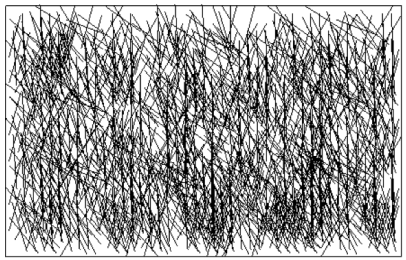

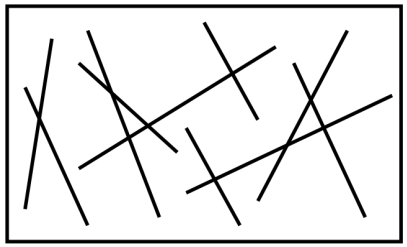

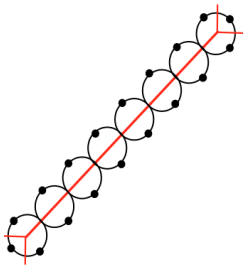

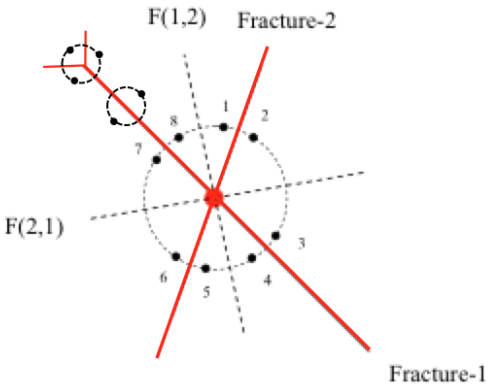

Direct simulation is not always feasible nor necessary!

1. Dual continuum (matrix-fracture) model:
   - Regard fractures as part of the pore volume
   - DPDP [Warren, Root 1963; Blaskovich et al. 1983]
   - Well developed, connected, without localized anisotropy
2. Equivalent porous media model: generalization of DCM
   - Representative elementary volume
   - Multiple INteraction Continua (MINC): [Wu, Pruess 1988]
3. Discrete fracture model (DFM): large-scale / isolated fractures
   - Representing fracture aperture / shape / direction explicitly
   - Unstructured grid / high computational cost
   - Flow-geomachanics coupling [Karimi-Fard et al. 2004]
   - Complex multi-phase flows inside the fracture network?
4. Embedded discrete fracture model (EDFM) [Li, Lee 2008]

No single model is good for every cases!

Darcy–Darcy Model for Fractured Reservoir

Fine-resolution direct simulation

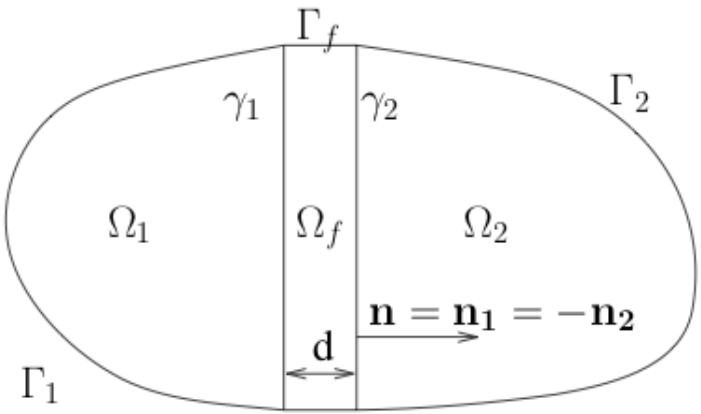

$$
\begin{cases}
\mathbf{u}_i = -\kappa_i \nabla p_i, & \Omega_i,\ i = 1, 2, f, \\
\nabla \cdot \mathbf{u}_i = f_i, & \Omega_i,\ i = 1, 2, f, \\
\mathbf{u}_1 \cdot \mathbf{n} = \mathbf{u}_f \cdot \mathbf{n}, & \gamma_i,\ i = 1, 2, \\
p_i = p_f, & \gamma_i,\ i = 1, 2, \\
p_i = p_D, & \Gamma_i,\ i = 1, 2, f.
\end{cases}
$$

Some comments on fracture modeling

- Fractures usually have higher permeability than the surrounding medium
  - Fluid tend to flow into the fracture other than along the fracture
  - Darcy velocity is not identical on the two sides of the fracture
- But the opposite situation could happen at some cases
- Accurate approximation of flow in complex fractures of variable aperture
- Requires large number of cells in partition and hence very costly
- May replace the Darcy's law for the flow in fractures by the NS equation

Darcy–Stokes/NS Model for Fractured Reservoir

Sometimes aperture of fracture might not be small and can't be neglected!

Why considering Stokes/NS? (e.g. vuggy carbonate reservoir)

- Seepage of water in sand (from lake into ground, from sea to sand beach, ...)
- Averaging incompressible flow through porous medium $\Longrightarrow$ Darcy (small to medium pore size, homogeneous in all directions)
- For thicker fractures and cavities/caves, a different flow model is needed

Beavers–Joseph–Saffman interface condition: slip velocity proportional to shear stress

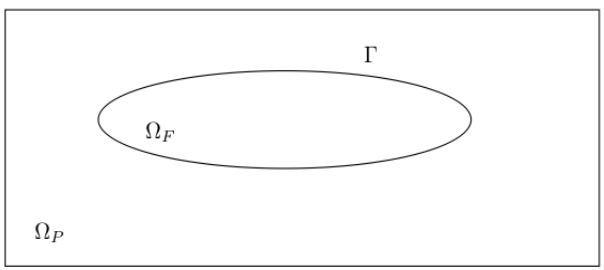

$$
\begin{cases}
\mathbf{u} = -\kappa \nabla p_P, & \Omega_P, \\
-\mu \Delta \mathbf{u} + \nabla p_F = \mathbf{f}, & \Omega_F, \\
\nabla \cdot \mathbf{u} = g, & \Omega, \\
\mathbf{u}_F \cdot \mathbf{n} = \mathbf{u}_P \cdot \mathbf{n}, & \Gamma, \\
p_F - 2\mu(\nabla \mathbf{u}_F\, \mathbf{n}) \cdot \mathbf{n} = p_P, & \Gamma, \\
\mathbf{u}_F \cdot \mathbf{t} = -2\beta\mu\, (\nabla \mathbf{u}_F\, \mathbf{n}) \cdot \mathbf{t}, & \Gamma, \\
\mathbf{u} \cdot \mathbf{n} = 0, & \partial\Omega.
\end{cases}
$$

[Beavers, Joseph 1967; Saffman 1971; Jager, Mikelic 2000; Layton et al. 2003]

Continuum Models

Dual Permeability Dual Porosity (DPDP) model

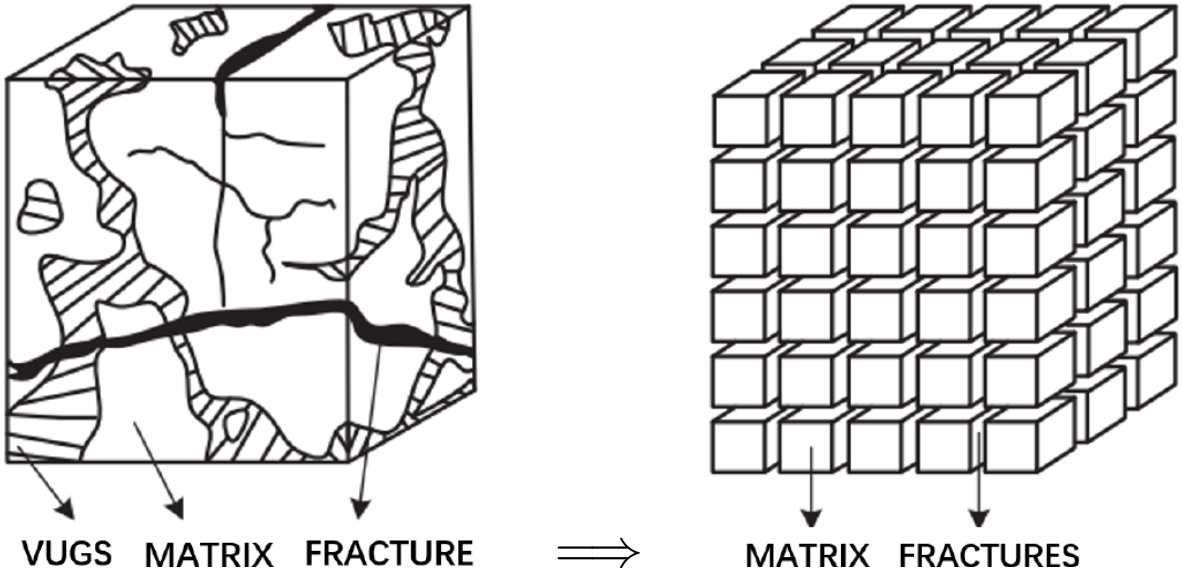

- Using upscaling to obtain effective transmissibility between fractures/matrix
- Effective when fractures are fully developed and do not change in time
- Legacy code can be easily adapted for DP or DPDP (via NNC)

Difficult to apply on (natural/hydraulic) fractures of multiple length-scales

Naturally fractured reservoirs $\Longrightarrow$ Induced fractures in shale reservoirs

[Barenblatt, Zheltov, Kochina 1960; Warren, Root 1963]

Discrete Fracture Model

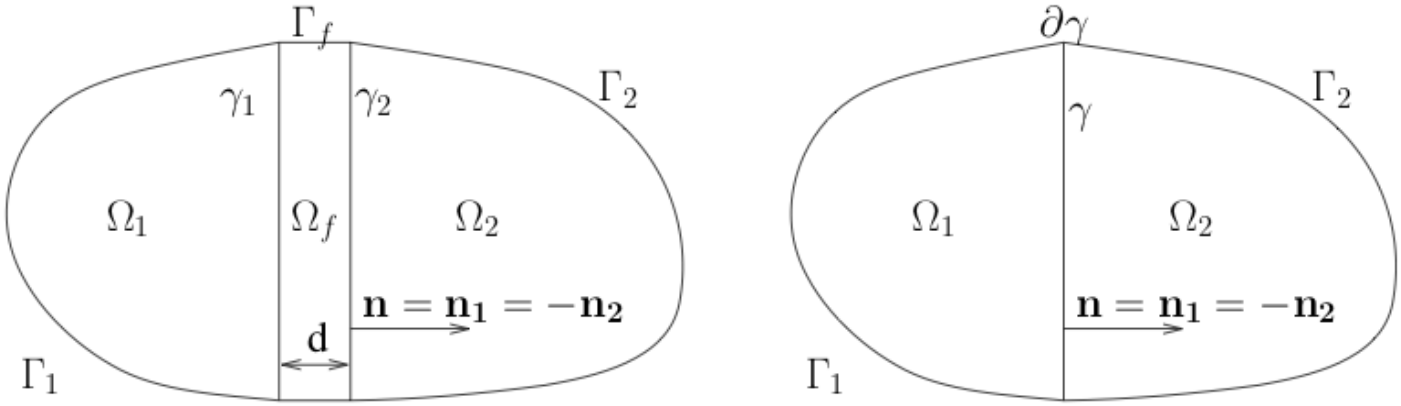

$$
\begin{cases}
\mathbf{u}_i = -\kappa_i \nabla p_i, & \Omega_i,\ i = 1,2 \\
\nabla \cdot \mathbf{u}_i = f_i, & \Omega_i,\ i = 1,2 \\
\mathbf{u}_f = -\kappa_{f,\tau} \mathrm{d} \nabla_\tau p_f, & \gamma, \\
\nabla_\tau \cdot \mathbf{u}_f = f_f + (\mathbf{u}_1 \cdot \mathbf{n}_1 + \mathbf{u}_2 \cdot \mathbf{n}_2)|_\gamma, & \gamma, \\
-\xi \mathbf{u}_1 \cdot \mathbf{n}_1 + \alpha_f p_1 = \alpha_f p_f - (1-\xi)\mathbf{u}_2 \cdot \mathbf{n}_2, & \gamma, \\
-\xi \mathbf{u}_2 \cdot \mathbf{n}_2 + \alpha_f p_2 = \alpha_f p_f - (1-\xi)\mathbf{u}_1 \cdot \mathbf{n}_1, & \gamma,
\end{cases}
\quad + \text{B.C.}
$$

where $\alpha_f = 2\kappa_{f,\mathbf{n}}/\mathrm{d}$ and $\xi = \frac{1}{2}, \frac{3}{4}, 1$ can be chosen for different types of fractures.

[Martin, Jaffré, Roberts 2005; Alboin, Jaffré, Roberts, Serres 1999]

Gridding for DFM Is Challenging

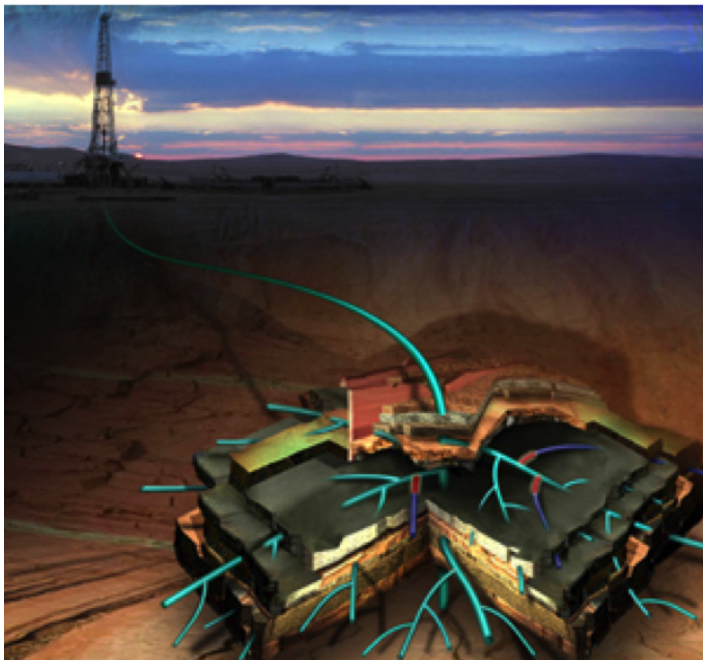

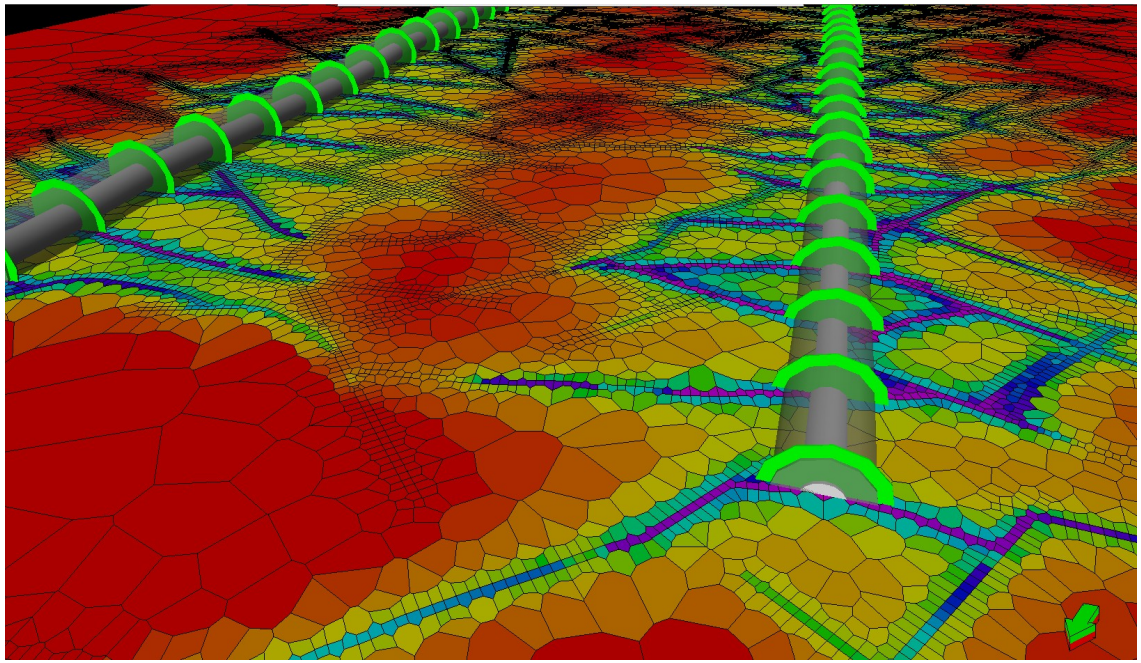

Different length scales:

- Vertical grid size $\sim$ 10cm–1m
- Horizontal grid size $\sim$ 10m–100m
- Lots of large fractures near wells
- Well radius $\sim$ 1cm
- Well length $\sim$ 100m
- Fractures $\sim$ 1cm–10m

Pictures from Saudi Aramco and Schlumberger

Embedded Discrete Fracture Model

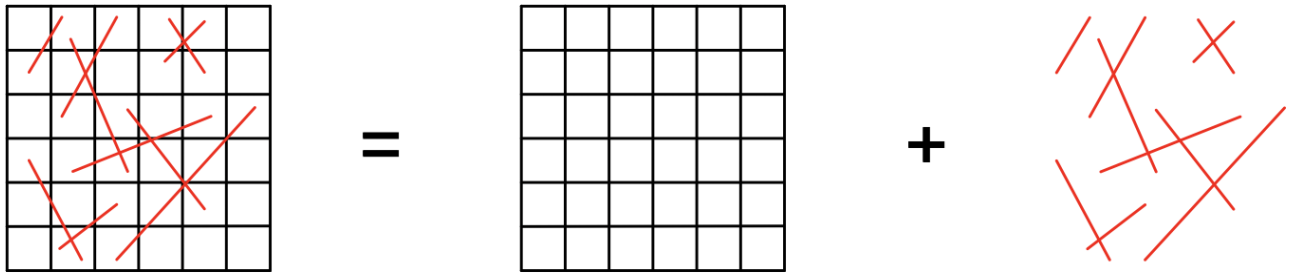

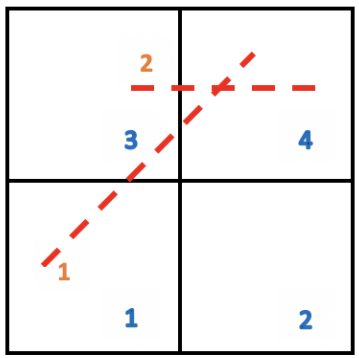

Matrix	1	2	3	4
Fracture1	5		6	7
Fracture2			8	9

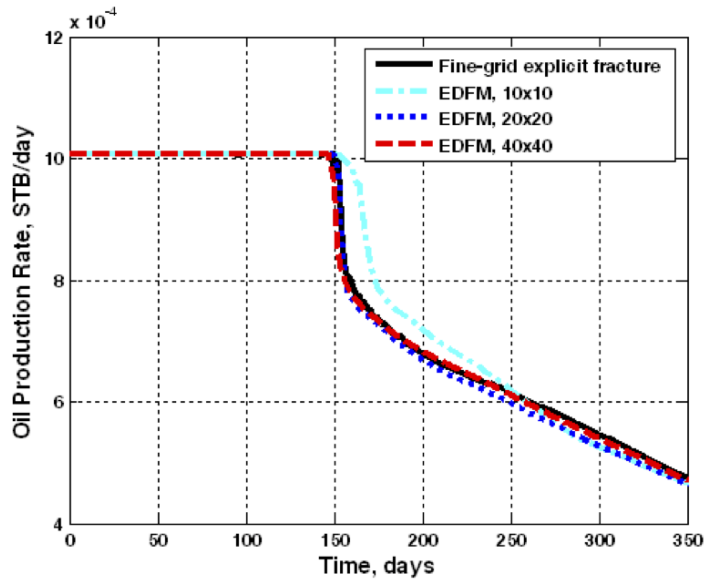

EDFM v.s. fine-grid direct simulation [Moinfar 2013, PhD Thesis]

- Three types of NNCs needed: M–M, Fi–Fi, Fi–Fj
- How to obtain transmissbility between discrete and continuum parts accurately?
- dual continuum approach is employed to describe the dense small-scale fractures and DFM or EDFM is used to model the large-scale fractures [Li, Lee 2008]

Permeability Thickening of Wormlike Micellar Fluid

- Chemical injection (polymer, gel, surfactant, ...) are widely applied in EOR
- Shear rate will greatly affect gelation process $\Longrightarrow$ How to quantify it?

A three-species model for wormlike micellar fluid: [Dai, Lee, Z.]

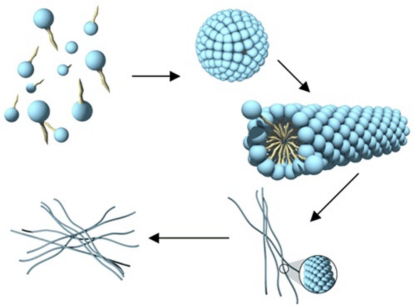

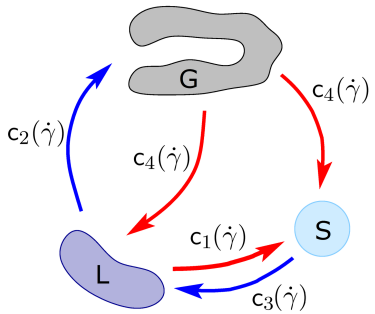

$L \to pS$	$c_1(\dot\gamma)L$
$qL \to G$	$c_2(\dot\gamma)L^q$
$pS \to L$	$c_3(\dot\gamma)S^p$
$G \to \alpha L + \beta S$	$c_4(\dot\gamma)G$

$$
\begin{aligned}
\dot{S} &= pc_1(\dot\gamma)L - pc_3(\dot\gamma)S^p + \beta c_4(\dot\gamma)G \\
\dot{L} &= -c_1(\dot\gamma)L - qc_2(\dot\gamma)L^q + c_3(\dot\gamma)S^p + \alpha c_4(\dot\gamma)G \\
\dot{G} &= c_2(\dot\gamma)L^q - c_4(\dot\gamma)G
\end{aligned}
$$

where S, L, and G are quantities of spherical, cylindrical, and gel micelles.

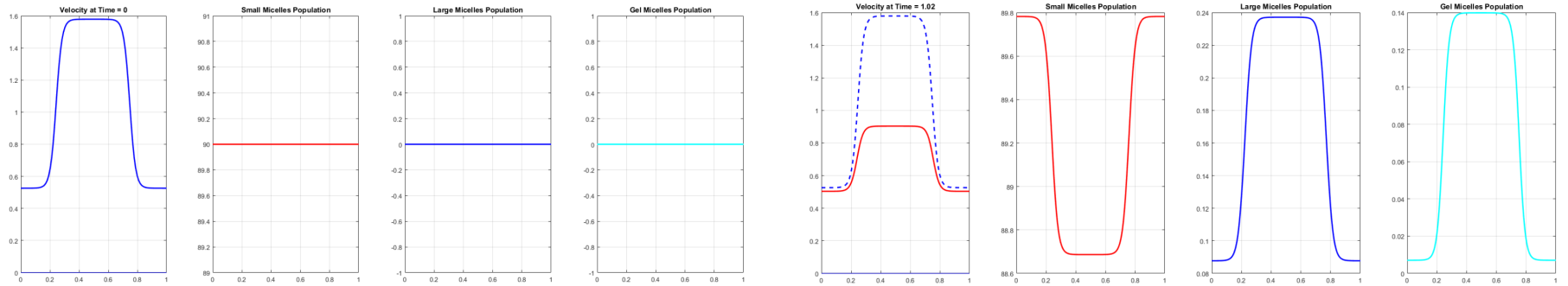

Multiscale hybrid-mixed method for DFM

20 Multiscale Methods

21 Multiscale Hybrid-Mixed Methods

22 Numerical Analysis of MHM

23 MHM-$H^1(\Omega)$ Formulation

24 MHM-$H(\mathrm{div}, \Omega)$ Formulation

25 Volumetric and Fracture Flows in DFM

26 Multiscale Hybrid-Mixed Method for DFM

27 Generalization to 3D DFM

28 Implementation of MHDFM

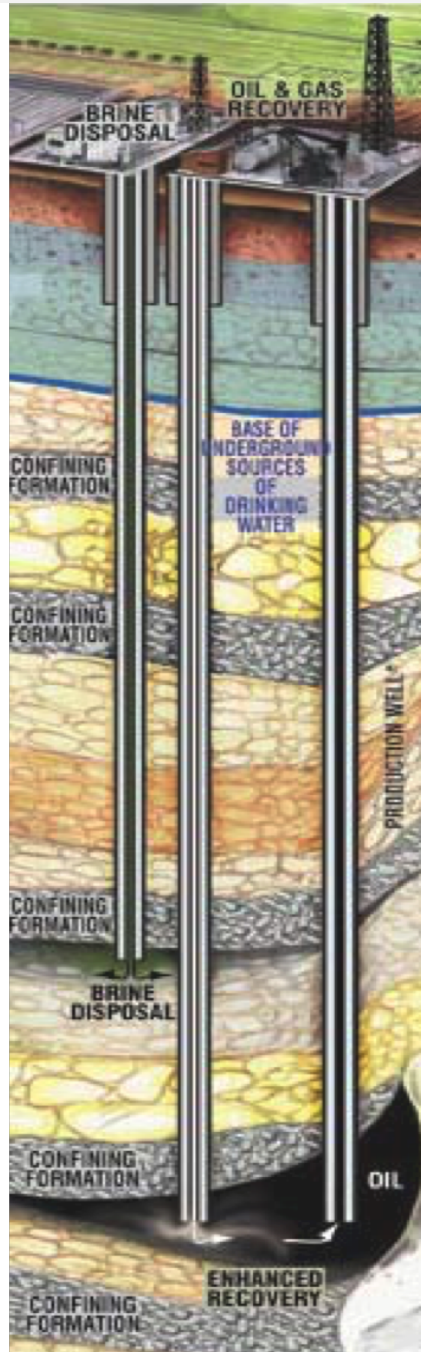

Multiscale Methods

Main ideas of multiscale methods

- Model physical phenomena on coarse grids while using small-scale features that impact the coarse-grid solution in a systematic way
- Incorporate subgrid information by utilising solutions of local flow problems to build a set of equations on a coarser scale

Localized multiscale basis methods

- MsFEM/MsMFEM [Hou, Wu 1997; Chen, Hou 2002]
- MsFVM [Jenny, Lee, Tchelepi 2003]
- Heterogeneous multiscale method [E, Engquist 2003; E, Ming, Zhang 2005]
- Petro-Galerkin MsFEM to reduce cell resonance error [Hou, Wu, Zhang 2004]
- MsFEM using limited global info [Efendiev, Ginting, Hou, Ewing 2006]
- MsFEM for high-contrast problems [Efendiev, Galvis, Wu 2011; Owhadi, Zhang 2011]
- FE-MsFEM using penalty method for the interface [Deng, Wu 2014]
- Survey with numerical experiments [Aarnes, Kippe, Lie, Rustad 2007]
- . . . . . .

Multiscale Hybrid-Mixed Methods

Basic ideas of MHM methods

1. Approximate the dual variable on the macro element boundaries and then solve the conservation law (for flux and pressure) at the interior of each macro element
2. MHM approximation contains two (or more) scaling operators:
   - Downscaling: The fine-scale behavior of solution is captured by solving local flow equations at the interior of the macro elements
   - Upscaling: The fine-scale properties are transferred to a small global problem associated with the fluxes

A two-scale pictorial demo of MHM

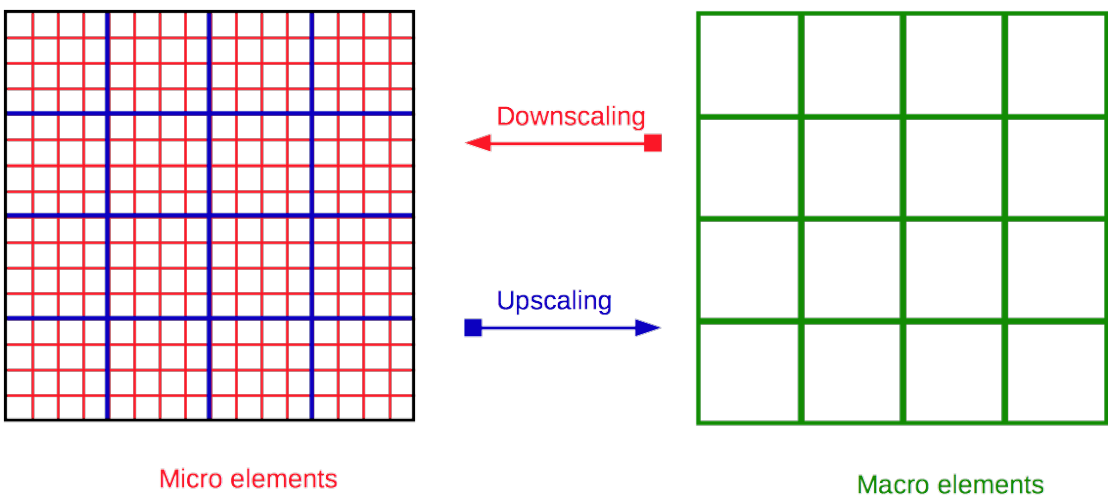

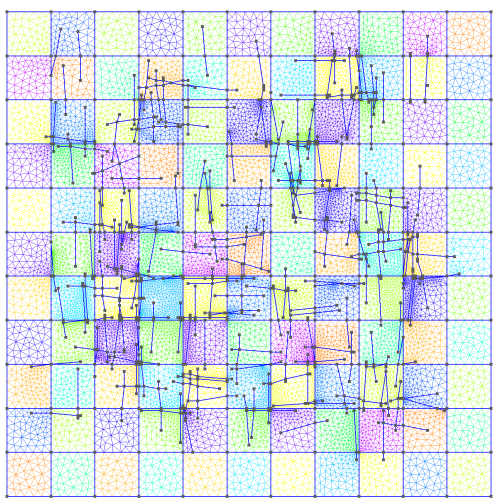

Numerical Analysis of MHM

- Well-posedness and best approximation property hold
- Locally mass conservative (on marco or micro elements)
- Can be implemented by regular FE basis or static condensation

- Error analysis of MHM-H^1 [Araya, Harder, Paredes, Valentin 2013]
- MHM for advective-reactive equation [Harder, Paredes, Valentin 2015]
- Robustness of MHM-H^1 [Paredes, Valentin, Versieux 2016]
- MHM for linear elasticity equation [Harder, Madureira, Valentin 2016]
- MHM for Stokes and Brinkman [Araya, Harder, Poza, Valentin 2017]
- MHM-$H(\mathrm{div})$ for DFM [Devloo, Teng, Z. 2019]
- MHM-$H(\mathrm{div})$ for Darcy [Duran, Devloo, Gomes, Valentin 2019]
- MHM-H^1 for DFM [Chen, Devloo, Z.]
- . . . . . .

MHM-$H^1(\Omega)$ Formulation

Weak formulation: Find $p \in V = H^1(\mathcal{T}_h), \lambda \in \Lambda = H^{-\frac{1}{2}}(\mathcal{E}_h)$ such that

$$a_h[p, \lambda;\, q, \mu] = F(q, \mu), \quad q \in V, \mu \in \Lambda$$

with $a_h[p, \lambda;\, q, \mu] := (\alpha \nabla p, \nabla q)_{\mathcal{T}_h} + (\lambda \mathbf{n}, [q])_{\mathcal{E}_h} + (\mu \mathbf{n}, [p])_{\mathcal{E}_h}$ and $F(q, \mu) := (f, q)_{\mathcal{T}_h}$.

Space decomposition: $V = V_0 \oplus W$, with $W = V \cap L_0^2(\mathcal{T}_h)$ and V_0 is p.w. const.

We can divide the weak formulation as the following two parts:

$$a_h[p, \lambda;\, q_0, \mu] = F(q_0, \mu), \qquad \forall\, q_0 \in V_0, \mu \in \Lambda; \tag{1}$$

$$a_h[p, \lambda;\, q_w, 0] = F(q_w, 0), \qquad \forall\, q_w \in W. \tag{2}$$

Static condensation: Using (2), on each macro element $\tau \in \mathcal{T}_h$, we solve

$$a_h[p^f + p^\lambda, \lambda;\, q_w, 0] = (f, q_w), \quad \forall\, q_w \in W(\tau),$$

where $p^f \in W$ and $p^\lambda \in W$

$$(\alpha \nabla p^f, \nabla q_w)_\tau = (f, q_w), \qquad \forall\, q_w \in W(\tau);$$

$$(\alpha \nabla p^\lambda, \nabla q_w)_\tau = -(\lambda \mathbf{n} \cdot \mathbf{n}_\tau, q_w)_{\partial\tau}, \qquad \forall\, q_w \in W(\tau).$$

Global problem: Find $\overline{p} \in V_0$ and $\lambda \in \Lambda$ such that the equation (1) holds.

[Harder, Paredes, Valentin 2013; Araya, Harder, Paredes, Valentin 2013]

MHM-$H(\mathrm{div}, \Omega)$ Formulation

Mixed formulation of Darcy's law: Find $(\mathbf{u}, p) \in \mathbf{H}_0(\mathrm{div}, \Omega) \times L^2(\Omega)$ such that

$$\int_\Omega \kappa^{-1}\mathbf{u} \cdot \mathbf{v}\, dx + \int_\Omega p \nabla \cdot \mathbf{v}\, dx = 0,$$

$$\int_\Omega \nabla \cdot \mathbf{u}\, q\, dx = \int_\Omega f q\, dx,$$

for any $(\mathbf{v}, q) \in \mathbf{H}_0(\mathrm{div}, \Omega) \times L^2(\Omega)$.

Main steps of MHM-$H(\mathrm{div})$ [Duran, Devloo, Gomes, Valentin 2019]

(1) Decompose $\mathbf{u} = \sigma + \lambda$, where σ is the inner flux diminishing on the macro element boundaries and λ is the outer flux between macro elements

(2) Write the system on each macro element as a function of inner flux, pressure, outer flux, and average pressure

(3) Obtain a global system by applying static condensation

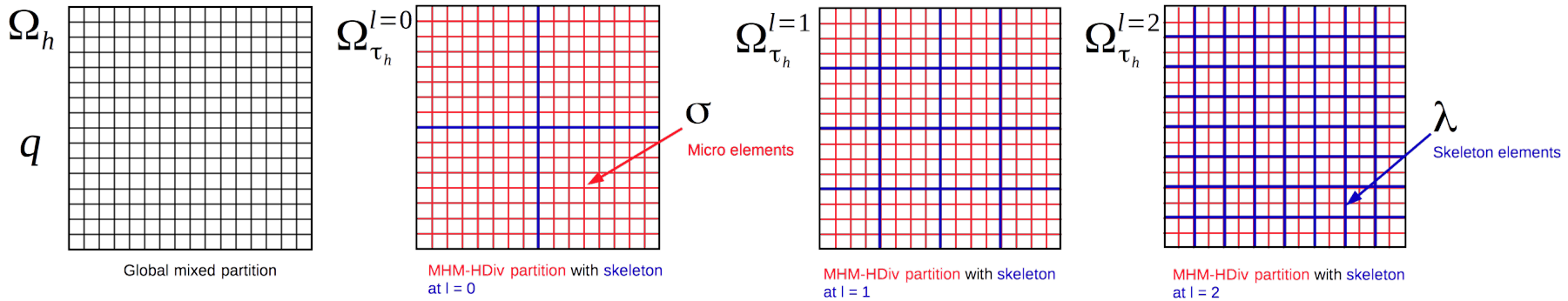

Volumetric and Fracture Flows in DFM

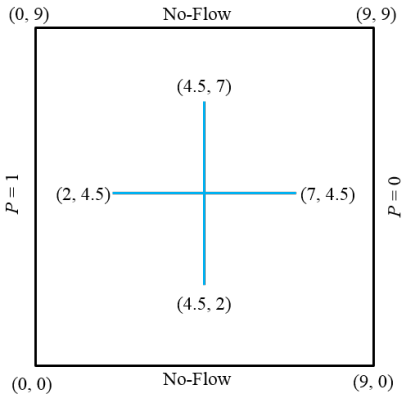

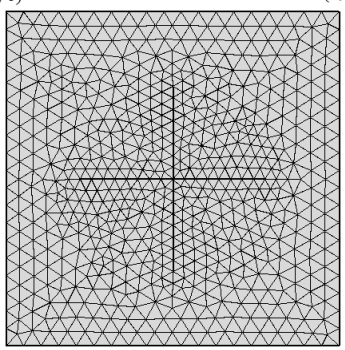

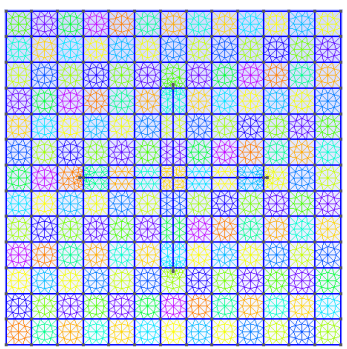

$$\int_{T_2} \kappa_{2,m}^{-1}\mathbf{u}_2\cdot\mathbf{v}_2 - \int_{T_2} p_2\,\nabla\cdot\mathbf{v}_2 + \int_{T_1} p_1\,\Sigma(\mathbf{v}_2\cdot n) = 0$$

$$-\int_{T_2} \nabla\cdot\mathbf{u}_2\,q_2 = \int_{T_2} f\,q_2$$

$$\int_{T_1} \Sigma(\mathbf{u}_2\cdot n)\,q_1 = 0 \qquad \Longleftarrow$$

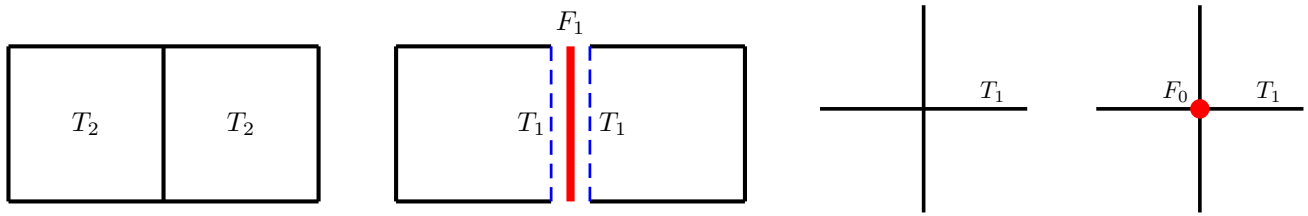

$$\int_{F_1} \kappa_{1,f}^{-1}\mathbf{u}_1\cdot\mathbf{v}_1 - \int_{F_1} p_1\,\nabla\cdot\mathbf{v}_1 + \int_{F_0} p_0\,\Sigma(\mathbf{v}_1\cdot n) = 0$$

$$-\int_{F_1} \nabla\cdot\mathbf{u}_1\,q_1 = 0 \qquad \Longleftarrow$$

$$\int_{F_0} \Sigma(\mathbf{u}_1\cdot n)\,q_0 = 0$$

Assume no resistivity (large permeability, small aperture): $\frac{1}{\alpha_f} \approx 0 \Longrightarrow p_1|_{\gamma_1} = p_2|_{\gamma_2} = p_f$

Multiscale Hybrid-Mixed Method for DFM

Two-dimension, no resistivity ($p_1|_{\gamma_1} = p_2|_{\gamma_2} = p_f$), homogenous B.C.

$$\int_{T_2} \kappa_{2,m}^{-1} \mathbf{u}_2 \cdot \mathbf{v}_2 - \int_{T_2} p_2 \nabla \cdot \mathbf{v}_2 + \int_{F_1} p_1 \Sigma(\mathbf{v}_2 \cdot n) = 0$$

$$- \int_{T_2} \nabla \cdot \mathbf{u}_2 \, q_2 = \int_{T_2} f \, q_2$$

$$\int_{T_1} \kappa_{1,f}^{-1} \mathbf{u}_1 \cdot \mathbf{v}_1 - \int_{T_1} p_1 \nabla \cdot \mathbf{v}_1 + \int_{F_0} p_0 \Sigma(\mathbf{v}_1 \cdot n) = 0$$

$$- \int_{T_1} \nabla \cdot \mathbf{u}_1 \, q_1 + \int_{T_1} \Sigma(\mathbf{u}_2 \cdot n) \, q_1 = 0$$

$$\int_{T_0} \Sigma(\mathbf{u}_1 \cdot n) \, q_0 = 0$$

- Two dimensional fluxes $\mathbf{u}_2$ and corresponding test functions $\mathbf{v}_2$
- One dimensional fluxes $\mathbf{u}_1$ and corresponding test functions $\mathbf{v}_1$
- Two dimensional pressures p_2 and corresponding test functions q_2
- One dimensional pressures p_1 and corresponding test functions q_1
- Zero dimensional pressures p_0 and corresponding test functions q_0

Generalization to 3D DFM

- 3D volumetric flow + 2D fracture flow + 1D flow through fracture interactions

$$\int_{T_3} \kappa_{3,m}^{-1}\mathbf{u}_3\cdot\mathbf{v}_3 - \int_{T_3} p_3\,\nabla\cdot\mathbf{v}_3 + \int_{F_2} p_2\,\Sigma(\mathbf{v}_3\cdot n) = 0$$

$$-\int_{T_3} \nabla\cdot\mathbf{u}_3\,q_3 = \int_{T_3} f\,q_3$$

$$\int_{T_2} \kappa_{2,f}^{-1}\mathbf{u}_2\cdot\mathbf{v}_2 - \int_{T_2} p_{f,2}\,\nabla\cdot\mathbf{v}_2 + \int_{F_1} p_1\,\Sigma(\mathbf{v}_2\cdot n) = 0$$

$$-\int_{T_2} \nabla\cdot\mathbf{u}_2\,q_{f,2} + \int_{T_2} \Sigma(\mathbf{u}_3\cdot n)\,q_{f,2} = 0$$

$$\int_{T_1} \kappa_{1,f}^{-1}\mathbf{u}_1\cdot\mathbf{v}_1 - \int_{T_1} p_{f,1}\,\nabla\cdot\mathbf{v}_1 + \int_{F_0} p_0\,\Sigma(\mathbf{v}_1\cdot n) = 0$$

$$-\int_{T_1} \nabla\cdot\mathbf{u}_1\,q_{f,1} + \int_{T_1} \Sigma(\mathbf{u}_2\cdot n)\,q_{f,1} = 0$$

$$\int_{T_0} \Sigma(\mathbf{u}_1\cdot n)\,q_0 = 0$$

- Verification benchmarks for single-phase flow in 3D fractured porous media

3D benchmark problems [Berre, Boon, Flemisch, et al. 2018]

Implementation of MHDFM

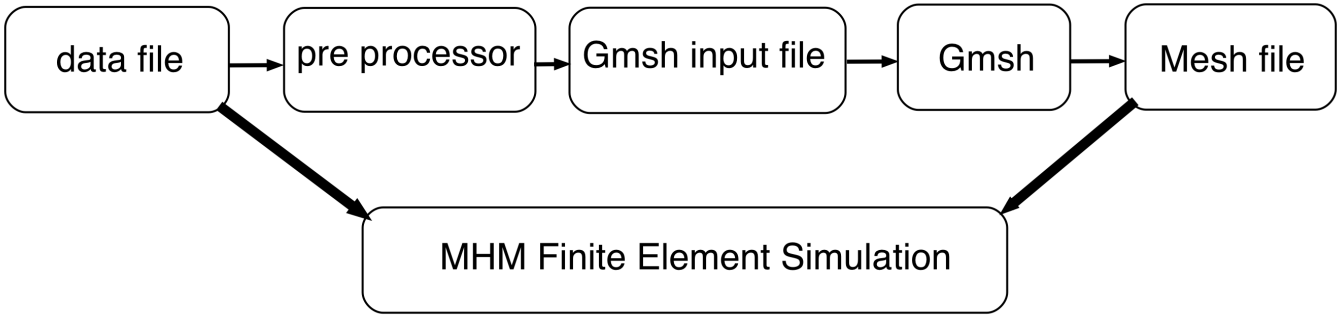


```
# Example 1
#
# Problem description
#
# 1000 ft X 1000 ft 2D planar region (1000 ft below earth surface)
# No flow boundary condition
# One producer (sink) at the center of the field
#

# Uniform permeability in x and y directions

PERMX
 1

PERMY
 1

PORO
 0.1

# Embedded fractures
#
# NAME: the name of a fracture
# CORNER: (x,y,z) of starting and ending points of a facture (z = 1000, ignore)
# PORO: porosity of fracture, ignore
# PERM: permeability of fracture
# THICK: aperture of facture, ignore
# SATMAP: ignore
#
# Since we assume area of any fracture is zero, we ignore PORO and THICK

EMBF
 NAME  'f1'
 CORNER    657.205181     153.584745     1000.000000   559.667835     131.528776     1000.000000
 PORO  0.001   PERM  500  THICK  0.1  SATMAP  2 /
 NAME  'f2'
 CORNER    860.631081     134.818298     1000.000000   761.925656     150.856961     1000.000000
 PORO  0.001   PERM  500  THICK  0.1  SATMAP  2 /
 NAME  'f3'
 CORNER    373.268623     169.009309     1000.000000   273.571195     176.782499     1000.000000
 PORO  0.001   PERM  500  THICK  0.1  SATMAP  2 /
 NAME  'f4'
 CORNER    711.399570     189.310648     1000.000000   611.428501     191.715858     1000.000000
 PORO  0.001   PERM  500  THICK  0.1  SATMAP  2 /
```

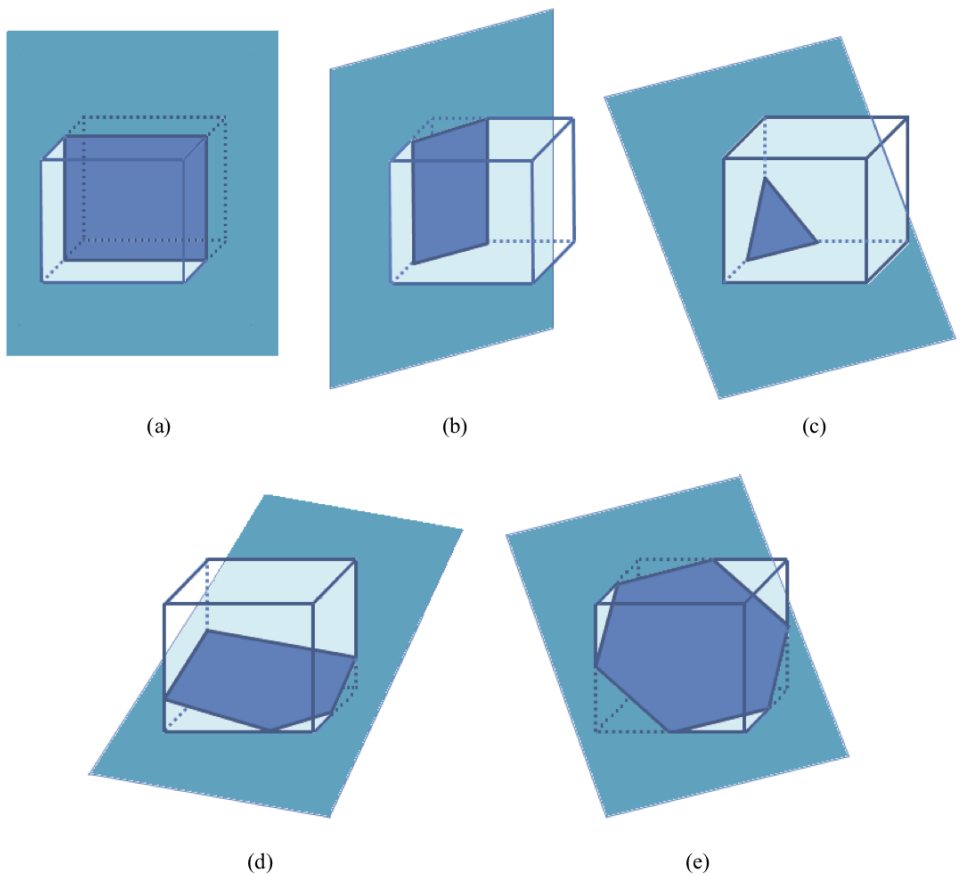

Benchmark problems and numerical results

29 Orthogonal Fracture Configurations

30 Unorthogonal Fracture Configurations

31 Comparisons with Direct Simulation

32 3D Benchmark 1

33 3D Benchmark 1

34 3D Benchmark 2

35 3D Benchmark 2

36 3D Benchmark 3

37 3D Benchmark 3

38 3D Benchmark 4

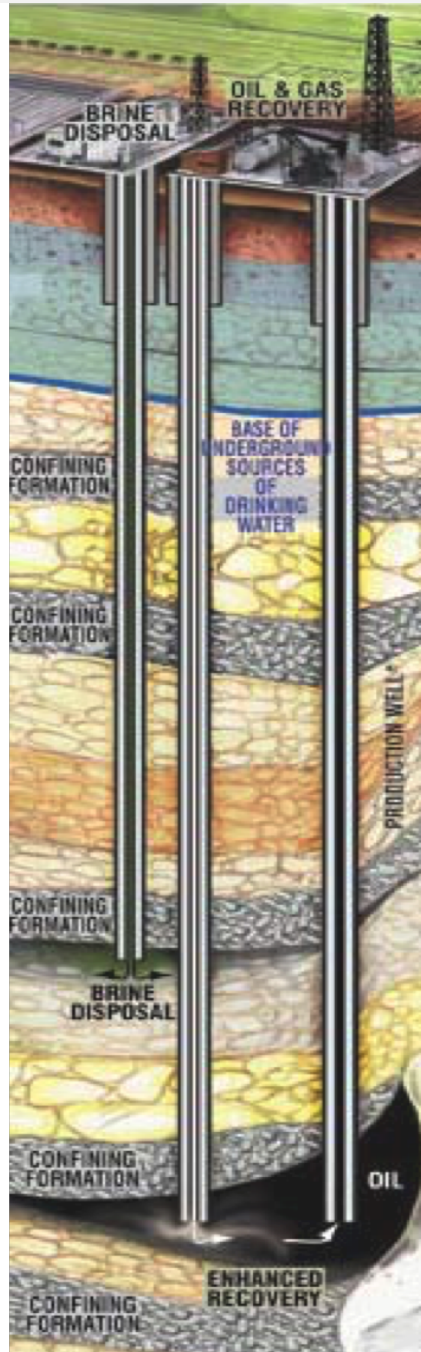

Orthogonal Fracture Configurations

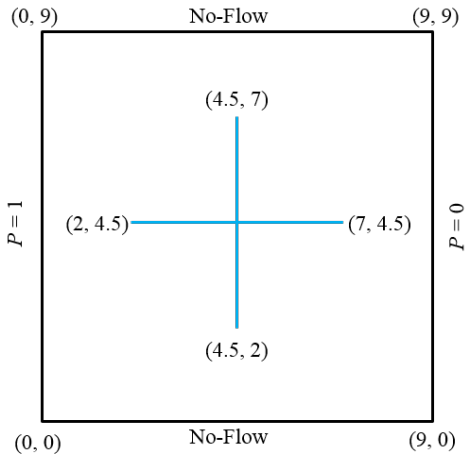

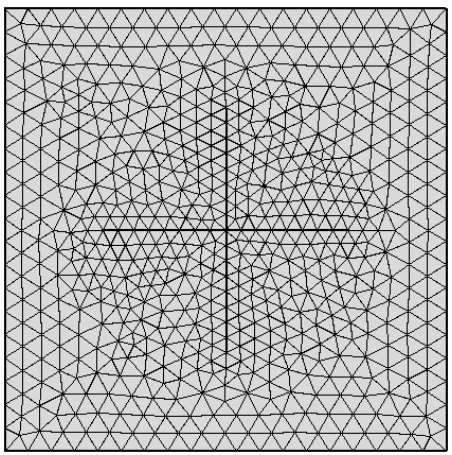

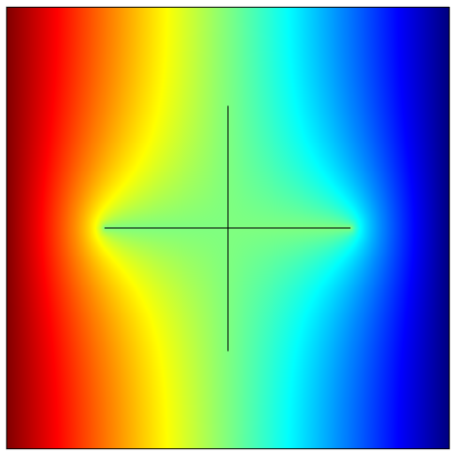

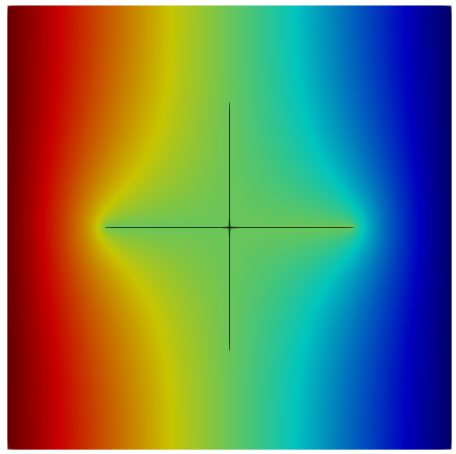

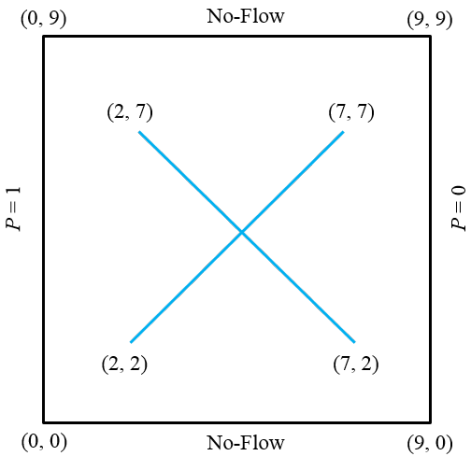

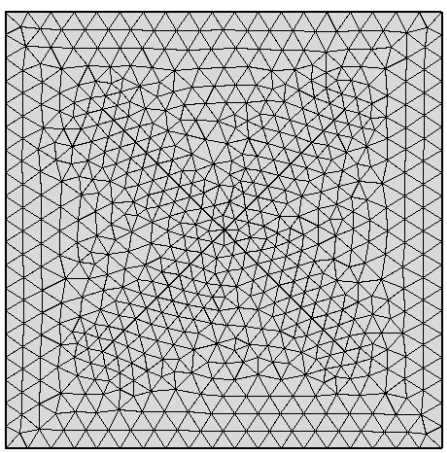

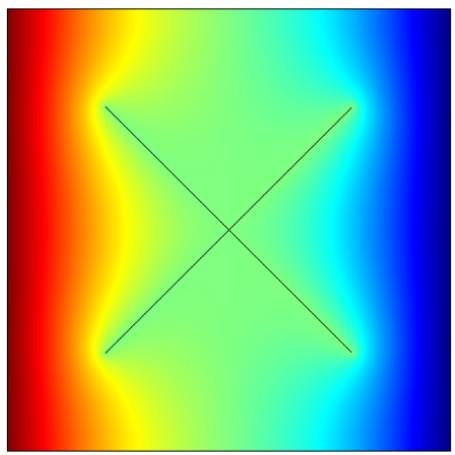

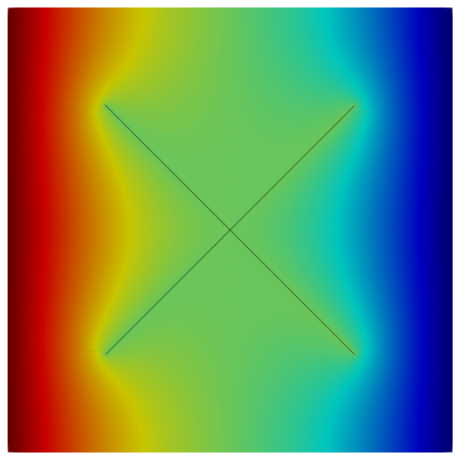

[Devloo, Teng, Z. 2019]

Unorthogonal Fracture Configurations

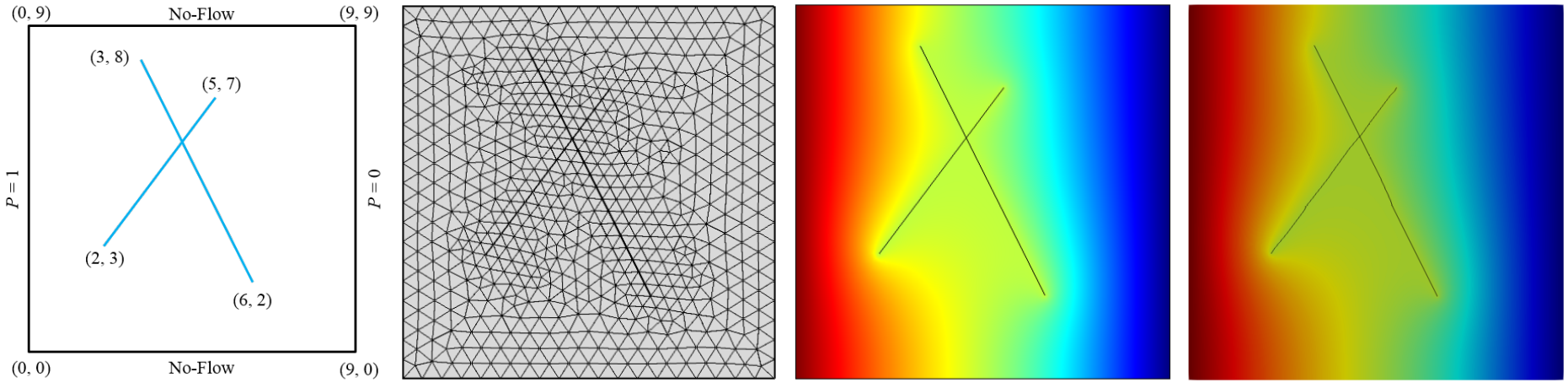

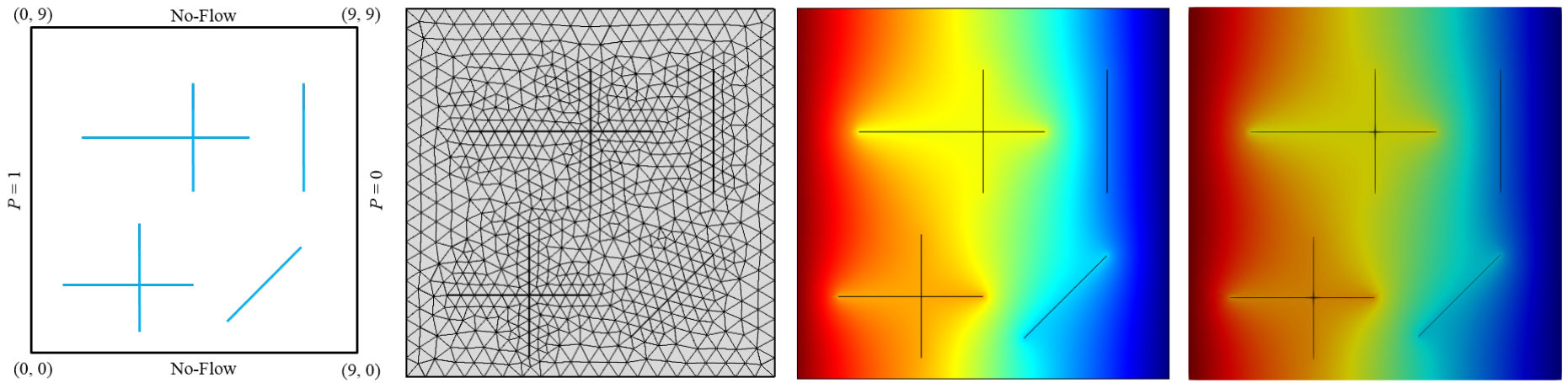

[Devloo, Teng, Z. 2019]

Comparisons with Direct Simulation

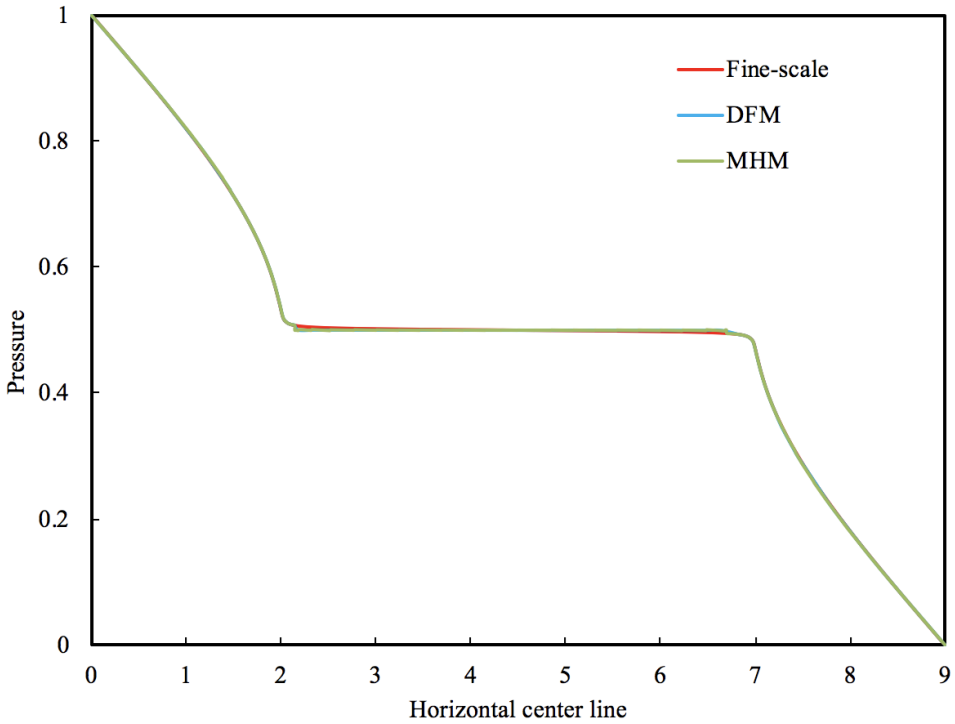

Case	MHDFM	DFM	Fine-Scale
1	841	2501	50625
2	809	2585	-
3	865	2517	-
4	883	2933	-

Case	MHDFM	DFM	Fine-Scale	Difference
1	1.2843	1.2876	1.2892	2.56E-3
2	1.6081	1.6122	—	2.54E-3
3	1.2661	1.2724	—	4.95E-3
4	1.3940	1.4070	—	9.24E-3

Table: Comparison of numerical flow rate by different methods

3D Benchmark 1

One fracture with thickness of 0.01m, simulation time is 10^9s

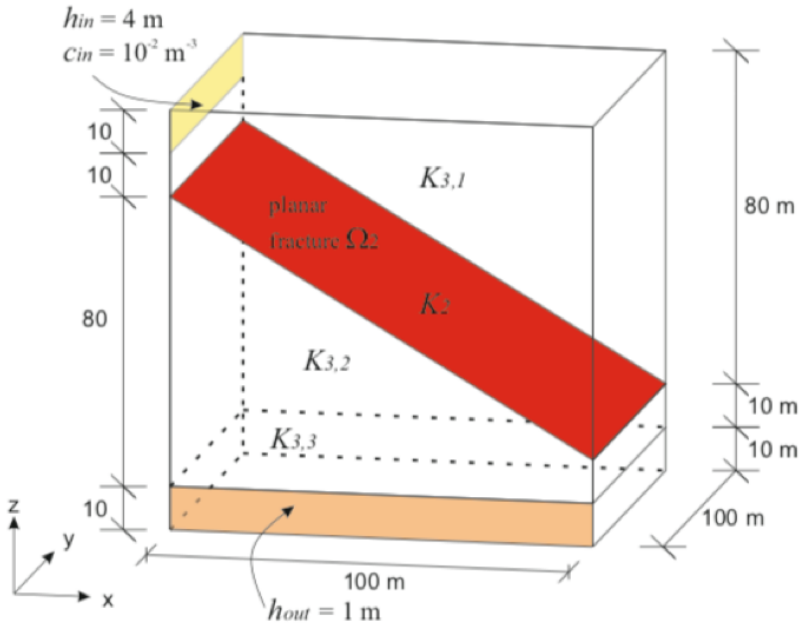

Matrix hydraulic conductivity $K_{3,1}$, $K_{3,2}$	$1 \times 10^{-6} I$	m/s
Matrix hydraulic conductivity $K_{3,3}$	$1 \times 10^{-5} I$	m/s
Fracture effective tangential hydraulic conductivity K_2	$1 \times 10^{-3} I$	m^2/s
Fracture effective normal hydraulic conductivity κ_2	20	1/s
Matrix porosity $\phi_{3,1}$, $\phi_{3,2}$	2×10^{-1}	
Matrix porosity $\phi_{3,3}$	2.5×10^{-1}	
Fracture porosity ϕ_2	4×10^{-1}	
Fracture cross-sectional length ε_2	1×10^{-2}	m

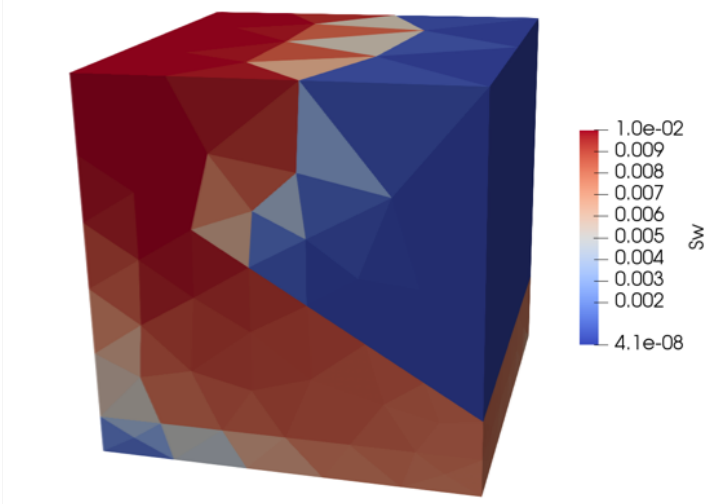

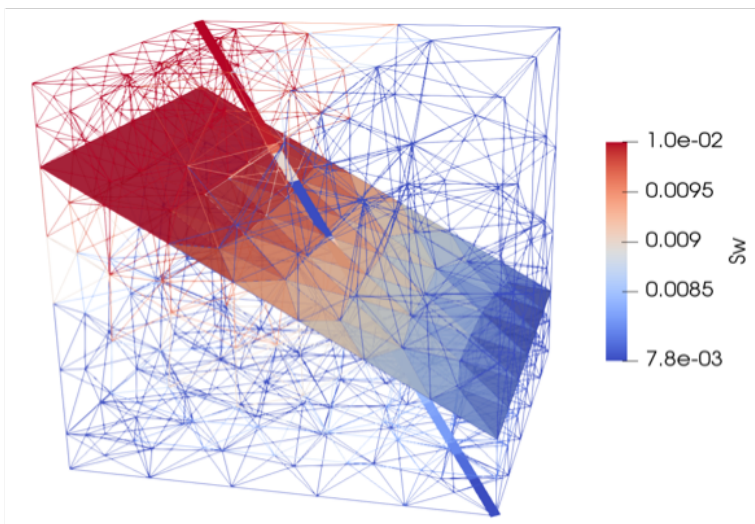

3D Benchmark 1

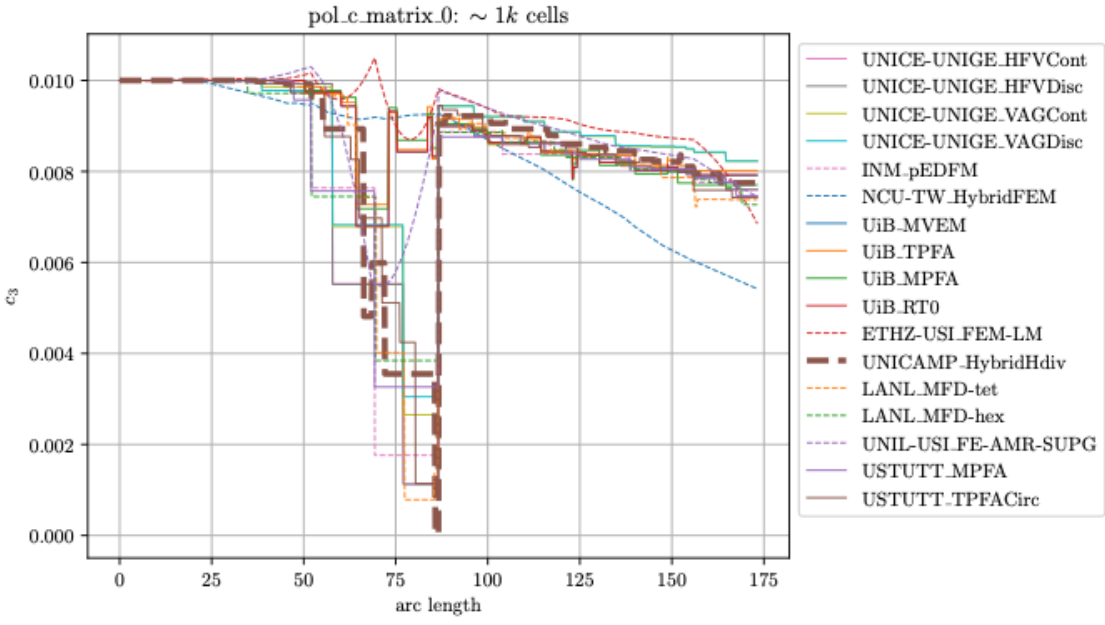

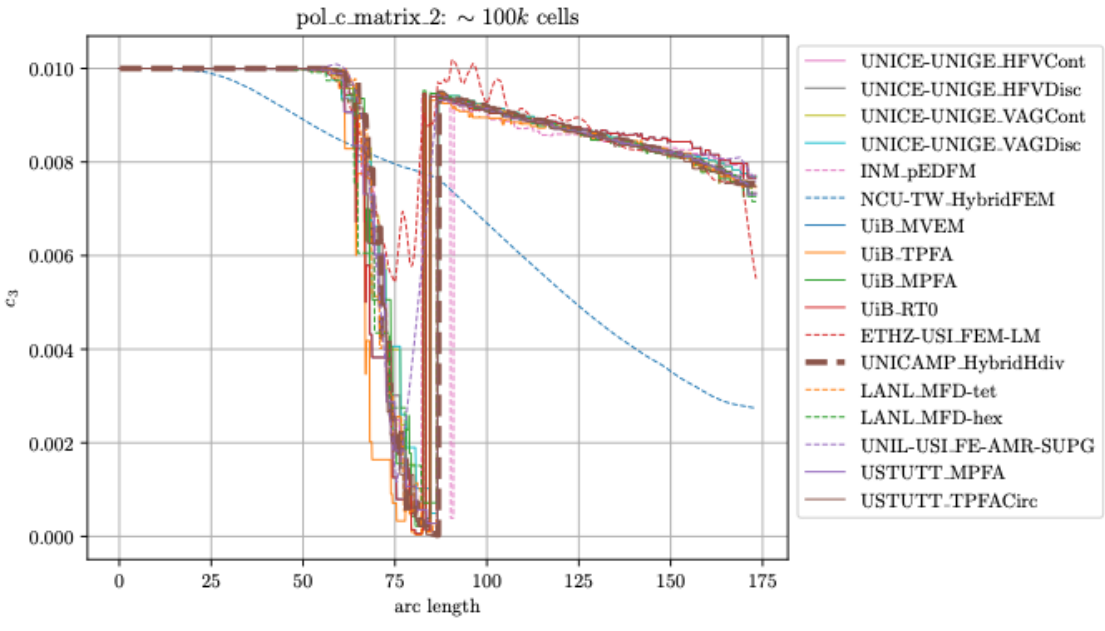

3D Benchmark 2

Nine fractures with high and low conductivity cases, simulation time is 0.25s

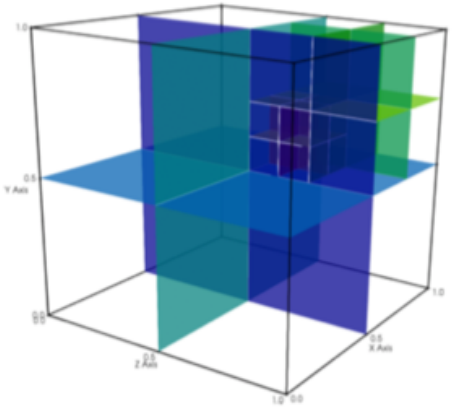

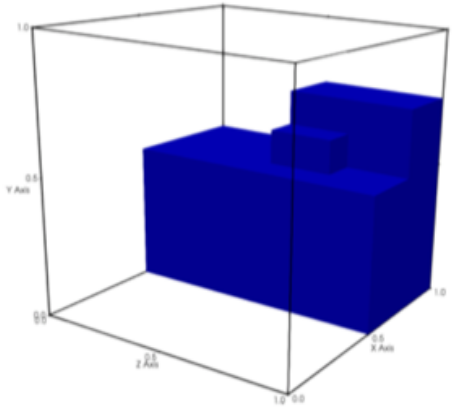

	${COND} = 0		${COND} = 1	
Matrix hydraulic conductivity $K_3\|_{\Omega_{3,0}}$	$\boldsymbol{I}$	m/s	$\boldsymbol{I}$	m/s
Matrix hydraulic conductivity $K_3\|_{\Omega_{3,1}}$	$1 \times 10^{-1}\boldsymbol{I}$	m/s	$1 \times 10^{-1}\boldsymbol{I}$	m/s
Fracture effective tangential hydraulic conductivity K_2	$\boldsymbol{I}$	m^2/s	$1 \times 10^{-8}\boldsymbol{I}$	m^2/s
Fracture effective normal hydraulic conductivity κ_2	2×10^8	1/s	2	1/s
Intersection effective tangential hydraulic conductivity K_1	1×10^{-4}	m^3/s	1×10^{-12}	m^3/s
Intersection effective normal hydraulic conductivity κ_1	2×10^4	m/s	2×10^{-4}	m/s
Intersection effective normal hydraulic conductivity κ_0	2	m^2/s	2×10^{-8}	m^2/s
Matrix porosity ϕ_3	1×10^{-1}		1×10^{-1}	
Fracture porosity ϕ_2	9×10^{-1}		1×10^{-2}	
Intersection porosity ϕ_1	9×10^{-1}		1×10^{-2}	
Fracture cross-sectional length ε_2	1×10^{-4}	m	1×10^{-4}	m
Intersection cross-sectional area ε_1	1×10^{-8}	m^2	1×10^{-8}	m^2
Intersection cross-sectional volume ε_0	1×10^{-12}	m^3	1×10^{-12}	m^3

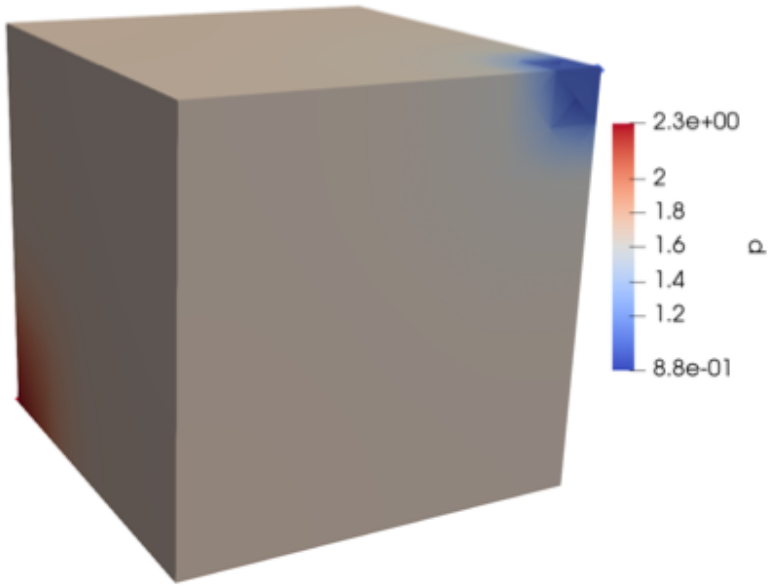

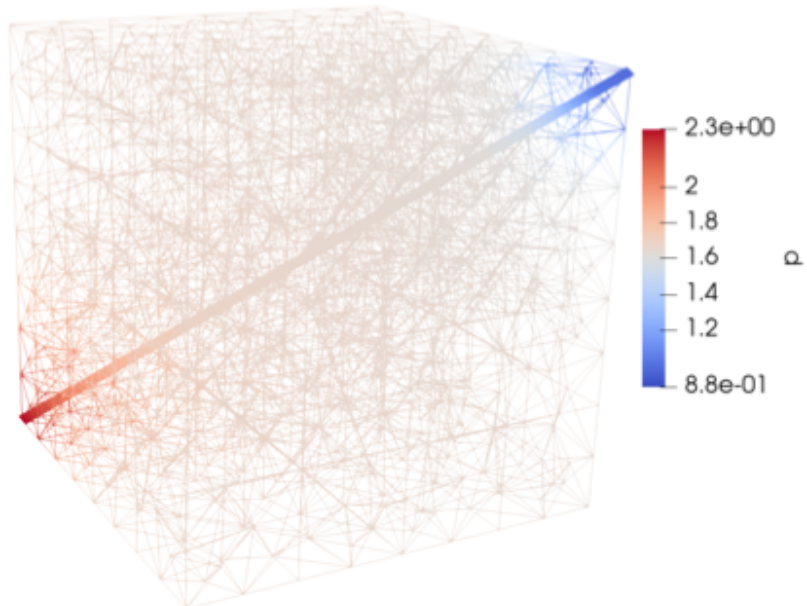

3D Benchmark 2

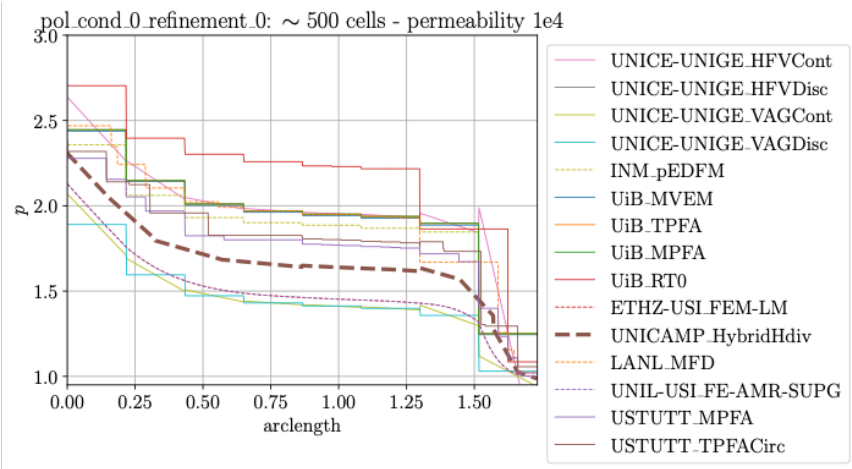

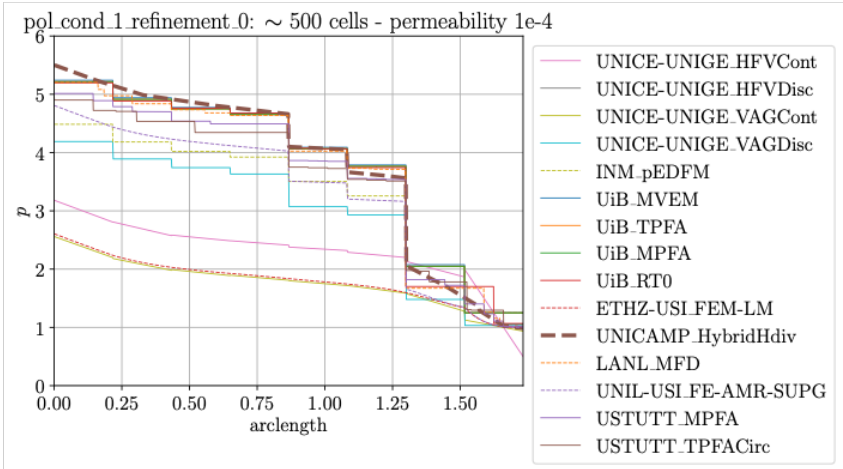

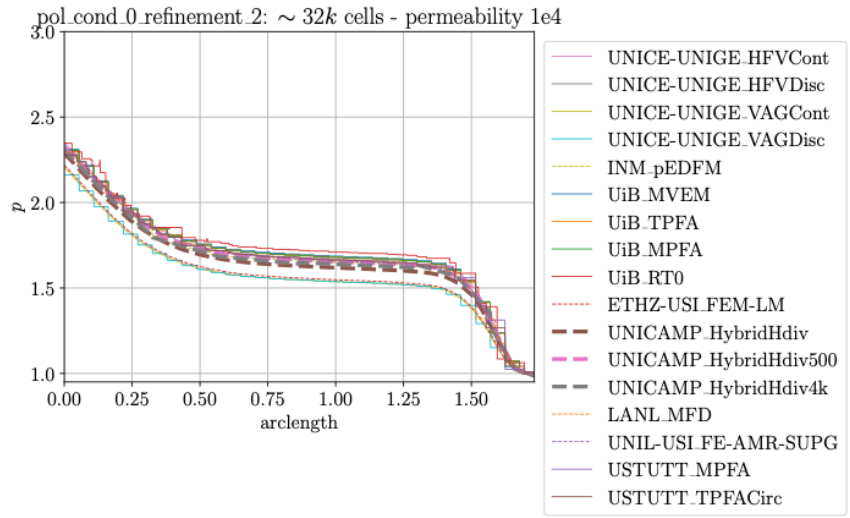

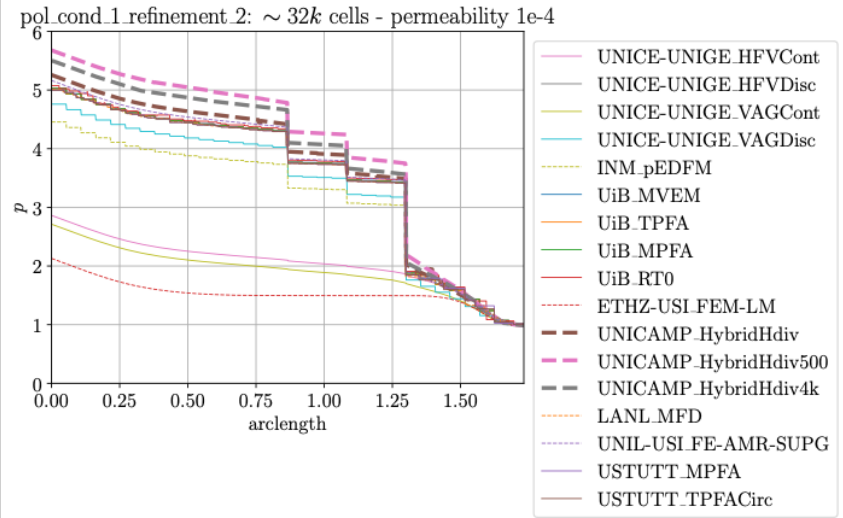

3D Benchmark 3

Eight fractures with barely touching fractures and small features, simulation time is 1s

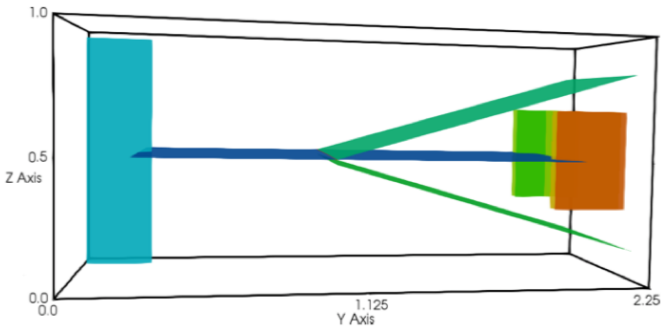

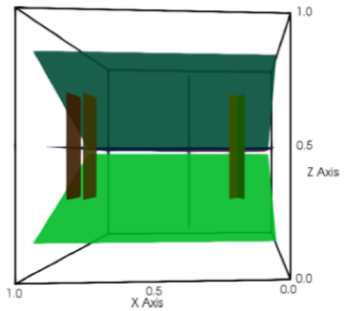

Matrix hydraulic conductivity K_3	$\boldsymbol{I}$	m/s
Fracture effective tangential hydraulic conductivity K_2	$1 \times 10^2 \boldsymbol{I}$	m^2/s
Fracture effective normal hydraulic conductivity κ_2	2×10^6	1/s
Intersection effective tangential hydraulic conductivity K_1	1	m^3/s
Intersection effective normal hydraulic conductivity κ_1	2×10^4	m/s
Matrix porosity ϕ_3	2×10^{-1}	
Fracture porosity ϕ_2	2×10^{-1}	
Intersection effective porosity ϕ_1	2×10^{-1}	
Fracture cross-sectional length ε_2	1×10^{-2}	m
Intersection cross-sectional area ε_1	1×10^{-4}	m^2

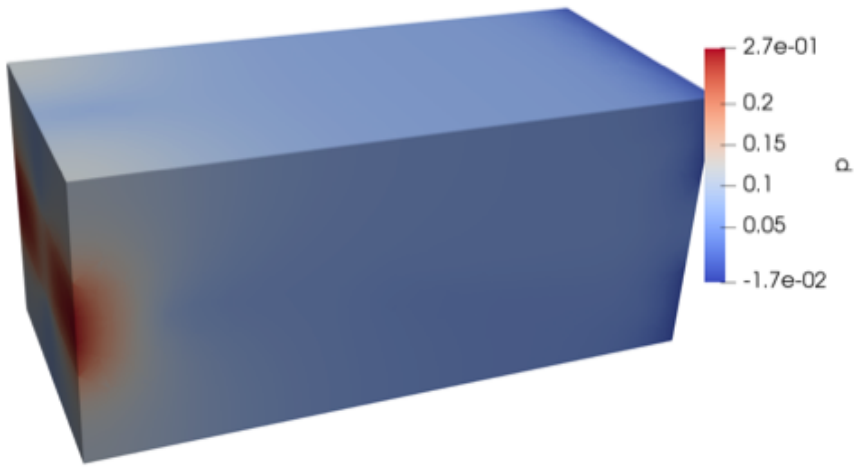

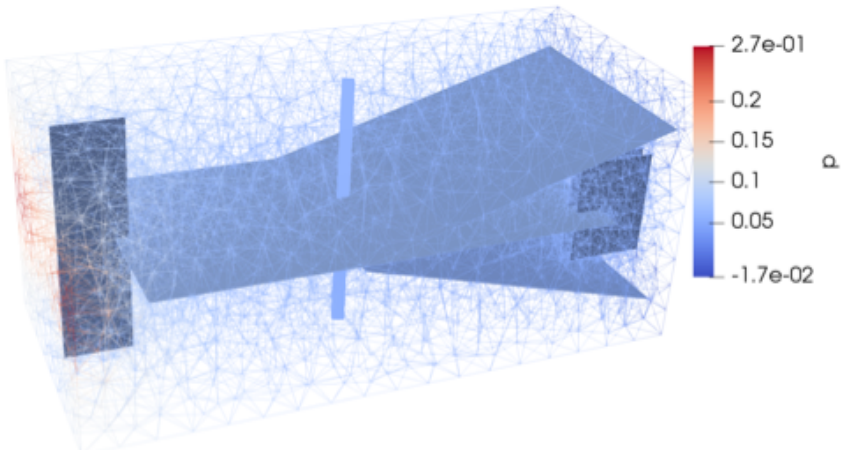

3D Benchmark 3

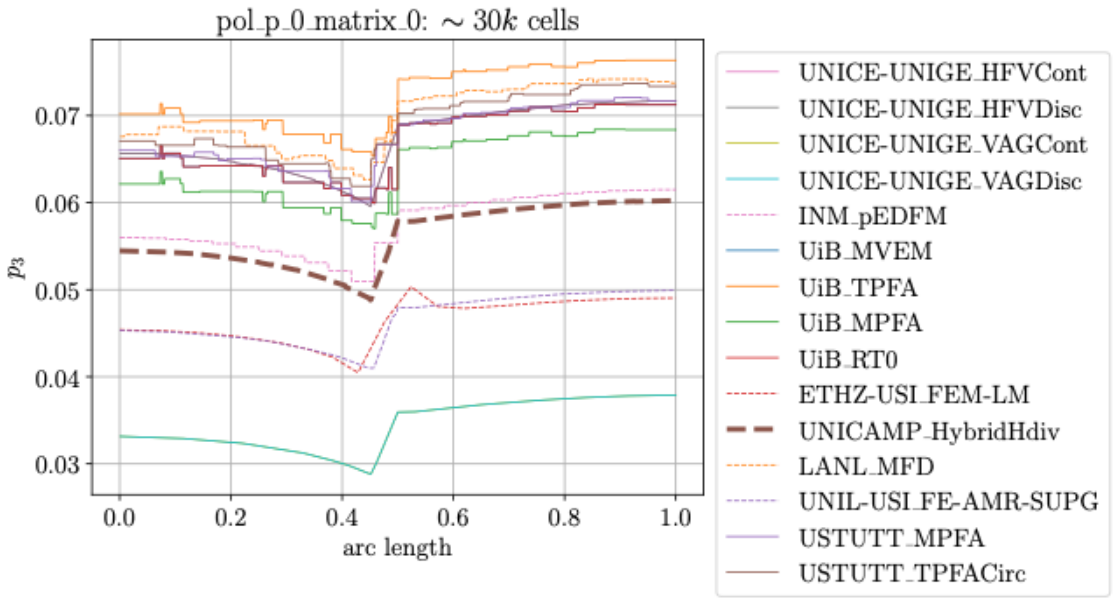

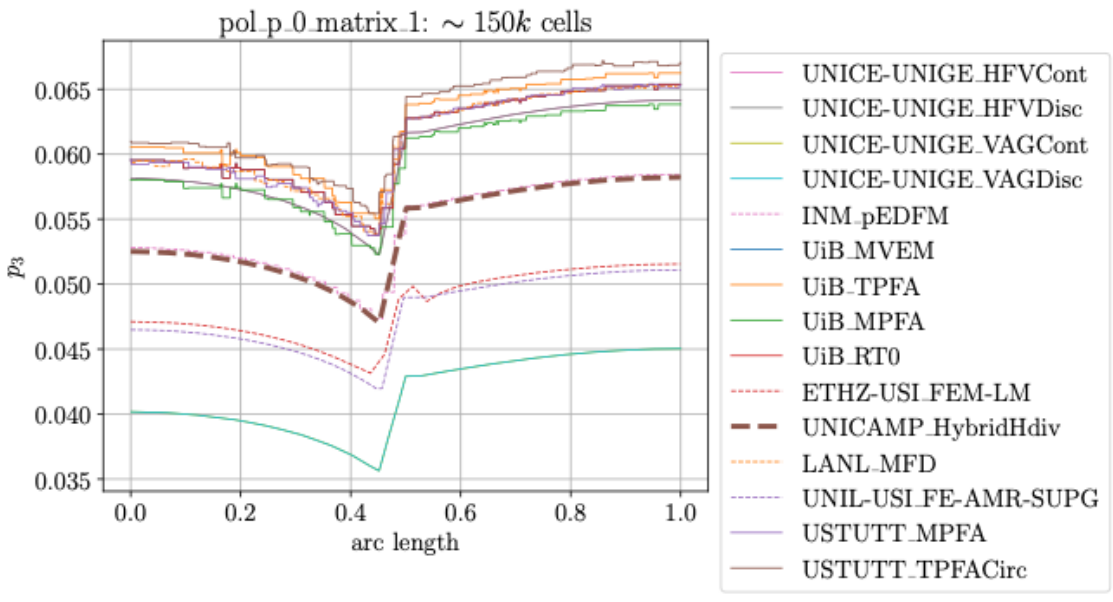

3D Benchmark 4

52 fractures with 106 intersections, simulation time is 50s

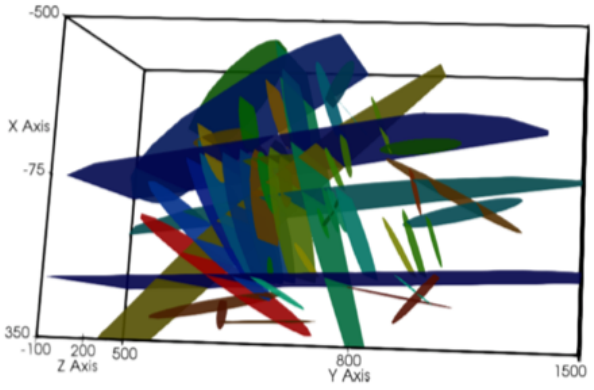

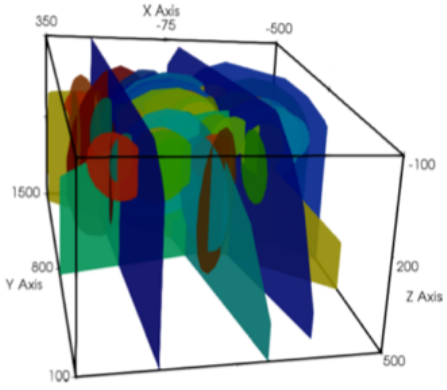

Matrix hydraulic conductivity K_3	$\boldsymbol{I}$	m/s
Fracture effective tangential hydraulic conductivity K_2	$1 \times 10^2 \boldsymbol{I}$	m^2/s
Fracture effective normal hydraulic conductivity κ_2	2×10^6	1/s
Intersection effective tangential hydraulic conductivity K_1	1	m^3/s
Intersection effective normal hydraulic conductivity κ_1	2×10^4	m/s
Matrix porosity ϕ_3	2×10^{-1}	
Fracture porosity ϕ_2	2×10^{-1}	
Intersection porosity ϕ_1	2×10^{-1}	
Fracture cross-sectional length ε_2	1×10^{-2}	m
Intersection cross-sectional area ε_1	1×10^{-4}	m^2

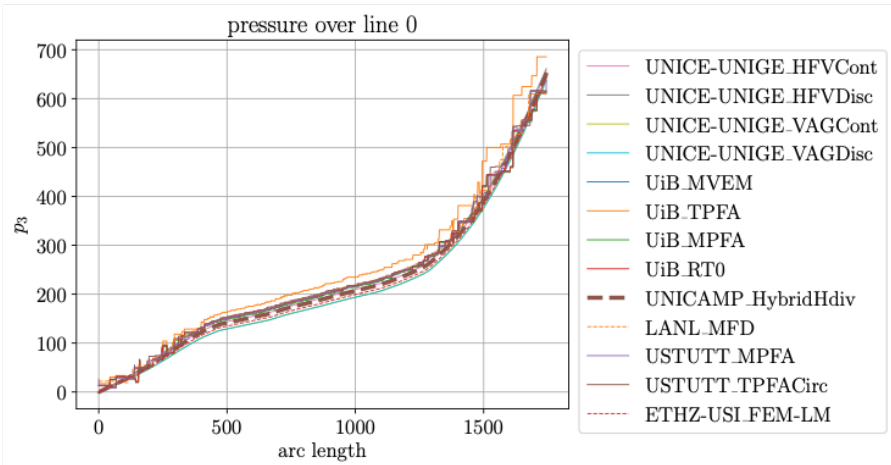

[Devloo, Durán, et al.]

Solution methods for field-scale simulation

39 Steps of Petroleum Reservoir Simulation

40 Large-Scale Reservoir Simulation

41 Case Study: Limitations of Upscaled Models

42 Case Study: Coarse and Fine Models

43 IMPES/IMPEC Discretization

44 Fully Implicit Discretization

45 Quick Review of Other Discretization Methods

46 Simulation and Preconditioning

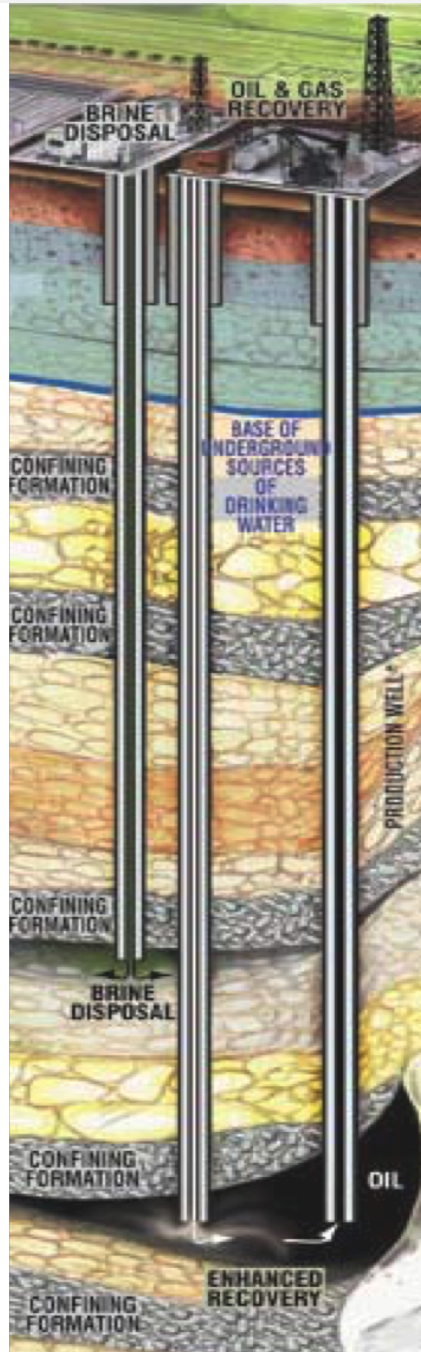

Steps of Petroleum Reservoir Simulation

Upstream Oil Industry: Finding and developing hydrocarbon deposits

1. Finding nearly horizontal and major fault surfaces
2. Determining detailed stratigraphic layers, faults, pinch-outs, ...
3. Generating reservoir characterization geomodel ($10^6 \sim 10^8$ cells)
4. Describing reservoir heterogeneity at multiple scales
5. Upscaling reservoir grids and properties ($10^4 \sim 10^6$ cells)
6. Finding fluid properties: PVT, relative permeability, ...
7. Reservoir initialization
8. Dynamic flow simulation
9. History matching
10. Calibrating model parameters, production forecast, & development planning

Large-Scale Reservoir Simulation

Challenges in large petroleum reservoir simulation

1. Modeling and discretization
   - Unconventional reservoirs and their modeling
   - Multiscale, heterogeneous, and anisotropic
   - Large number of grid cells with a lot of inactive cells
   - Complicated production requirements and well models
2. Nonlinear and linear solvers
   - Nonlinear algebraic equations for flash calculation
   - Nonlinear coupling between pressure and non-pressure variables
   - Large ill-conditioned linear system to solve
   - Non-symmetric (sometimes indefinite) Jacobian systems for FIM
3. Uncertainty and reliability

Why do we need lager computers for reservoir simulation?

- Need to solve fine-scale problems (1M∼1B grid cells)
- Need to simulate a long period of time (40∼60 years)
- Have many problems to solve ($10^2 \sim 10^3$ repetitions)

Case Study: Limitations of Upscaled Models

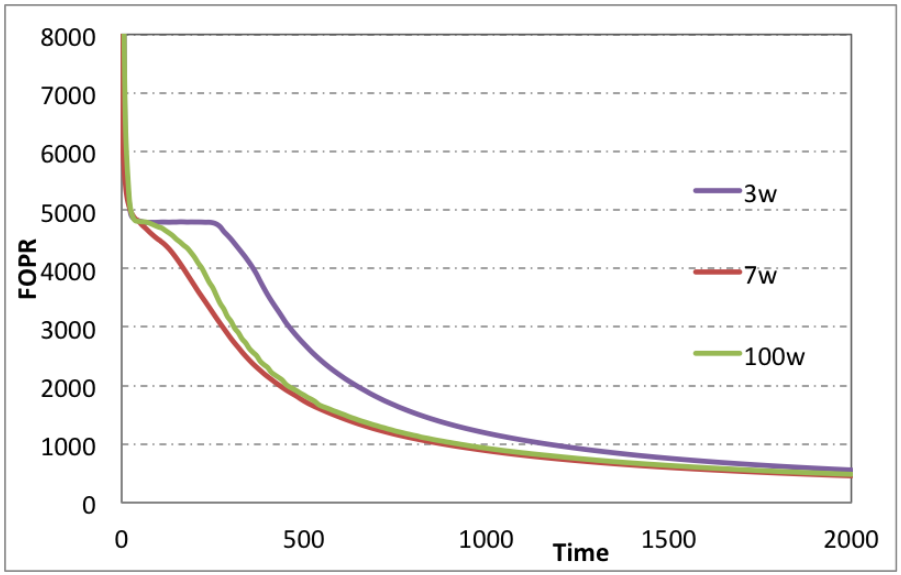

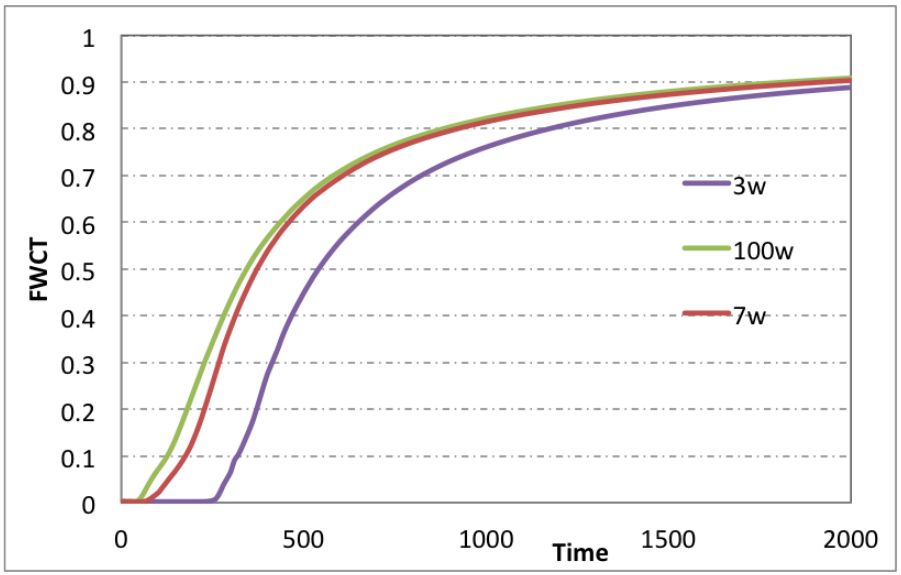

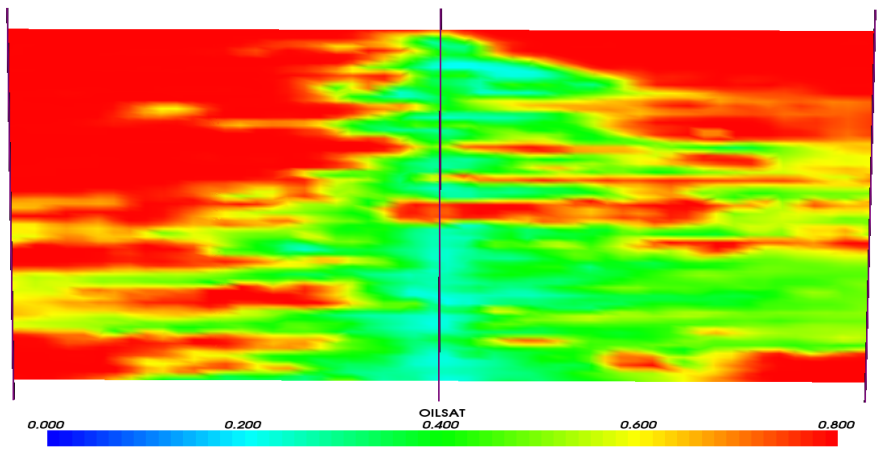

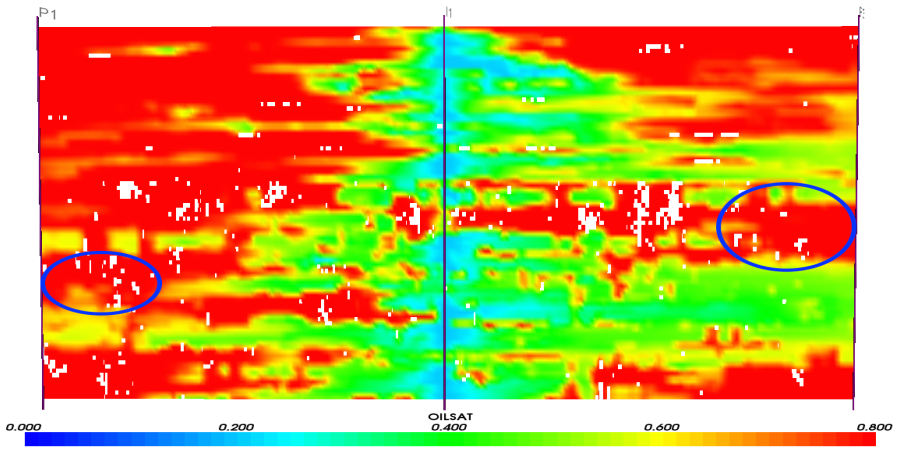

Effect of water injection. Left: 70K grid cells; Right: 1.1M grid cells.

[Wu, Xu, Z., et al. 2013]

Case Study: Coarse and Fine Models

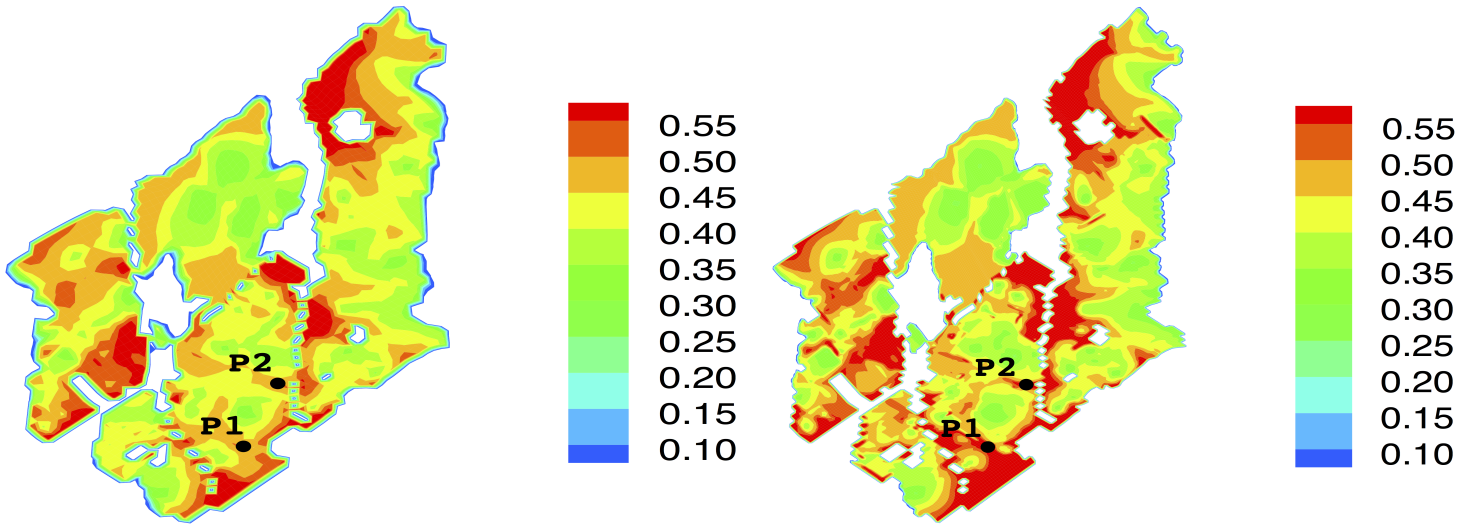

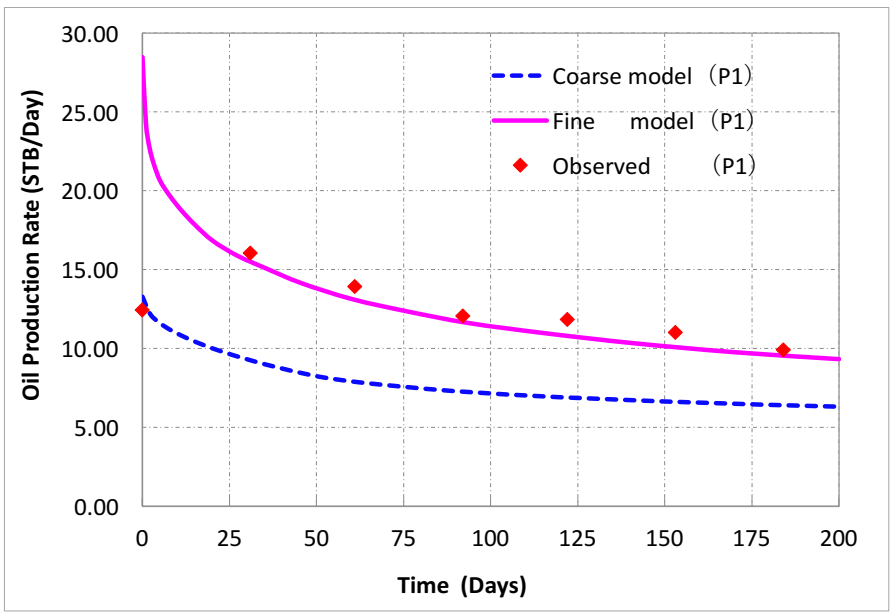

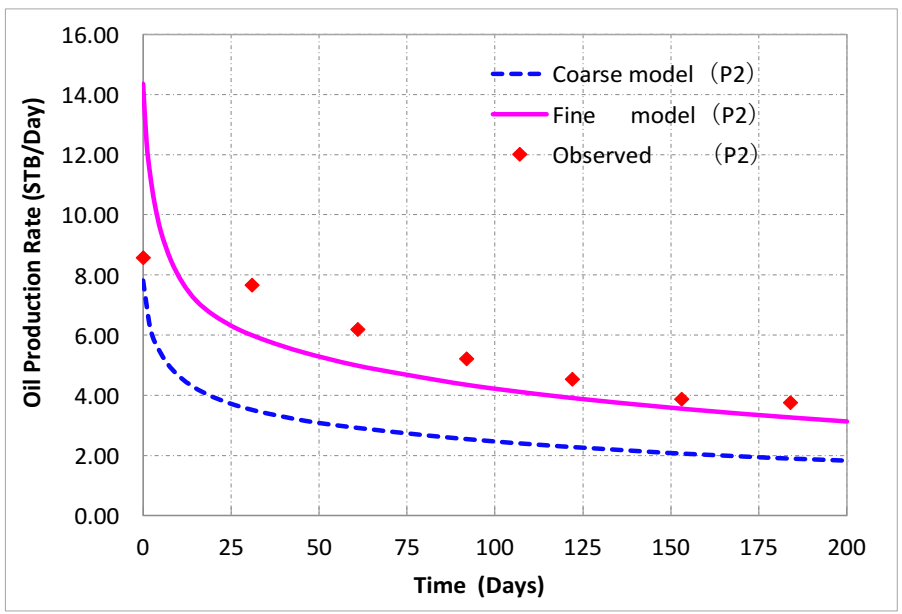

[Li, Wu, Li, Z., et al. 2016]

IMPES/IMPEC Discretization

Implicit pressure / explicit saturation (concentration)

- Separate computation of pressure from that of saturation / concentration
  [Sheldon, Zondek, Cardwell 1959; Stone, Garder 1961; Collins, et al. 1992]
- Two-phase classical IMPES: Define the total velocity $\mathbf{u} = \mathbf{u}_o + \mathbf{u}_w$ and then

$$\nabla \cdot \mathbf{u} = \frac{Q_w}{\rho_w} + \frac{Q_o}{\rho_o}$$

$$\mathbf{u} = -\kappa \left[\left(\frac{\kappa_{rw}}{\mu_w} + \frac{\kappa_{ro}}{\mu_o} \right) \nabla P - \left(\frac{\kappa_{rw}}{\mu_w} \rho_w + \frac{\kappa_{ro}}{\mu_o} \rho_o \right) \mathfrak{g} \nabla z \right]$$

- Obtaining an equation for pressure: $-\nabla \cdot (\alpha \nabla P) = Q$
- Updating saturation/concentration with explicit time-marching

Pros & Cons and Variants

- The discrete linear system to solve is SPD: solver-friendly

☞ Not very stable $\Longrightarrow$ requires small time stepsize (high flow velocity problems)

- Some modifications: Smaller Δt for saturation update; used in Newton iterations (Iterative IMPES); adaptive scheme; ...

Fully Implicit Discretization

Set of equations and unknowns

- FIM or SS discretization [Douglas, Peaceman, Rachford 1959]
- Primary equations: n_c mass conservation laws + volume balance:

$$V^{\text{fluid}}(P, N_1, \ldots, N_{n_c}) = V^{\text{pore}}(P)$$

- Secondary equations: phase equilibrium, density, relative permeability, ...
- Primary unknowns: $\vec{X} := (P, N_1, \ldots, N_{n_c})^T$ $\longleftarrow$ One more variable!
- Secondary unknowns: $\vec{Y} := (x_{11}, \ldots, x_{n_c n_p}, S_1, \ldots, S_{n_p})^T$

Discrete linear equations (no reaction term)

- Update the primary unknowns (Backward Euler + FVM + Newton)

$$\begin{aligned} \Psi_0 &:= V^{\text{pore}} - V^{\text{fluid}} = 0 \\ \Psi_i &:= \frac{N_i^{n+1} - N_i^n}{\Delta t} + \sum_s F_{i,s}^{n+1} - Q_i^{n+1} = 0, \quad i = 1 : n_c \end{aligned}$$

- Jacobian matrix $J := \dfrac{d\vec{\Psi}}{d\vec{X}} = \dfrac{\partial \vec{\Psi}}{\partial \vec{X}} + \dfrac{\partial \vec{\Psi}}{\partial \vec{Y}} \dfrac{\partial \vec{Y}}{\partial \vec{X}}$ $\longleftarrow$ More expensive!

Quick Review of Other Discretization Methods

1. Sequential Solution Method [MacDonald, Coats 1970]
   - Solve each equation separately and sequentially
   - Saturation functions use the saturations from the previous Newton iteration
   - Linear systems are decoupled in a straightforward way
2. Iterative IMPES Method [Young, Stephenson 1983]
   - Apply the IMPES technique inside the Newton iteration
   - The pressure unknown is obtained implicitly, which the other two explicitly
   - Linear systems to solved are just the pressure equations
3. Streamline-Based Method [Datta-Gupta, King 1995]
   - Exploit incompressibility and decouple the pressure and saturation calculations
   - Follow the streamline direction and reduce saturation calculation to 1D
   - Allow very large time stepsize for incompressible fluids
   - Difficult to apply to compressible fluids [Cheng, Osako, Datta-Gupta, King 2006]

[Chen, Huan, Ma 2006]

Simulation and Preconditioning

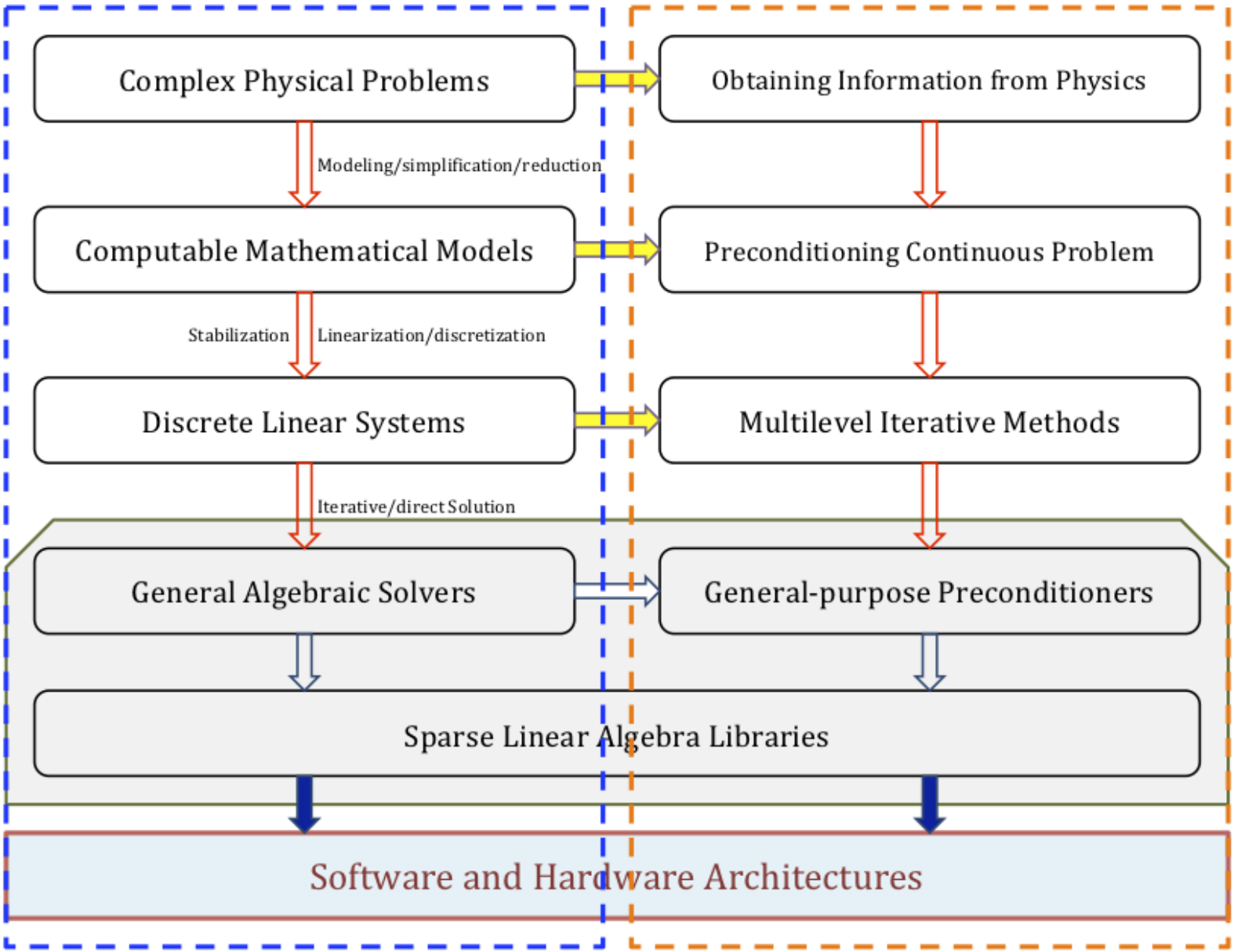

Decoupling, preconditioning, and iterative solvers

47 Linear Solution Methods for FIM

48 Multistage Preconditioners for FIM

49 Convergence and Robustness

50 Decoupling Strategies for FIM

51 Analytic Decoupling Methods: Basic Idea

52 Analytic Decoupling Methods: Matrix Form

53 Algebraic Decoupling Methods

54 Numerical Validation: Relation b/w D/B

55 Decoupling Strategies, Revisited

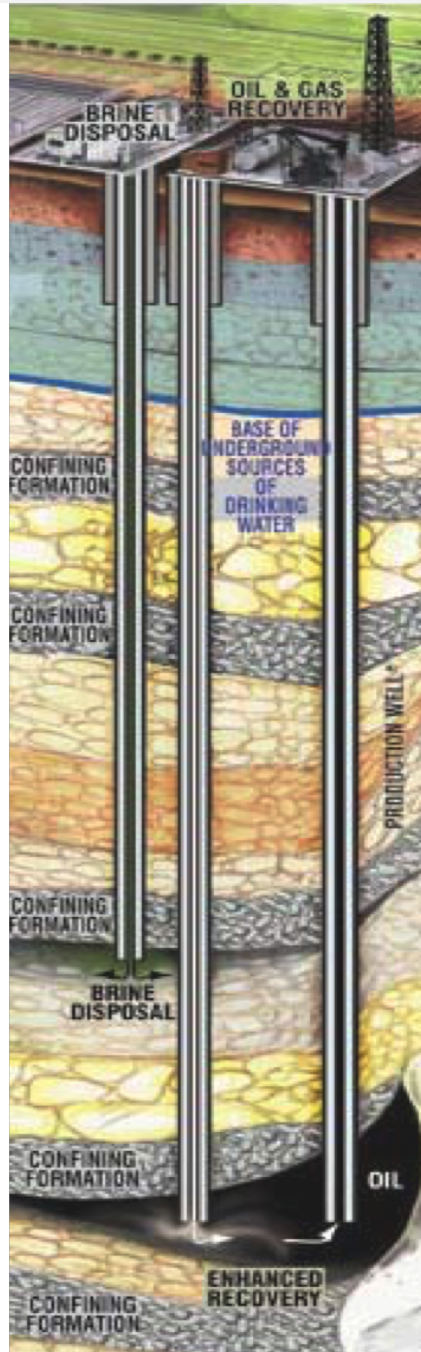

Linear Solution Methods for FIM

Now we consider linear algebraic solvers for the FIM discretization!

Solving the Jacobian system:

$$J\,u = r$$

1. Decoupling Step: Weaken the coupling between different physical variables

$$\tilde{J}\,u = \tilde{r}$$

where, in the decoupled Jacobian system, we have

$$\tilde{J} := DJ \quad \text{and} \quad \tilde{r} := Dr$$

2. Solution Step: Solving the preprocessed linear equation by a Krylov space method (e.g. GMRES or BiCGstab) with an efficient preconditioner

Difficulties in solving the Jacobian system:

- Fully-coupled, large, non-symmetric, ill-conditioned
- Usually takes more than 80% of the computing time
- Requires a robust iterative method and solver

Multistage Preconditioners for FIM

Define subspaces:

$$V = V_P + V_N$$

A two-stage preconditioner: Given u_0, $Bu_0 := u_2$, where

$$u_1 = u_0 + \Pi_P \tilde{J}_{PP}^{-1} \Pi_P^* (\tilde{r} - \tilde{J} u_0)$$

$$u_2 = u_1 + \Pi_N \tilde{J}_{NN}^{-1} \Pi_N^* (\tilde{r} - \tilde{J} u_1)$$

- Form subspaces according to physical properties
- Choose appropriate solvers for each subspace
- Example: CPR-type preconditioners [Wallis 1983]

- A decoupling stage is necessary before the solution stage
- Decouple different unknowns (P and N) effectively
- Obtain a reasonable pressure equation $\tilde{J}_{PP}$
- How to choose the decoupling (D) and preconditioning (B)?

[Hu, Xu, Z. 2013]

Convergence and Robustness

No	Name	Properties				Ecl100		HiSim	
		Model	# Total Cells	# Active Cells	Peroid (day)	Newton	Time (min)	Newton	Time (min)
1	SPE10-2	Two-phase	1122000	1094422	2000	——	——	295	41.82
2	SPE9-9k	Black-oil	9000	9000	900	339	0.12	269	0.20
3	SPE1	CO2 flooding	300	300	3656	536	0.04	445	0.08
4	SPE2	Three-phase coning	150	150	900	209	0.01	538	0.14
5	SPE10-3	Black-oil	1122000	1094422	2000	——	——	1462	354.12
6	SPE6	Dual porosity	100	100	7300	306	0.01	322	0.02
7	DPSP	Dual porosity	60984	40294	360	545	2.64	116	0.81
8	SPE7	Horizontal wells	488	488	1500	120	0.01	75	0.02
9	Voliatle	Extended black-oil	2100	2100	0.694			67	0.03
10	Zaoyuan	Field test (black-oil)	417480	143786	10653	3302	105.49	5204	66.20
11	Jidong	Field test (black-oil)	335664	154598	10587	1091	139.69	161	4.41
12	Chengbei	Field test (black-oil)	1646500	585123	2191	1971	155.57	420	28.47
13	Daqing1	Field test (black-oil)	1453248	466913	15616	——	——	5227	338.00
14	Daqing2	Field test (black-oil)	847895	241474	15096	8562	92.46	3072	88.05
15	SPE10-10M	Two-phase (large-scale)	11220000	10944220	2000	——	——	592	962.12
16	SPE9-9M	Black-oil (large-scale)	9000000	9000000	900	——	——	2460	10932.81

Tested by the Research Institute of Petroleum Exploration and Development, PetroChina (2015): Dell E5-2690 v2 CPU@3.0GHz, 200GB DDR3, Windows 7/VS2010/Intel Fortran Compiler 2015, HiSim 2.0, ECL 2012

Decoupling Strategies for FIM

Formal (semi-discrete) Jacobian matrix

$$J = \frac{1}{\Delta t}\begin{bmatrix} V_P^{\text{pore}} - V_P^{\text{fluid}} & -V_1^{\text{fluid}} & \cdots & -V_{n_c}^{\text{fluid}} \\ 0 & 1 & & \\ \vdots & & \ddots & \\ 0 & & & 1 \end{bmatrix} \longleftarrow A$$

$$+ \begin{bmatrix} 0 & 0 & \cdots & 0 \\ -\nabla\cdot(T_1\nabla\circ) - \nabla\cdot(\vec{\beta}_{1P}\circ) & -\nabla\cdot(\vec{\beta}_{11}\circ) & \cdots & -\nabla\cdot(\vec{\beta}_{1n_c}\circ) \\ \vdots & \vdots & \ddots & \vdots \\ -\nabla\cdot(T_{n_c}\nabla\circ) - \nabla\cdot(\vec{\beta}_{n_cP}\circ) & -\nabla\cdot(\vec{\beta}_{n_c1}\circ) & \cdots & -\nabla\cdot(\vec{\beta}_{n_cn_c}\circ) \end{bmatrix} \longleftarrow F$$

Decoupling methods [Lacroix, Vassilevski, Wheeler, 2001; ...]

$$\tilde{J} = DJ = \begin{bmatrix} \tilde{J}_{PP} & \tilde{J}_{PN} \\ \tilde{J}_{NP} & \tilde{J}_{NN} \end{bmatrix}$$

- Cheap to apply and give an easy-to-solve pressure equation
- Make $\tilde{J}_{PN}$ (sometimes $\tilde{J}_{NP}$ as well) not dominant

☞ Limiting behavior: $I - B\tilde{J}$ reduces to 0 as $\Delta t \to 0$, which is invalid for J

Analytic Decoupling Methods: Basic Idea

Decoupling at the PDE level:

$$\tilde{J}_{ANL} = \frac{1}{\Delta t}\begin{pmatrix} \alpha_P & 0 & \dots & 0 \\ 0 & 1 & \dots & 0 \\ \vdots & \vdots & \ddots & \vdots \\ 0 & 0 & \dots & 1 \end{pmatrix}$$

$$+\begin{pmatrix} -\nabla\cdot(\tilde{T}\nabla\circ)+\vec{\beta}_1\cdot(\nabla\circ)-\sum_{i=1}^{n_c}V_{ti}\nabla\cdot(\vec{\beta}_{iP}\circ) & -\sum_i V_{ti}\nabla\cdot(\vec{\beta}_{i1}\circ) & \dots & -\sum_i V_{ti}\nabla\cdot(\vec{\beta}_{in_c}\circ) \\ -\nabla\cdot(T_1\nabla\circ)-\nabla\cdot(\vec{\beta}_{1P}\circ) & -\nabla\cdot(\vec{\beta}_{11}\circ) & \dots & -\nabla\cdot(\vec{\beta}_{1n_c}\circ) \\ \vdots & \vdots & \ddots & \vdots \\ -\nabla\cdot(T_{n_c}\nabla\circ)-\nabla\cdot(\vec{\beta}_{n_cP}\circ) & -\nabla\cdot(\vec{\beta}_{n_c1}\circ) & \dots & -\nabla\cdot(\vec{\beta}_{n_cn_c}\circ) \end{pmatrix}$$

where $\alpha_P, \vec{\beta}_1, \vec{\beta}_{ik}, \vec{\beta}_{iP}$ are knowns.

- We know the underlying equations we are solving
- A multigrid-type solver friendly system can be formed
- Becomes diagonally dominant as Δt goes to 0

Analytic Decoupling Methods: Matrix Form

Decoupling in matrix form:

Consider the decomposition $J = A + F$. Let

$$A := \frac{1}{\Delta t}\begin{bmatrix} A_{PP} & A_{PN} \\ A_{NP} & A_{NN} \end{bmatrix} \quad \text{and} \quad D^{\text{ANL}} := \begin{bmatrix} I & X \\ 0 & I \end{bmatrix}$$

such that

$$D^{\text{ANL}}A = \frac{1}{\Delta t}\begin{bmatrix} \tilde{A}_{PP} & 0 \\ A_{NP} & A_{NN} \end{bmatrix} \Longrightarrow \tilde{J} = D^{\text{ANL}}J = \frac{1}{\Delta t}\begin{bmatrix} V_P^{\text{pore}} - V_P^{\text{fluid}} & 0 \\ 0 & I \end{bmatrix} + \cdots$$

General comments and advantages

☞ The coefficient matrix A is in a very special form

- Closely related to the IMPES discretization (eliminate N-terms)
- Black oil model $\Longrightarrow$ True-IMPES decoupling method [Coats 1999]
- Giving "good" pressure equations that work well with multigrid
- We have $I - B\tilde{J} \to 0$ as $\Delta t \to 0$

Algebraic Decoupling Methods

- Alternate Block Factorization [Bank-Chan-Coughran-Smith 1989; Klie 1997]:

$$D^{\text{ABF}} := \begin{bmatrix} \text{diag}(J_{PP}) & \text{diag}(J_{PN}) \\ \text{diag}(J_{NP}) & \text{diag}(J_{NN}) \end{bmatrix}^{-1}$$

☞ Eigenvalues clustered around 1, but the pressure equations difficult to solve

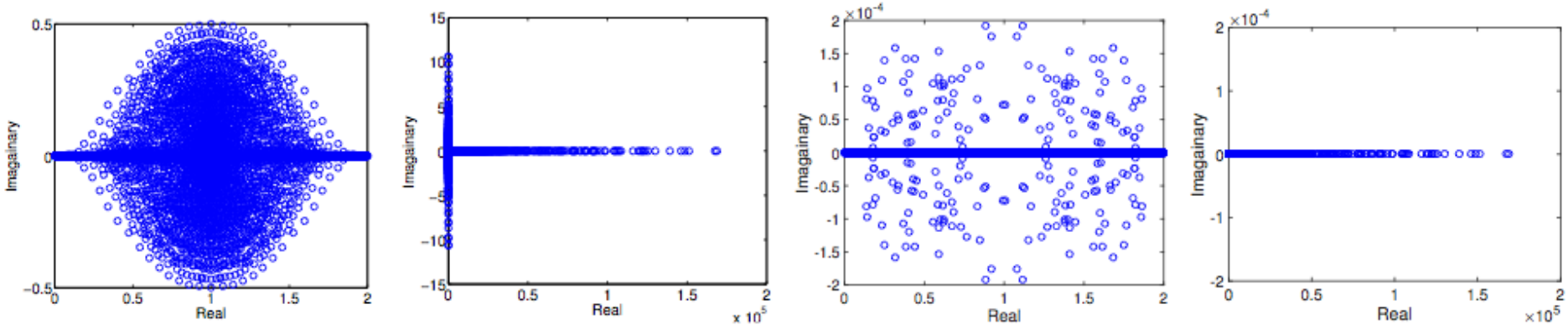

(a) $\tilde{J}^{\text{ABF}}$ (b) $\tilde{J}^{\text{ANL}}$ (c) $\tilde{J}^{\text{ABF}}_{PP}$ (d) $\tilde{J}^{\text{ANL}}_{PP}$

- There are several algebraic decoupling methods (Householder, Quasi-IMPES, CPR, ...) that are equiv. to ABF up to a scaling
- More stable and take less iterations if the pressure is approximated well

[Qiao, Wu, Xu, Z. 2017]

Numerical Validation: Relation b/w D/B

Pressure equations from ABF are difficult for AMG $\Longrightarrow$ Different solvers

Comparison of two preconditioners

- ☞ Method-I: Use one AMG V-cycle as a pressure solver
- ☞ Method-Ⅱ: Use AMG preconditioned GMRES as a pressure solver

No	Model	DAYS	GRID
1	Black-oil	900	9026
2	Black-oil	900	900026
3	Black-oil	15096	241474
4	Black-oil	15096	241471
5	Black-oil	15616	466913
6	Black-oil	10653	143786
7	Black-oil	9100	46825
8	Black-oil	11868	46574
9	Two-phase	5233	45156
10	Two-phase	4408	208842
11	Two-phase	21427	89339
12	Two-phase	2000	1094422
13	Two-phase	2000	10944220
14	Two-phase	19753	89048
15	Two-phase	708	51623
16	Two-phase	1825	104013

Speedup of Method-I / Method-Ⅱ (wall time)

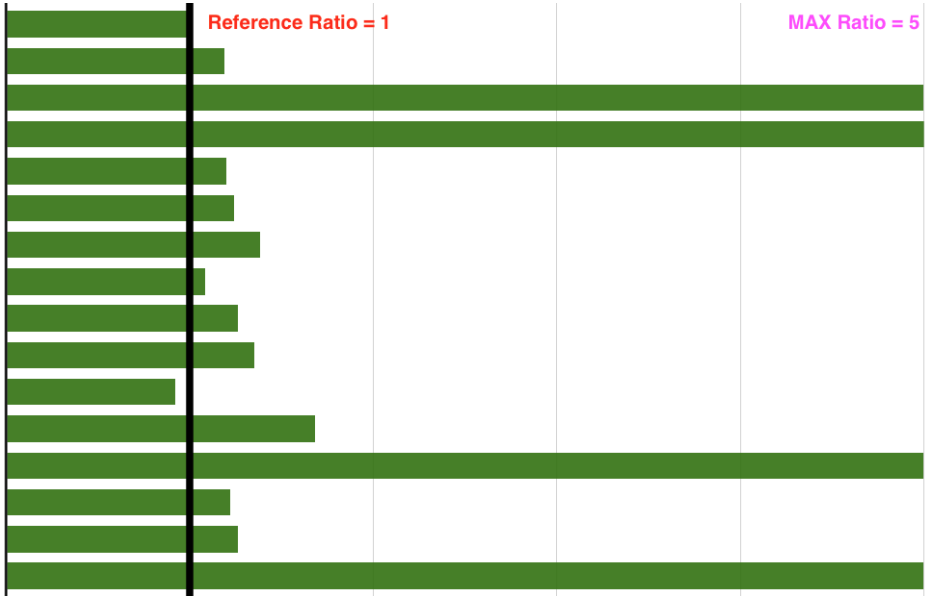

[Li, Wu, Z., et al. 2017]

Decoupling Strategies, Revisited

How to take advantages of both strategies?

- Combine analytical and algebraic decouplings?
  - Relatively cheap to compute
  - Obtain an easy-to-solve pressure equation
  - Improve (at least maintain) performance of outer iterations
  - Keep the asymptotic behavior $I - B\tilde{J} \to 0$ as $\Delta t \to 0$
- A semi-analytical decoupling method: [Qiao, Wu, Xu, Z. 2017]

$$D^{\text{SEM}} := \begin{bmatrix} D_{PP}^{\text{ANL}} & D_{PN}^{\text{ANL}} \\ D_{NP}^{\text{ABF}} & D_{NN}^{\text{ABF}} \end{bmatrix}$$

Some numerical results

Simulator performance for SPE10. Simulation period 2000 days.

Method	Time steps	Nonlinear iterations	Linear iterations	AMG iterations	Linear solver time (s)
ABF	60	352	2505	37235	7756
Analytical	57	332	2209	16212	3149
Semi-analytical	56	320	1338	13813	2464

Using PennSim and FASP to solve SPE10 in compositional formulation

Development of petroleum reservoir simulator

56 Solution Algorithm Flow Chart

57 Software Structure of PennSim

58 FASP Software Project

59 Numerical Validation: SPE 1

60 Numerical Validation: Field Test

61 Field Test: Polymer Flooding

62 Benchmark Test: SPE10

63 Strong Scaling Tests on Tianhe-2

64 Weak Scaling Tests on Tianhe-2

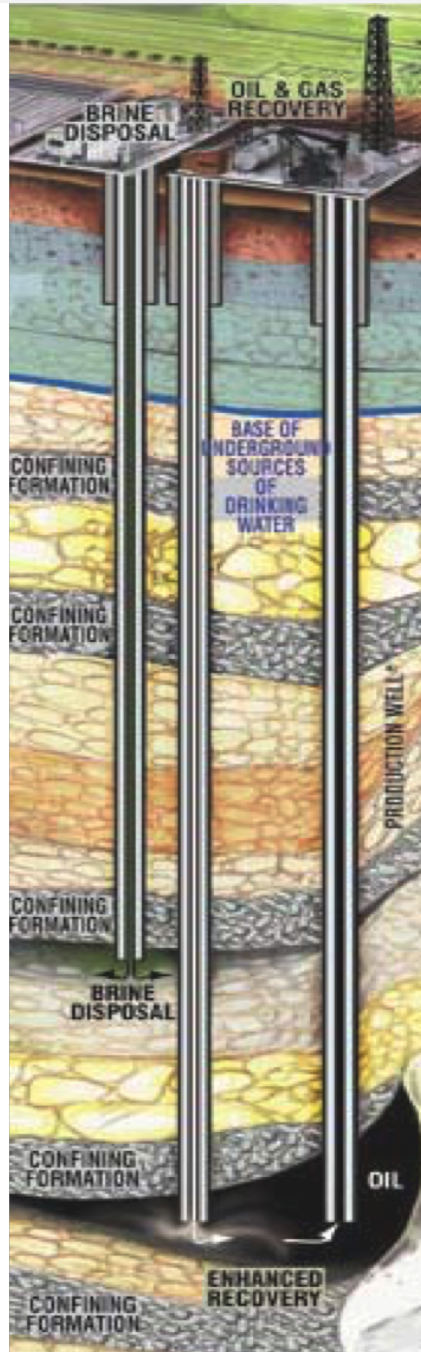

Solution Algorithm Flow Chart

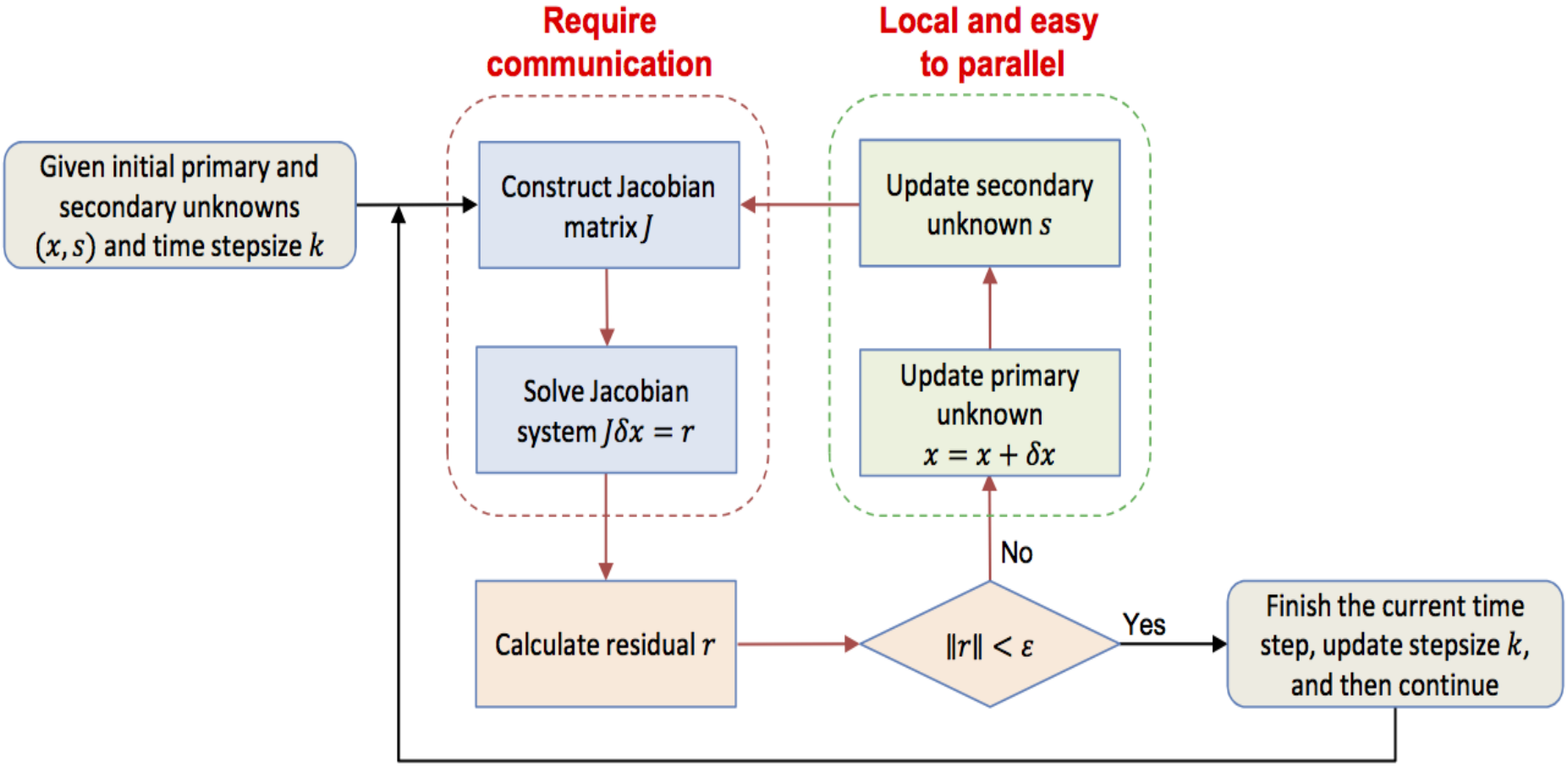

Need a scalable parallel linear algebraic solver to make it work!

[Guan, Qiao, Zhang, et al. 2015]

Software Structure of PennSim

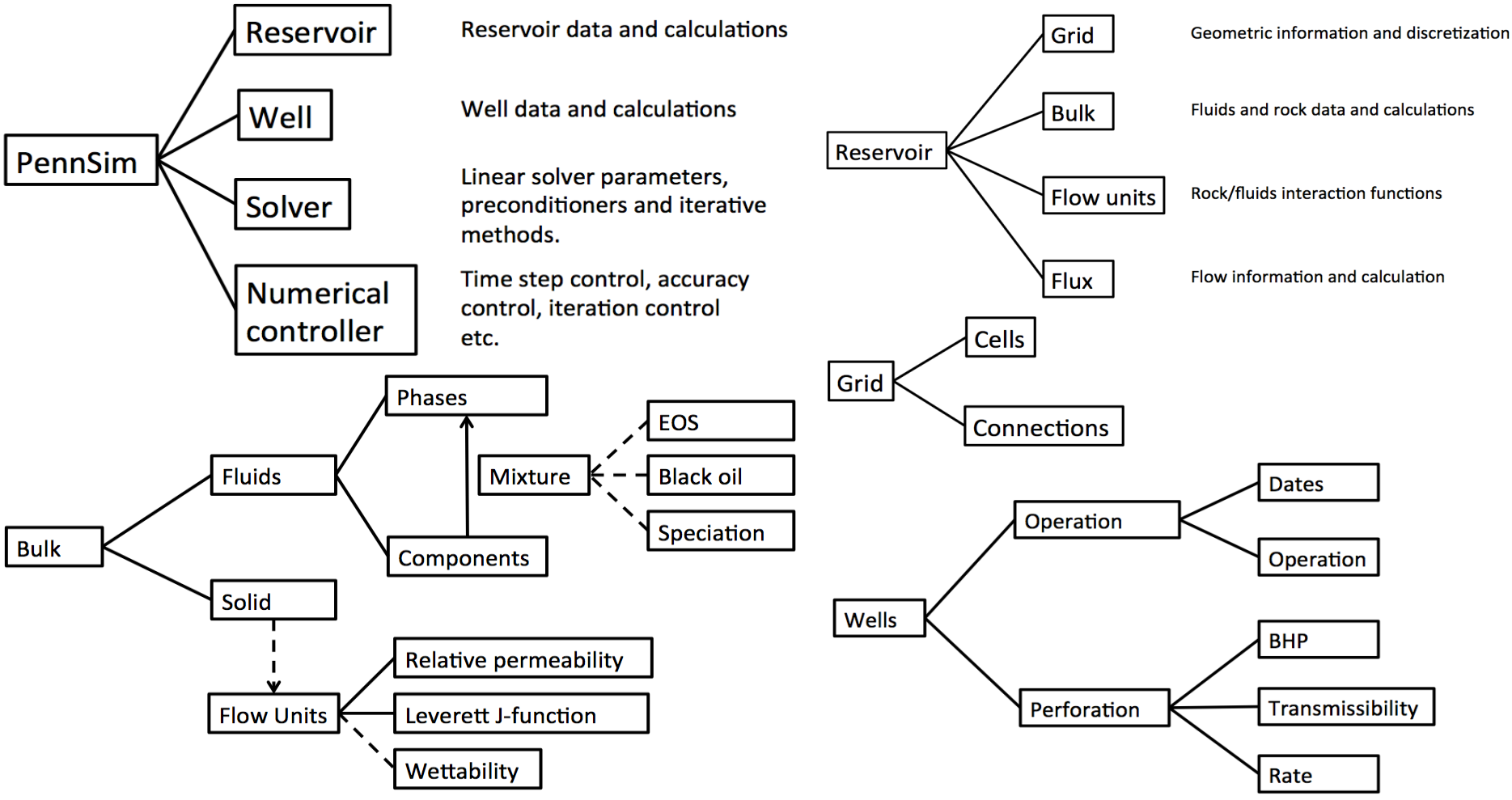

Range: Developer ⇒ Team ⇒ Local ⇒ Widespread ⇒ General public

[Qiao 2016, PhD Thesis]

FASP Software Project

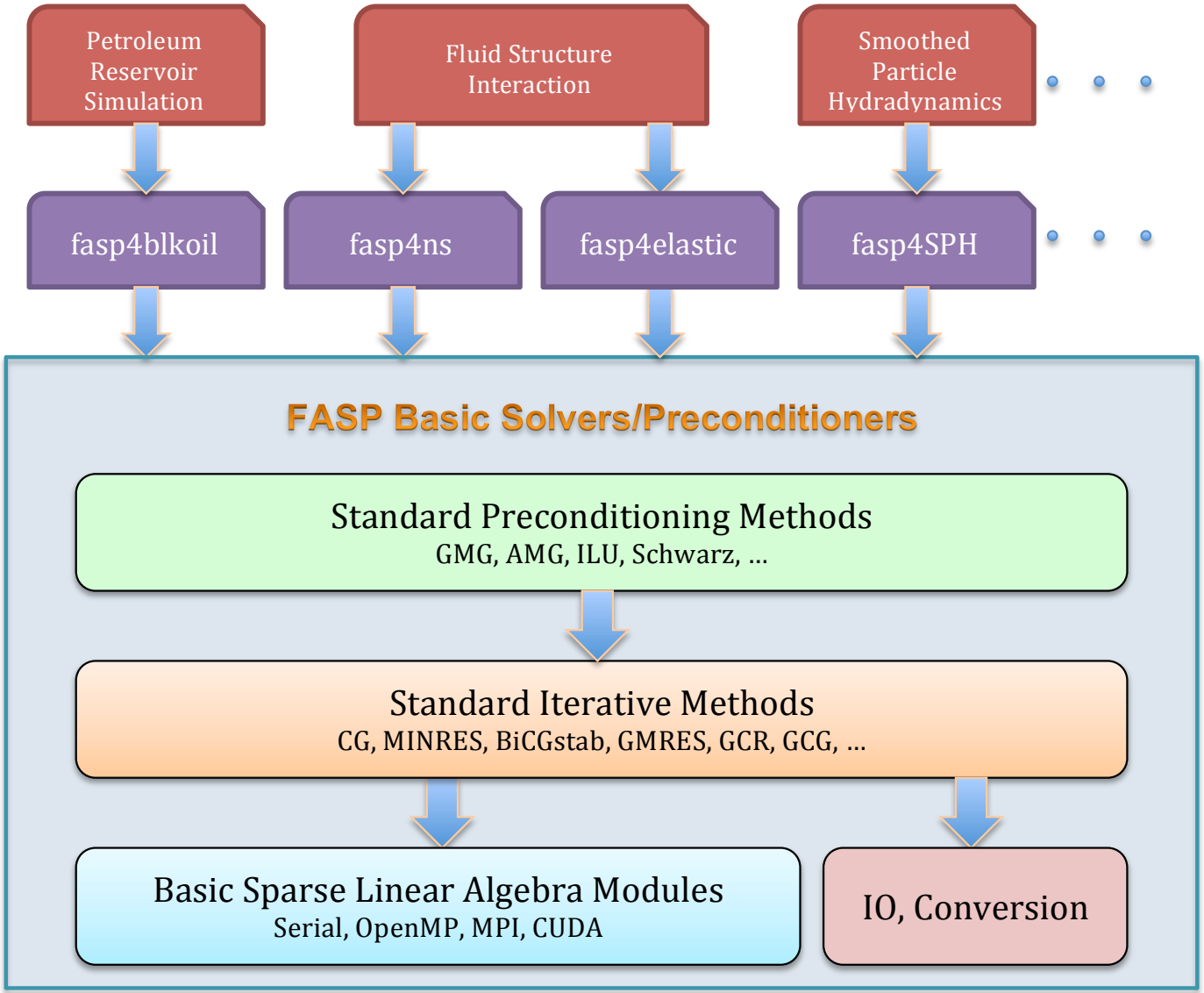

Supported by NSF DMS-0915153 and NSFC 91130011. http://www.multigrid.org/fasp

Numerical Validation: SPE 1

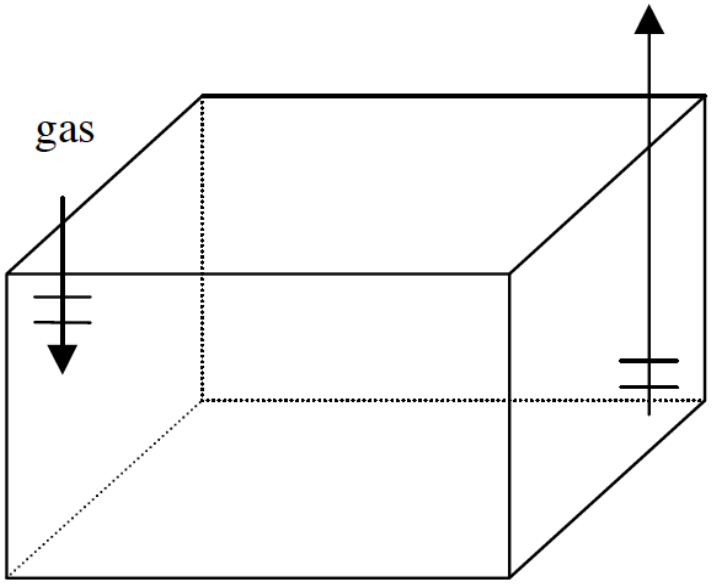

Figure: SPE 1 benchmark

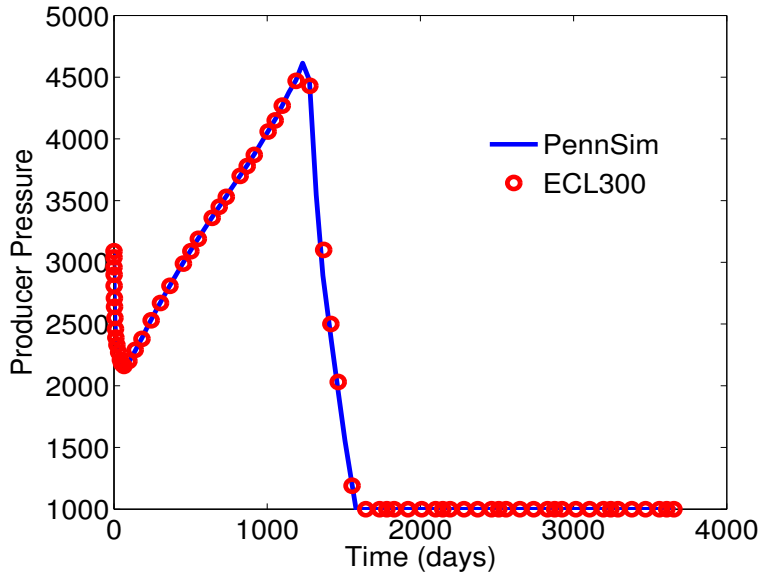

Figure: Producer pressure

- Three dimensional, three-phase, gas injection
- Adaptive time stepping strategies are applied for both IMPES and FIM
- IMPEC: 3815 time steps, 4.0 seconds
- FIM: 75 time steps, 0.76 seconds

FIM discretization is much more stable, but requires a good solver!

Numerical Validation: Field Test

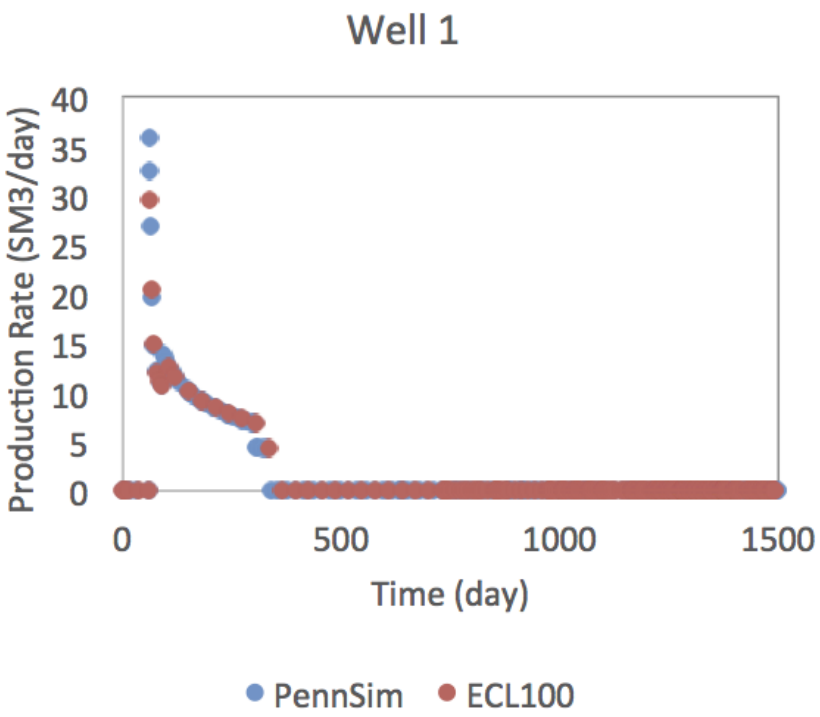

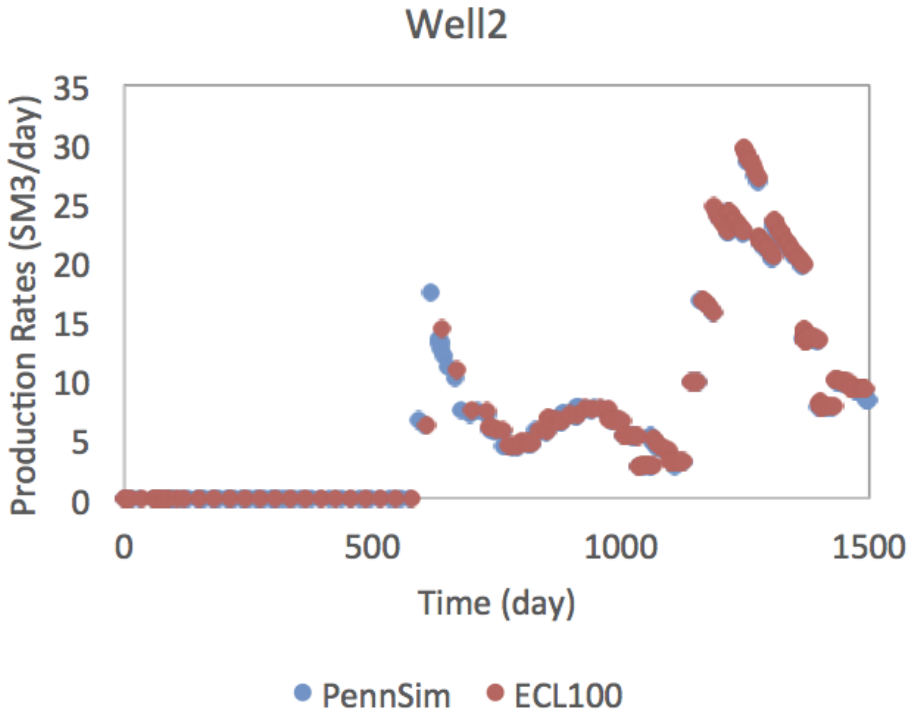

- Real data from an European field (60K corner-point grid)
- Qualitatively matches the results of commercial software
- Simulate five-year period (PennSim≈3hr, ECL100≈6hr)
- Cost only half of the CPU time compared with ECL100

Field Test: Polymer Flooding

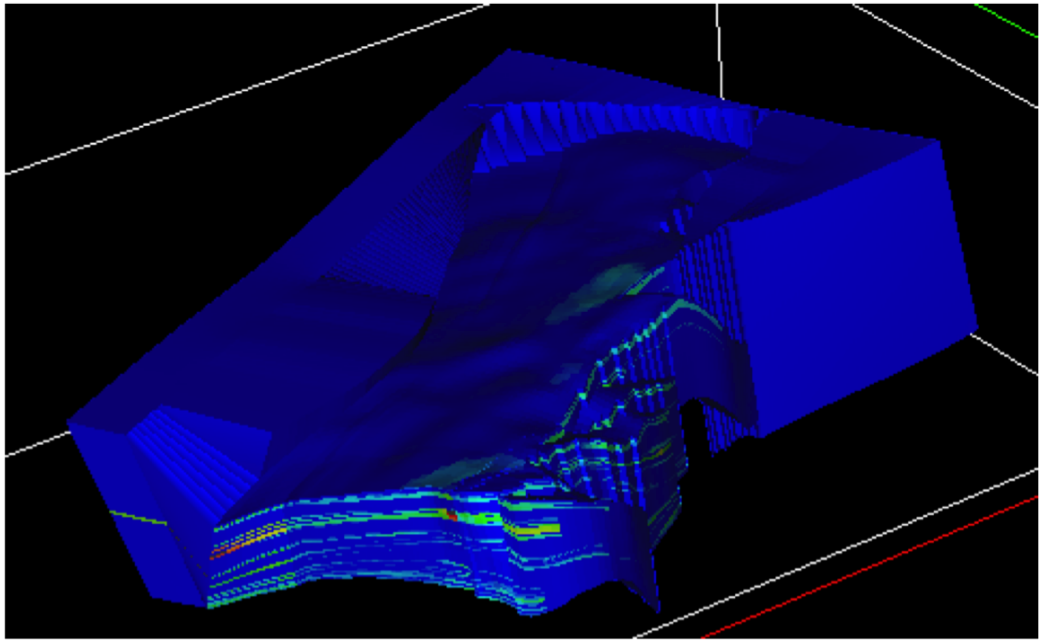

- Tested by CNOOC 2011
- Polymer flooding
- Number of grids: $157 \times 53 \times 57$
- Several geological faults
- 37 wells (peak)
- 7 years of water flooding
- 3 years of polymer flooding

Simulator	# Newton Iter.	Total CPU time	CPU time/Newton
ECL100	1562	81.0 (min)	3.11 (sec)
SOCF	1653	40.0 (min)	1.45 (sec)

Table: Tested by CNOOC, using FASP as its solver.

Benchmark Test: SPE10

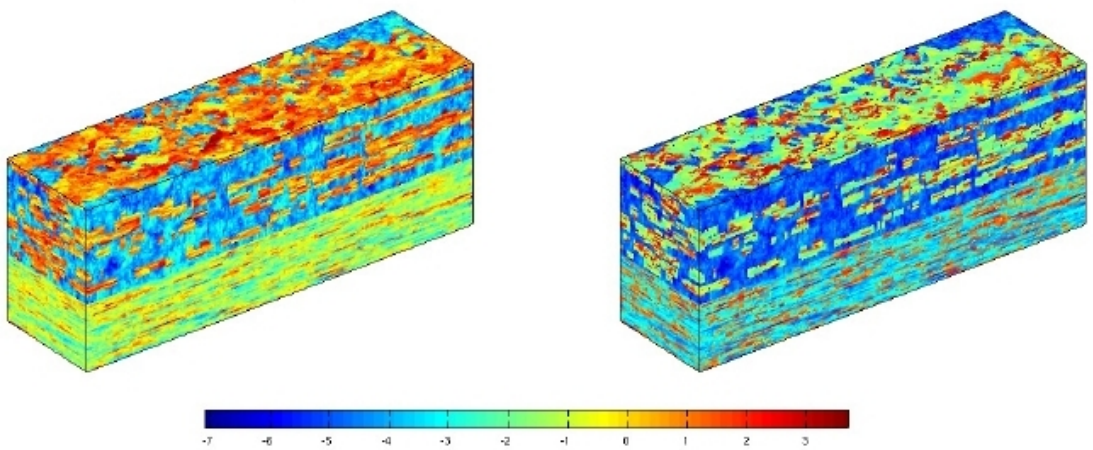

- A benchmark for upscaling
- Two phase (water and oil)
- Number of grids: 1.1 M
- One injector, four producers
- Total simulation time: 2000 days

Simulator	ECL100	tNavigator	MURS	HiSim	HiSim (P100)
Wall Time	100+ hr	18 hr	29 hr	40 min	6 min

- Tested by PetroChina 2012
- SLB claimed: ECL300 8-node cluster 2.8GHz CPU, 5 hr
- Average wall-time for each Jacobian system is 6s on one CPU core
- Modify SPE10 to three-phase black-oil: HiSim+FASP takes 4 hr

Strong Scaling Tests on Tianhe-2

Problem	Size	# Nodes	# Processes	Efficiency	Total time (s)	Solver time(s)	# Newton	# Linear
SPE1-refine	75M cells	40	960		888	583.205	76	614
		60	1440	94%	631	425.531	76	631
		80	1920	89%	497	341.551	76	688
		100	2400	68%	520	367.979	87	958
SPE1-refine	150M cells	80	1920		1294	899.789	81	884
		100	2400	118%	878	609.921	82	818
		120	2880	108%	802	566.173	84	860
		160	3840	95%	678	472.916	92	907
		200	4800	84%	614	438.111	100	1095
SPE9-refine	90M cells	32	768		1953	1079.351	133	277
		128	3072	86%	567	307.249	148	525
		256	6144	64%	381	241.309	148	525

SPE1 and SPE9 benchmark problems first refined and then tilted. Tested on the Tianhe-2 cluster, Guangzhou: 1st in the Top500 list (June 2015), 3.12M cores (2 Xeon CPU's + 3 Xeon Phi's), Rmax 33.86PFlops, Rpeak 54.90PFlops, 1.408PB RAM, Peak Power 17.8MW. Upgraded version: Tianhe-2A, 4th in the Top500 list (Nov 2018).

[Guan, Qiao, Zhang, et al. 2015]

Weak Scaling Tests on Tianhe-2

# CPU Cores	24	48	96	192	384	768	1536
# Grid Block	3M	6M	12M	24M	48M	96M	192M
# Linear Iterations	723	724	726	727	723	725	715
Total CPU Time (s)	2741	2838	2846	2907	2711	2881	3026

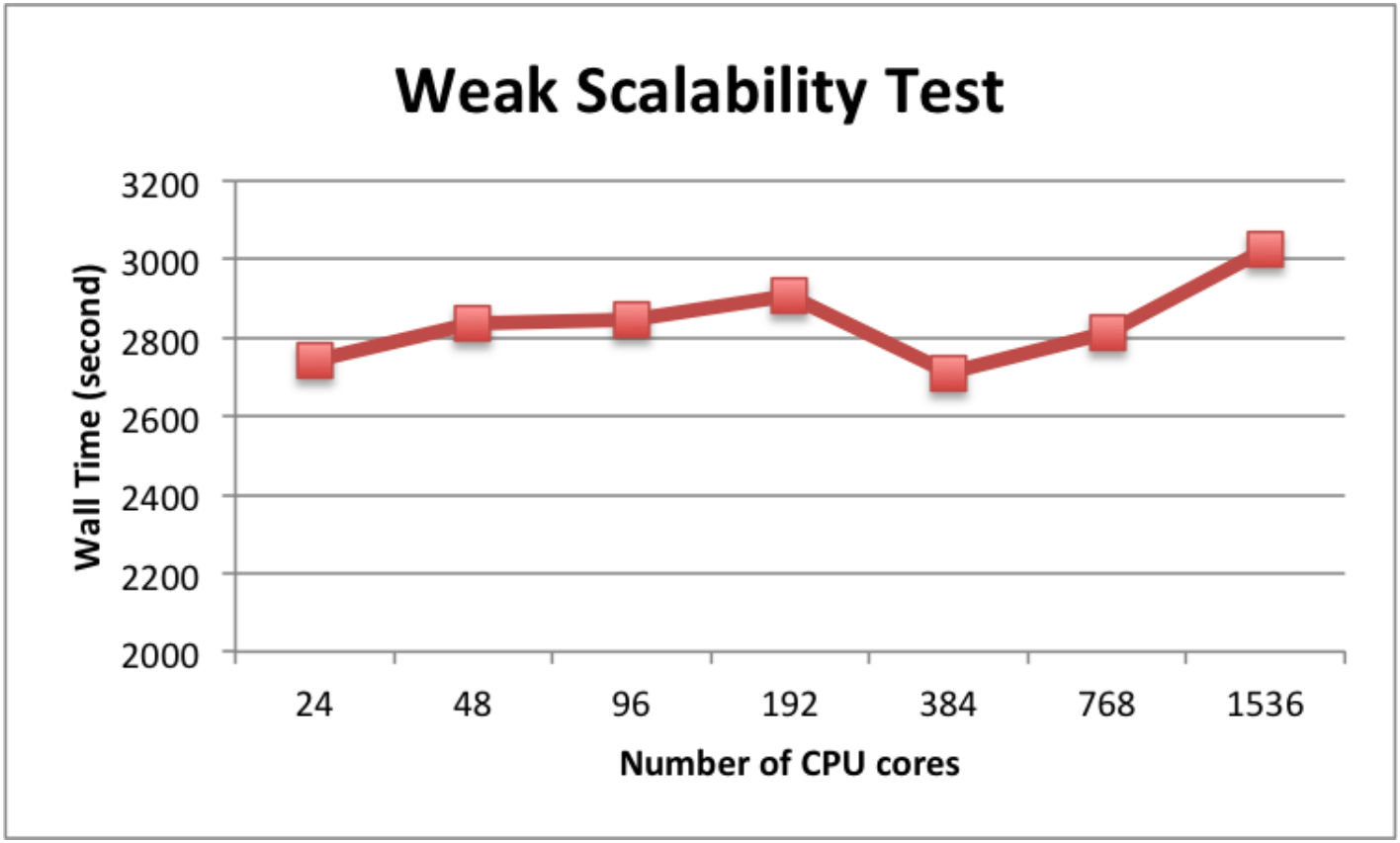

[Guan, Qiao, Zhang, et al. 2015]

Fluid-rock interaction in carbonate formation

65 Fluid-Rock Interaction

66 Geo-Mechanical Interaction

67 Darcy–Stokes–Brinkman Model

68 Reactive-Transport Model

69 Modeling Rock Property

70 Solving the Coupled Model

71 Numerical Validation

72 Effect of Porosity Heterogeneity

73 Evolution of Rock Porosity

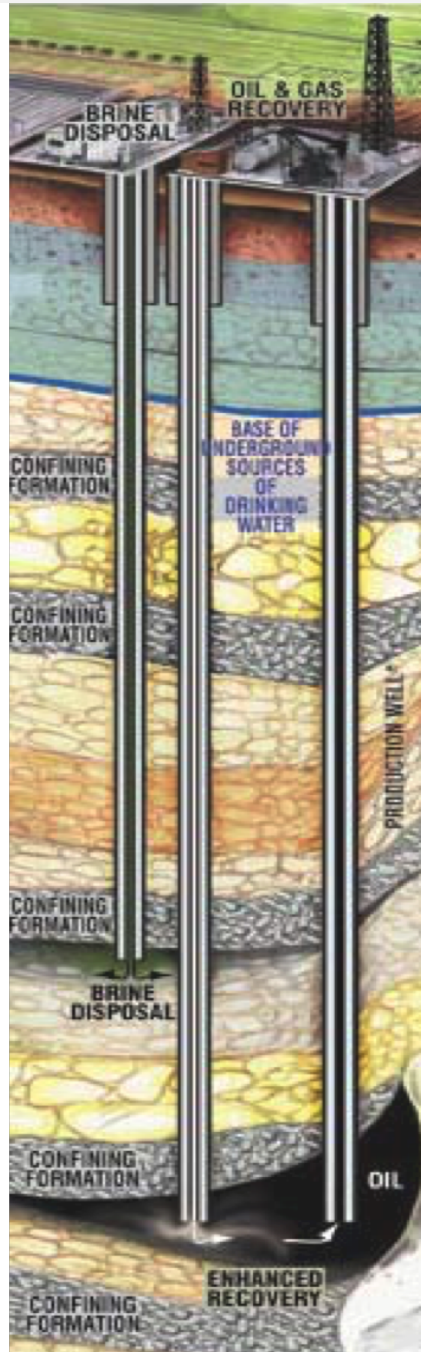

Fluid-Rock Interaction

Fluid and rock in carbonate formations

- Carbonate rocks undergo various chemical reactions with the injecting fluids
- This leads to evolution of fracture network $\Longrightarrow$ Bad predictions if ignored
  - Water flooding / polymer flooding
  - Geological CO_2 sequestration (GCS)
  - Matrix acidizing in carbonate formations

Main goals

- Simulating dynamic behavior of fracture evolution in carbonate reservoirs
- Coupling multiphase flow, chemical reactions, and geo-mechanical responses

So far, we have done:

1. Black oil and compositional model simulator (parallel), dual continuum model
2. An efficient linear solver/preconditioner based on FASP
3. Fluid-rock (chemical) interaction based a single-domain approach

Missing: Geo-mechanical response, energy equation, and coupling

Geo-Mechanical Interaction

Conventional approach: simple models

$$\begin{cases} \phi = \phi_0\big(1 + c_{_P}(p - p_0)\big) & \text{poro compressibility} \\ \rho = \rho_0\big(1 + c_{_F}(p - p_0)\big) & \text{fluid compressibility} \end{cases}$$

Why consider more complicated models: geo-mechanics / poroelasticity?

> Many applications require an understanding of the porous flow of fluids as well as rock stresses & displacements. Geo-mechanics can significantly influence reservoir engineers' predictions! [Settari, Mourits 1998]

Biot poroelasticity [Biot 1941]: stress-dependent flow simulation

$$\begin{cases} \dfrac{\partial}{\partial t}\left(\dfrac{p}{M} + b\varepsilon_v\right) - \dfrac{\kappa}{\mu}\nabla^2 p = Q_f, & \text{mass conservation} \\ K_s\Delta u + \left(K_d + \dfrac{K_s}{3}\right)\nabla(\nabla\cdot u) = b\nabla p, & \text{force balance} \end{cases}$$

M is the Biot modulus, b is the Biot stress coefficient, K_s is the rock shear modulus, K_d is the drained bulk modulus, and the volumetric strain $\varepsilon_v := \sum_i \varepsilon_{ii}$.

Remark: If assume no matrix deformation, then $\phi_0(c_{_P} + c_{_F})\frac{\partial}{\partial t}p - \frac{\kappa}{\mu}\nabla^2 p = Q_f$.

Darcy–Stokes–Brinkman Model

A single model with strongly discontinuous coefficients

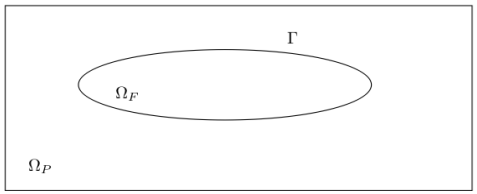

$$\begin{cases} -\nabla \cdot (\mu(x)\nabla \mathbf{u}) + \kappa^{-1}\,\mathbf{u} + \nabla p = \mathbf{f}, & \Omega, \\ \nabla \cdot \mathbf{u} = g, & \Omega, \\ \mathbf{u} = \mathbf{0}, & \partial\Omega. \end{cases}$$

- Single domain approach for both matrix and fractures [Brinkman 1947]
- Matrix domain: Small viscosity and transmissibility $\Longrightarrow$ Darcy
- Fracture domain: Large viscosity and transmissibility $\Longrightarrow$ Stokes
- Straightforward internal interface conditions (compared with Darcy–NS)
- Meshing is much easier, especially for evolving internal interfaces

Problems with the single-domain model

- How to give appropriate and accurate coefficients?
- Standard $H(\mathrm{div})$-conforming FEM not uniformly stable [Xie, Xu, Xue 2008]
- Linear solution becomes more difficult after discretization

Reactive-Transport Model

Chemical reactions and transport in carbonate reservoirs

- Processes of solute transport and chemical reactions [Steefel, Lasaga 1994]
- Mineral–water reactions: cannot reach an equilibrium state locally
- Aqueous reactions: rapid and local $\Longrightarrow$ formulated via the mass action law

A reactive-transport model for mineral-water interaction [Yuan, Ning, Qin 2016]

$$\frac{\partial}{\partial t}\left(\phi C_i^{\text{total}}\right) + \nabla \cdot \left(\mathbf{u} C_i^{\text{total}} - \mu \nabla C_i^{\text{total}}\right) = R_i^{\text{min}}, \qquad i = 1, \ldots, n_c$$

- n_c is the number of primary components
- C_i^{total} is the total concentration of the primary component i
- R_i^{min} is the sum of all mineral-water reactions of the primary component i
- R_i^{min} are nonlinear w.r.t. the molar concentrations of primary species

During mineral dissolution / precipitation, mineral volume also changes!

- R_i^{min} are also coupled with rock volume changes
- When pore volume changes, rock pemeabiltity also changes

[Reed 1982; Langmuir 1997; Lasaga 1998; Steefel 2009; Bundschuh, Ziberbrand 2012; ...]

Modeling Rock Property

Rock volume change

$$\phi := 1 - \sum_{m=1}^{n_m} \phi_m \quad \text{and} \quad \frac{d\phi_m}{dt} = V_m r_m$$

- ϕ is the rock porosity and there are n_m minerals
- ϕ_m is the volume fraction of an individual mineral m
- V_m is the molar volume of an individual mineral m
- r_m is the rate of precipitation/dissolution of mineral m per unit volume

Rock permeability change

- The Kozeny–Carman model ignoring changes in grain size is written

$$K := K_0 \left(\frac{1-\phi_0}{1-\phi}\right)^2 \left(\frac{\phi}{\phi_0}\right)^3,$$

  where K_0 and ϕ_0 are initial absolute permeability and porosity
- Many possible models to empirically predict absolute rock permeability

[Mavis, Wilsey 1936; Berg 1972; Ehrenberg et al. 2006; ...]

Solving the Coupled Model

A decoupled numerical algorithm [Yuan, Wei, Z., Qin 2019]

- Implicit time-stepping and decoupled Newton iteration
- MAC for the Brinkman equation
- FDM for the reactive-transport equation
- FASP solvers for the discrete linear systems
- In both Cartesian and cylindrical coordinates

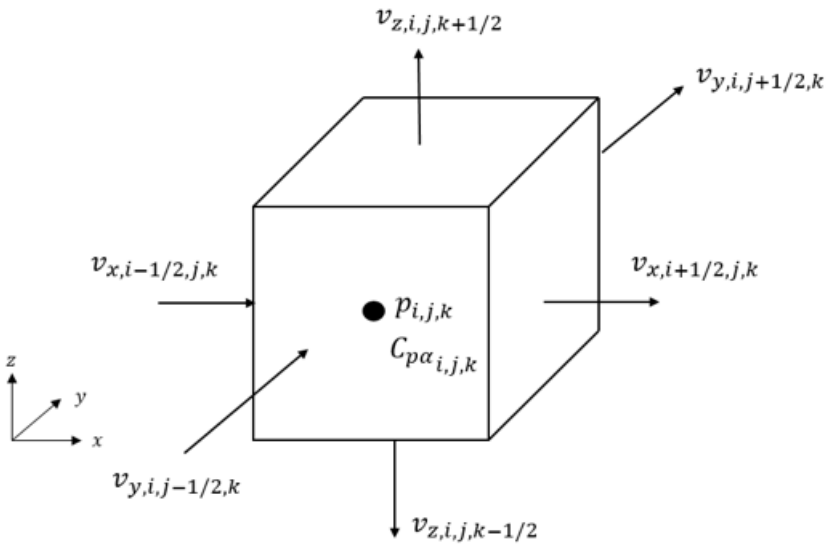

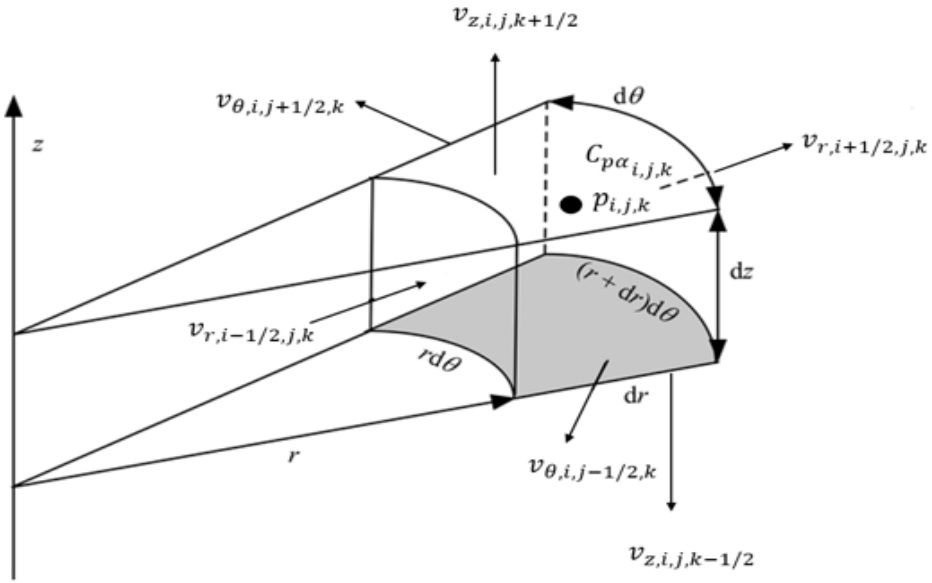

This decoupled algorithm is only a proof-of-concept for the coupled model!

Numerical Validation

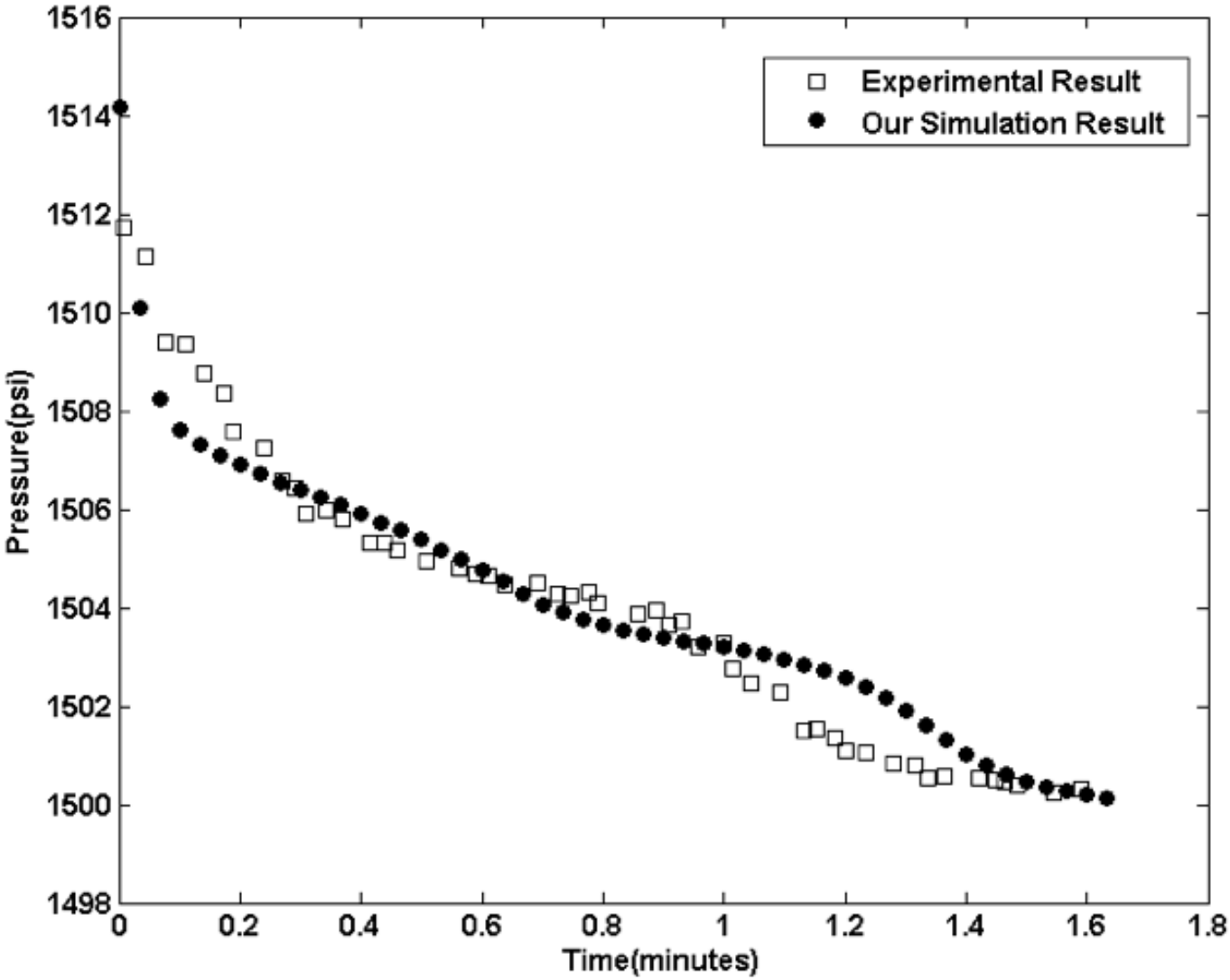

Pressure at the inlet during acid injection [Tardy, Lecerf, Christanti 2007]

Effect of Porosity Heterogeneity

Table 1 Initial and injected concentrations of aqueous species

	$Ca^{2+(a)}$	$Na^{+(a)}$	$Al^{3+(a)}$	$SiO_2^{(a)}$	pH
Initial Condition (mol/L)	6.05×10^{-4}	1.38×10^{-4}	2.93×10^{-6}	7.38×10^{-5}	7
Injected CO_2-saturated brine (mol/L)	1.57×10^{-2}	1.03	4.08×10^{-7}	1.21×10^{-6}	3

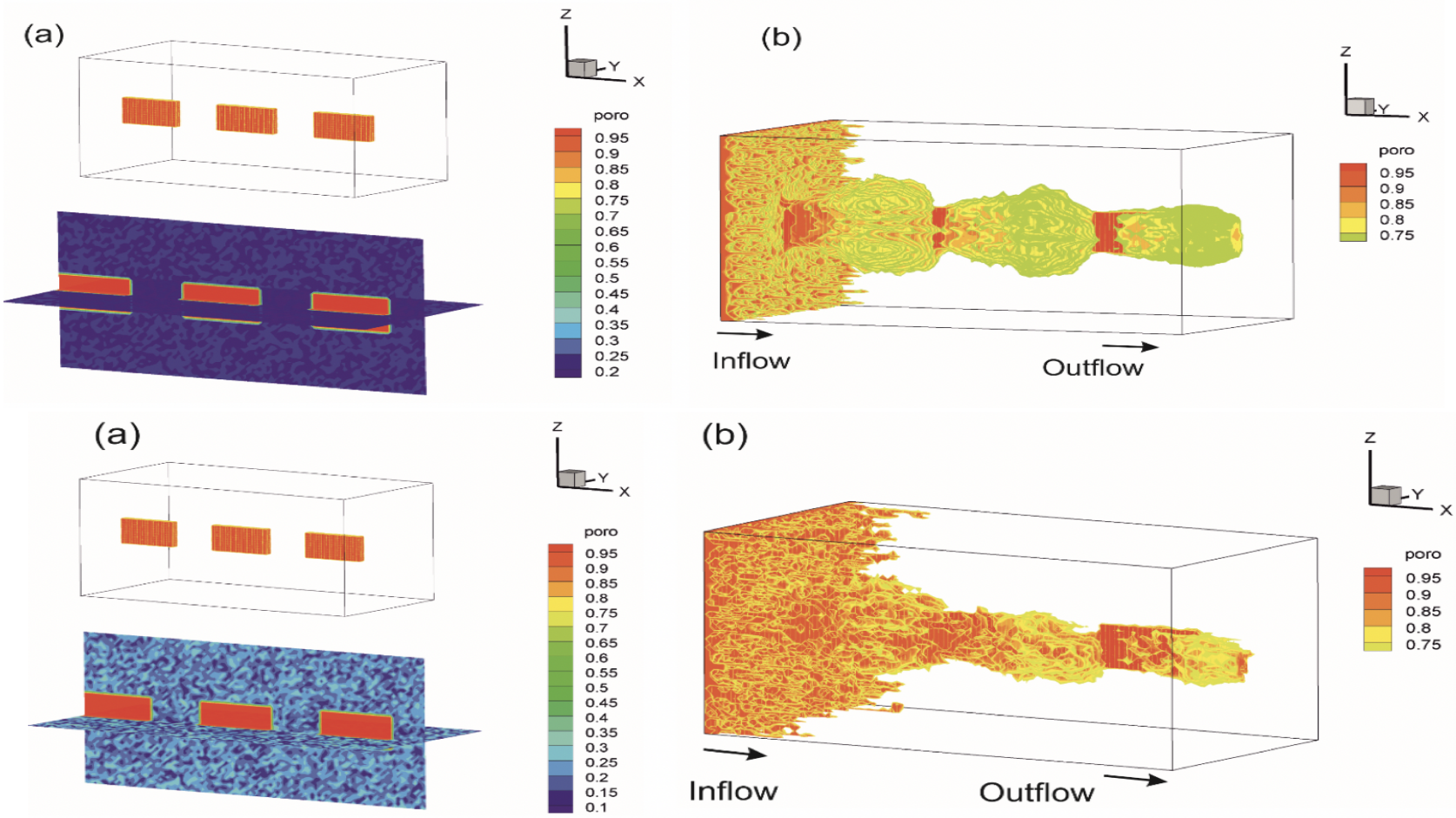

Porosity profile of fractured rock of the dominant wormhole

Evolution of Rock Porosity

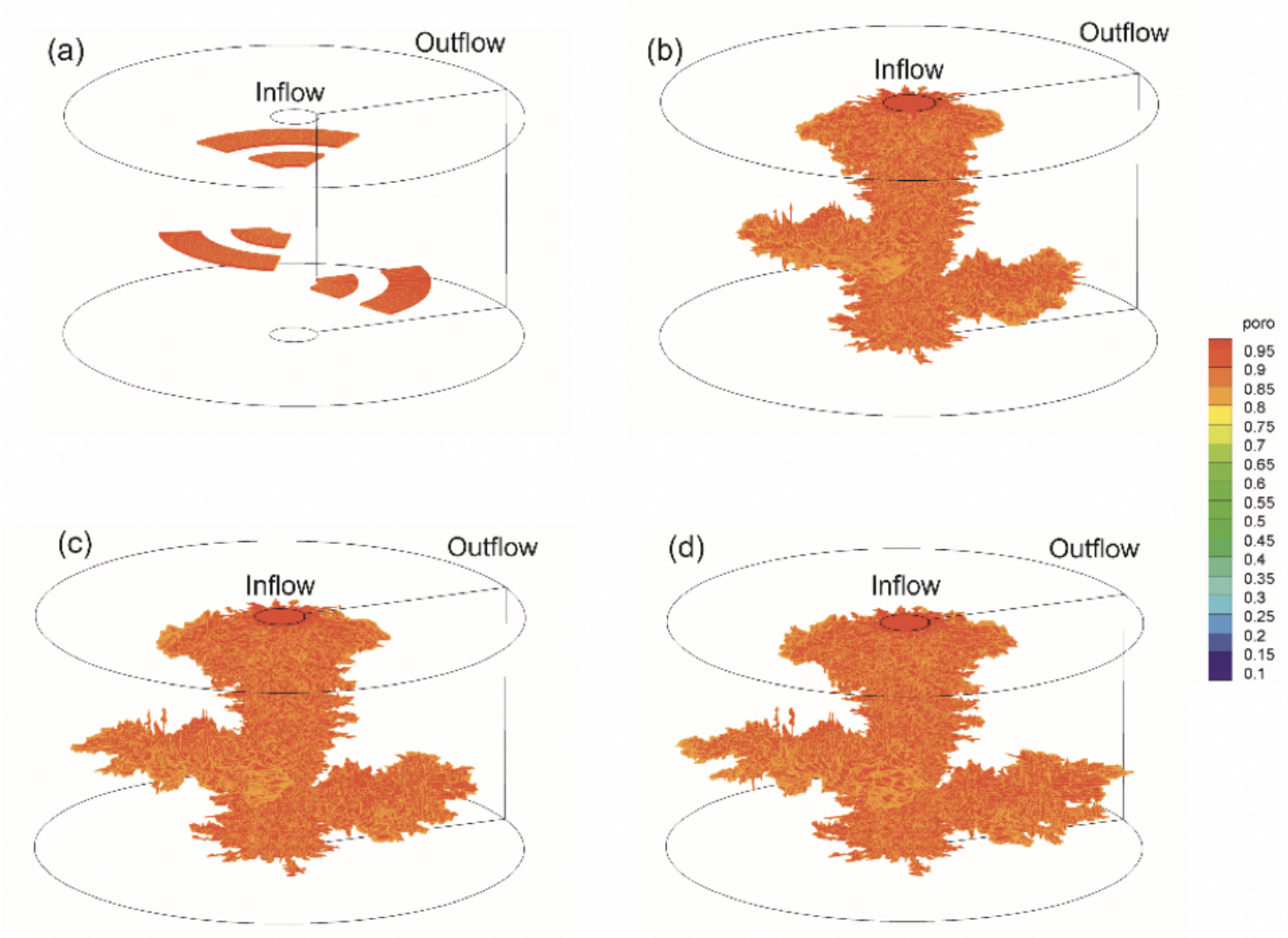

Porosity profiles at different injection time: (a) initial time, (b) 14.4 minutes, (c) 28.8 minutes, (d) 47.4 minutes (water breakthrough time)

Managing uncertainty and improve reliability

74 Quantifying Uncertainty

75 Forward UQ: Uncertainty Propagation

76 Sources of Uncertainty in Simulation

77 History Matching in Reservoir Simulation

78 History Matching Methods

79 Surrogate Models

80 Surrogate Models with Deep Learning

81 So... Problem Solved?

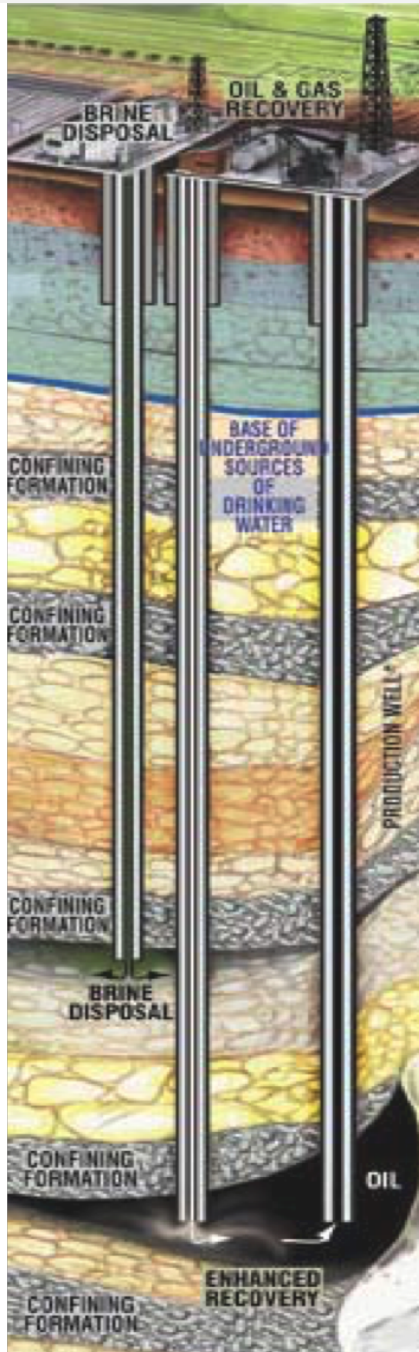

Quantifying Uncertainty

Uncertainty v.s. Error

- Lack of knowledge? Types: aleatoric (statistical) and epistemic (systematic)
- Sources of uncertainty: model, measurements, initial/boundary conditions
- "All models are wrong, but some are useful" [George Box 1976] $\Longrightarrow$ V&V
- Where does uncertainty make a big difference (compared with error)?

Uncertainty quantification: SIAM/ASA-joint conference on UQ 2012

- Predict model responses with quantified and reduced uncertainties
  - Identification and characterization
  - ☞ Forward propagation (UP): MC, Surrogate model, ...
  - Inverse propagation
  - Sensitivity analysis
- Difficulties when applied in petroleum reservoir simulation
  - In practice: curse of dimensionality
  - Identifiability: Combinations of uncertainties might yield same prediction
  - "... an uncertain input parameter will lead not only to an uncertain solution but to an uncertain error ..." [Trucano 2004]

Forward UQ: Uncertainty Propagation

Model problem and uncertainty propagation using PCE

$$y = \mathcal{F}(x) \implies Y = \mathcal{F}(X), \text{ where } X \text{ is a random variable}$$

- Polynomial Chaos Expansion: represent the random variable of interest as a polynomial expansion of another random variable ξ with distribution ρ
- $\{\psi_j\}$ are the orthogonal polynomials w.r.t. $(\cdot,\cdot)_\rho$
  - We have $\psi_0 = 1$ and $E(\psi_j) = 0$, $j = 1, 2, \ldots$
  - Variance of ψ_j is $(\psi_j, \psi_j)_\rho$ and covariance $(\psi_i, \psi_j)_\rho = 0$ if $i \neq j$
  - A few possible choices, for example:
    Uniform $[-1, 1] \Rightarrow$ Legendre; Gamma $[0, \infty) \Rightarrow$ Laguerre; Normal $\Rightarrow$ Hermite

Non-intrusive UP with PCE

- Suppose $X \approx \sum_{j=0}^{m} x_j \psi_j(\xi)$ and $Y \approx \sum_{j=0}^{m} y_j \psi_j(\xi)$
- $\sum_{j=0}^{m} y_j \psi_j(\xi) = \mathcal{F}\big(\sum_{j=0}^{m} x_j \psi_j(\xi)\big) \implies y_k = \dfrac{\big(\mathcal{F}\big(\sum_{j=0}^{m} x_j \psi_j(\xi)\big), \psi_k\big)_\rho}{(\psi_k, \psi_k)_\rho}$
- Need to compute the integral: $\int_\Omega \mathcal{F}(\sum_{j=0}^{m} x_j \psi_j(\xi)) \psi_k(\xi) \rho(\xi)\, d\xi$

Sources of Uncertainty in Simulation

What we know about subsurface rock and fluid in formation is very limited

Heterogeneity and Multiscale Behavior

- Accurate information is very limited and localized
- Difficult to obtain accurate information of reservoir formation
- Lab experiments and simulation are in rather small scale
- Field-scale simulation have nothing to use other than lab-scale results

Physical Complexity

- Initial and boundary conditions
- Different constitutive laws can be tried for different cases
- Multiple constitutive laws might be needed even in one case
  - Porous media flow models: Darcy, nonlinear Darcy, ...
  - Free flow models for large fractures, vugs, ...

Competing Objectives: economics, human, risk, environment, ...

Decision variables: volumes, rate and time of extraction, fluid movement

History Matching in Reservoir Simulation

HM is a process that integrates a static model with dynamic data to obtain a more accurate model for predicting reservoir performance

2D test (mesh size 100×12) [Tavassoli, Carter, King 2004]

- Three parameters: low perm $[0, 50]$, high perm $[100, 200]$, fault throw $[0, 60]$
- Three years of HM (using 160K random sampling) and one year for prediction

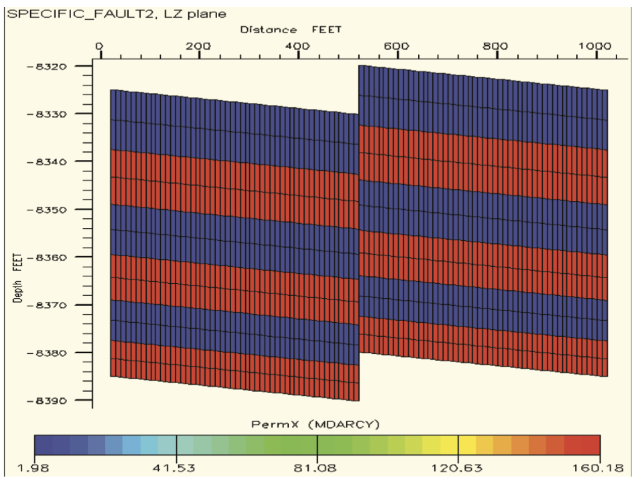

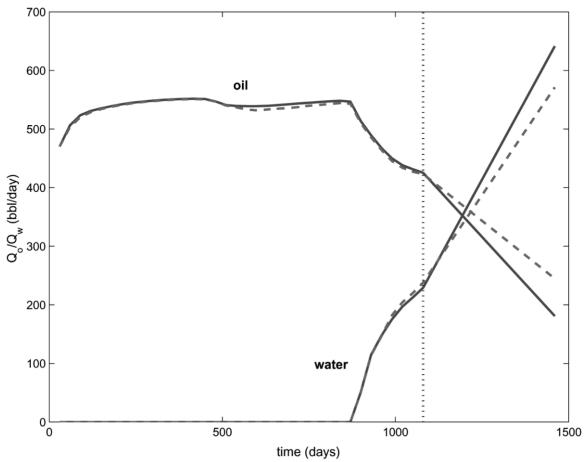

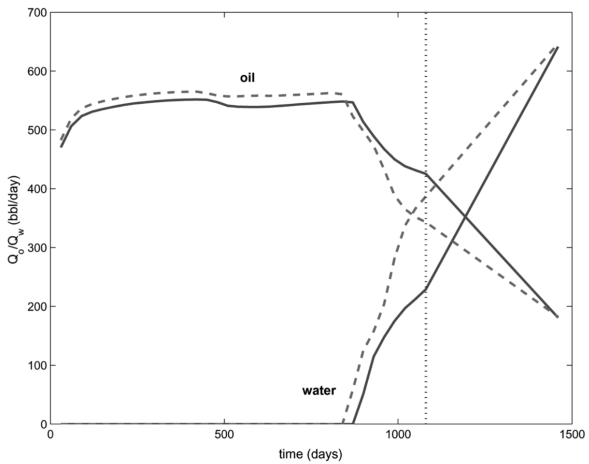

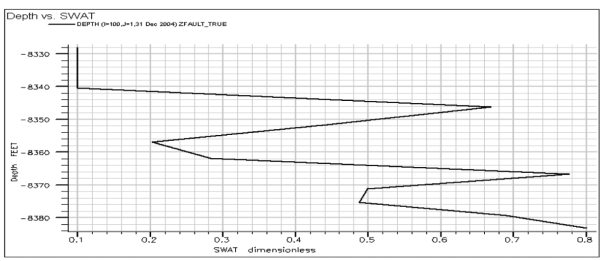

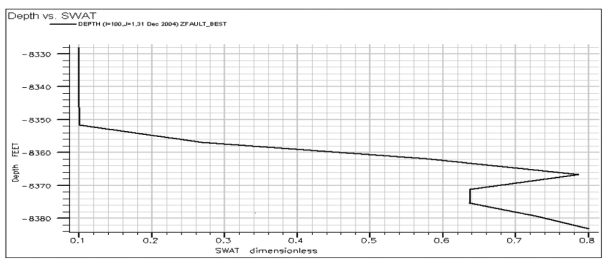

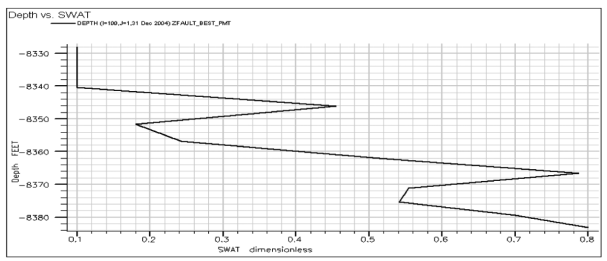

History Matching Methods

Q: How to improve the performance (in terms of accuracy and cost) of HM?

Manual matching (MHM) [Kabir, Landa 2003]

- MHM (trial and error) is subjective and labor-intensive
- Driven by experience of the engineers and, more importantly, the budget

Automatic matching (AHM)

- A nonlinear regression problem — Many attempts to "solve" the problem
  - Gradient-based optimization
  - Genetic method
  - Optimal control
  - Stochastic modeling
  - Sensitivity analysis
  - Gradual deformation method

However it is still difficult for 3D multiphase flow problems due to its highly nonlinear nature and large computational requirements

Surrogate Models

How to improve AHM performance?

- Using flow-based upscaling (coarsening) for flow simulation
  - Employ a coarse model for flow simulation [Durlofsky, et al. 1996; ...]
  - Adaptive local coarsening and dynamic fluid representation [Kabir, et al. 2003]
- Using surrogate models:
  - Radial basis functions [Park, Sandberg 1991; ...]
  - Polynomial chaos expansions [Xiu, Karniadakis 2002, 2003; ...]
  - Gaussian processes [Bilionis, Zabaras 2012, JCP; Bilionis, et al. 2013; ...]
  - Relevance vector machines [Bilionis, Zabaras 2012, SISC]

Model order reduction: Large number of input stochastic dimension

- Using low-rank approximation of covariance
  - Karhunen-Loève expansion (KLE) [Spanos, Ghanem 1989; ...]
  - Principle component analysis (PCA) [Word, Esbensen, Geladi 1987; ...]
- Using automatic relevance determination [Neal 1998; ...]
- Using sensitivity analysis [Saltelli, et al. 2000; ...]
- Using active subspace method [Constantine, Gleich 2014; ...]

Surrogate Models with Deep Learning

Problems with existing methods

- Work for linear problems, mostly
- Unsupervised learning, mostly

Construction of a surrogate model

$$\hat{\mathcal{F}}(X) := g(\, h(X)\,),$$

where h is the projection function (encoder) and g is the link function (decoder)

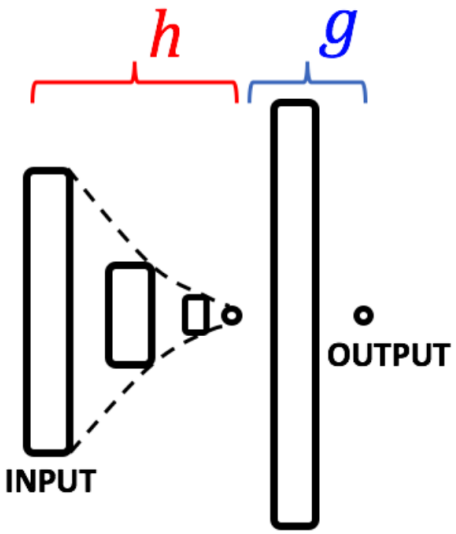

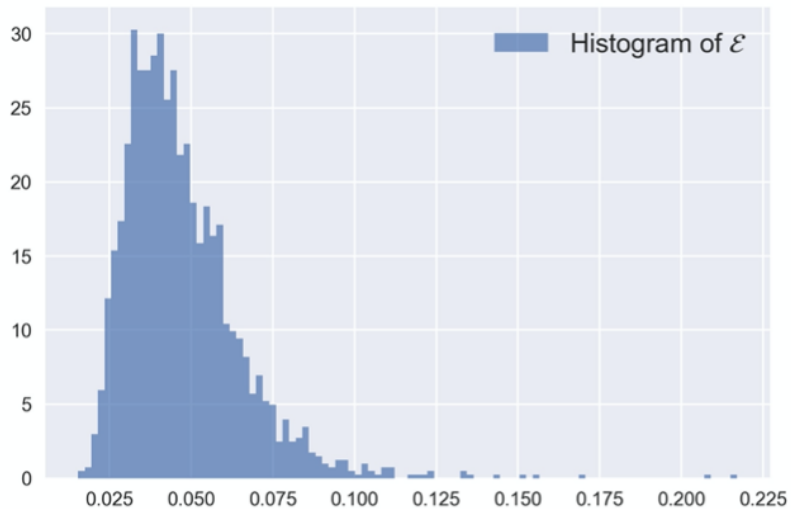

DeepUQ (2D Poisson-like equation, 32×32 input parameters, 2000 training, 2000 testing)
[Tripathy, Bilionis 2018]

So... Problem Solved?

- Not even close ... History matching is an ill-posed inverse problem
- The real problem is really complicated!
  - Time-dependent problem
  - Training set might not be representative
  - Hard evidence (observation) is limited (small data)
  - Requires a large set of training data
- Some questions to consider:
  - How to combine with expert experiences?
  - How to zoom in (fine resolution) to the interested area?
  - How to effectively combine observation and simulation data?
  - How to adjust model when production procedure changes?
  - How to solve the training problem more "accurately"?
  - How to solve the training problem more efficiently?

Gridding techniques for reservoir simulation

82 Grid Partitions for Reservoir Simulation

83 Subdivision and Triangulation

84 Angle Conditions and Approximation

85 Angle Conditions and Stiffness Matrix

86 Delaunay Triangulation

87 Algorithms for Delaunay Triangulation

88 Voronoi Diagram

89 Adaptive Mesh Refinement

90 Adaptive Mesh and Nonlinear Approximation

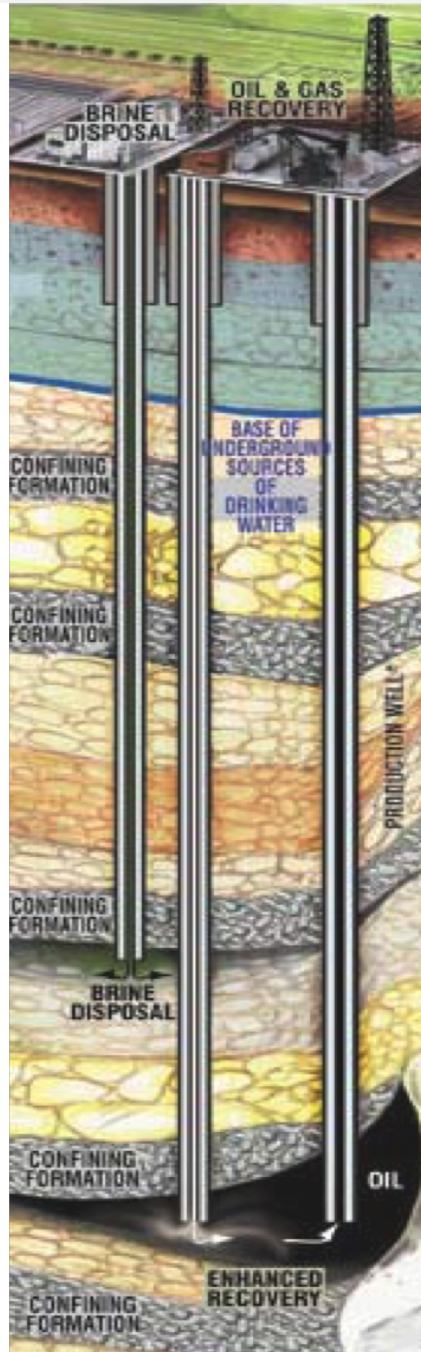

Grid Partitions for Reservoir Simulation

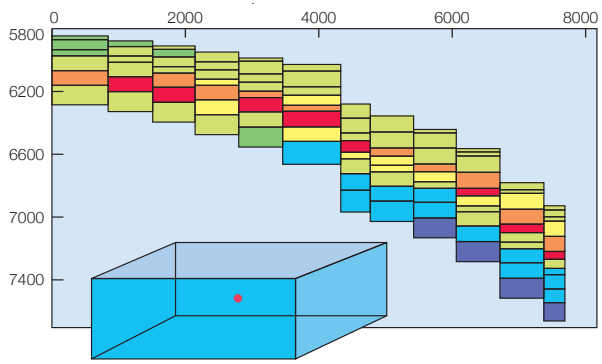

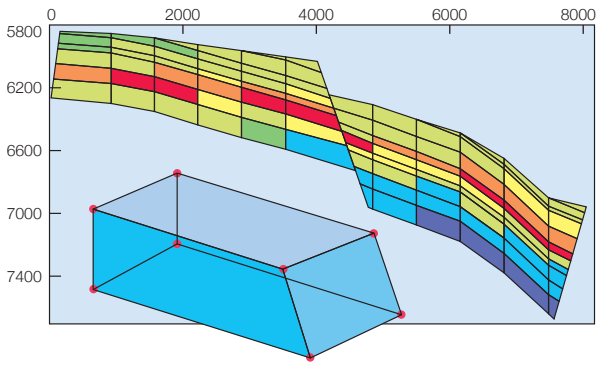

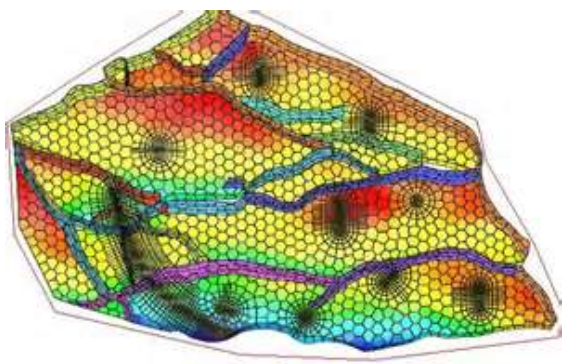

1. Cartesian block-centered grids
   - CNOOC: SOCF (2009.12—2011.6)
   - Easy for implementation
   - Multiple-domain, local refinement
   - Difficult to simulate fault/dip
2. Corner-point grids
   - PetroChina: HiSim (2011.1—2015.12)
   - A type of hexahedral grid
   - Logically still structured
   - Difficult to compute flux accurately
3. Unstructured grids (PEBI and beyond)
   - PennSim (2013.1—2016.12) $\Longrightarrow$ ExSim
   - Voronoi, 2.5D
   - Better description of faults and wells
   - Incompatible with structured seismic data
   - Challenges in discretizations and solvers

[Goldthorpe et al. 1985; Heirich 1987; Heinemann 1989; SPE8 1993; Palagi 1994]

Subdivision and Triangulation

Subdivision and (conforming) triangulation

- Subdivision (partition) of Ω: $\cup_i \tau_i = \overline{\Omega}$ and $\text{int}\,\tau_i \cap \text{int}\,\tau_j = \emptyset$ (if $i \neq j$)
- Triangulation: A subdivision in which no vertex lies in the interior of any edge
- Find a triangulation $\mathcal{T}(\mathbb{P})$ of a set of sites (points) $\mathbb{P} := \{p_1, \ldots, p_n\}$
- An important problem in computational geometry with MANY applications

What is a "good" triangulation?

- Need to give mathematical conditions on "good" and "bad"
- Need to give algorithms to generate a good triangulation

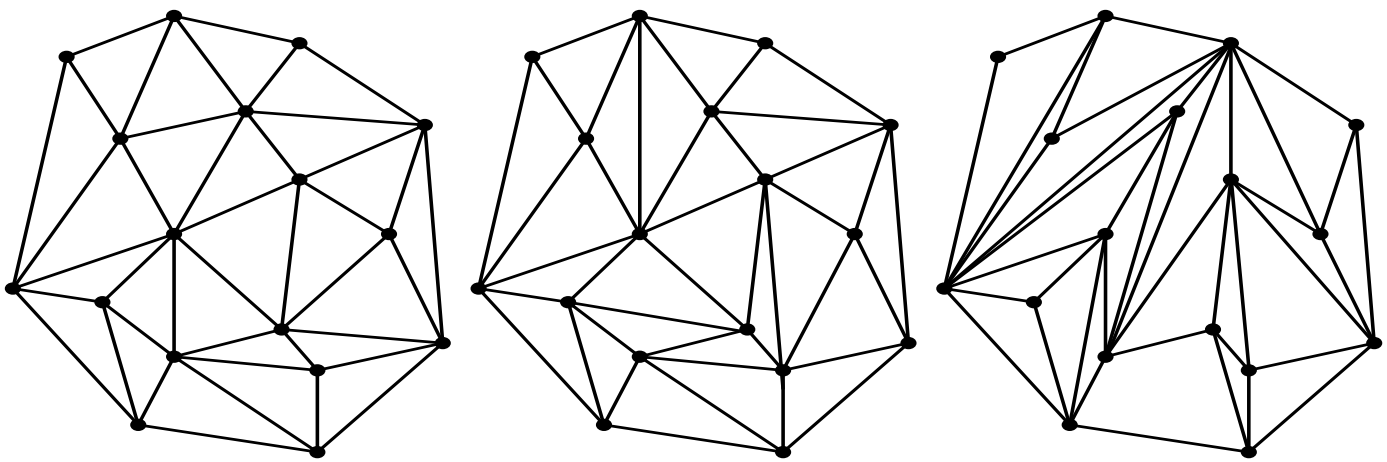

Angle Conditions and Approximation

- Minimal angle condition: $\exists\, \alpha_{\min} > 0,\ \alpha_\tau \geq \alpha_{\min},\ \ \forall\, \tau \in \mathcal{T}_h,\ h \to 0$
  - P_2-FEM for Poisson $\|u - u_h\|_1 \lesssim h^2 / \sin \alpha_{\min}$ [Zlámal 1968; Zenisek 1969]
  - Similar estimate for the fourth-order clamped plane problem
  - Inscribed ball condition or $|\tau| \geq Ch^d$ [Ciarlet 1978; Lin, Lin 2003]
- Maximal angle condition: $\exists\, \alpha_{\max} < \pi,\ \alpha_\tau \leq \alpha_{\max},\ \ \forall\, \tau \in \mathcal{T}_h,\ h \to 0$
  - Minimal angle cond. $\Rightarrow$ maximal angle cond. $\Rightarrow$ essential for convergence
  - Interpolation error $\|u - I_h u\|_{1,\infty} \lesssim h|u|_{2,\infty}$ [Synge 1957]
  - Sufficient for convergence of P_1-FEM [Feng 1965; Babuška, Aziz 1976]

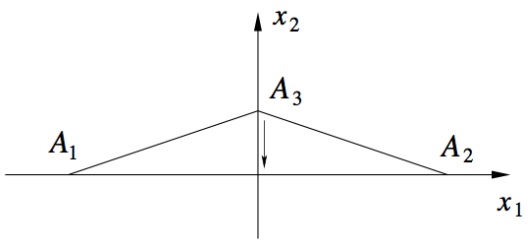

$$A_1 = (-h, 0), A_2 = (h, 0), A_3 = (0, h^5)$$

$$u(x) = x_1^2,\ \|u - I_h u\|_1^2 \geq h^{-6} \cdot \tfrac{1}{2}(2h)h^5 = 1$$

Large interpolation error [Strang, Fix 1973]

- Nonobtuse condition: $\alpha_\tau \leq \pi/2,\ \ \forall\, \tau \in \mathcal{T}_h$
  - Obtuse triangles can destroy the discrete maximum principle $f \geq 0 \Rightarrow u_h \geq 0$
  - Nonobtuse simplicial triangulations yields diagonally dominant stiffness matrices

Angle Conditions and Stiffness Matrix

- Eigenvalues of stiffness matrix on quasi-uniform meshes:
  - $h^d \lesssim \lambda(A) \lesssim h^{d-2} \quad \Longrightarrow \quad \mathrm{cond}(A) \sim h^{-2}$
- Element size and shape affect matrix conditioning:
  - Smallest eigenvalue: Not strongly affected by element shape [Fried 1972]:

$$\lambda_{\min}(A) \sim \min_{\tau \in \mathcal{T}_h} |\tau|$$

  - Largest eigenvalue: Can be arbitrarily large by a single bad-shaped element:

$$\max_{\tau \in \mathcal{T}_h} \lambda_{\max}^{\tau} \leq \lambda_{\max}(A) \leq m \max_{\tau \in \mathcal{T}_h} \lambda_{\max}^{\tau}$$

    where m is the maximum number of elements meeting at a single vertex
  - If an angle of τ approaches zero, $\lambda_{\max}^{\tau}$ goes to infinity
- Small angles can ruin matrix conditioning:
  - Small angles $\Longrightarrow$ ill-conditioned linear systems [Xu 1989; Shewchuk 2002]
  - A mesh with only a small number of bad elements will typically impose only a few large eigenvalues
  - Krylov subspace iterative methods can work around a few bad eigenvalues; but need to be careful if restarting is used

Delaunay Triangulation

Delaunay triangulation

- Many possible partitions; but which one is better? How to check?

Delaunay triangulation: a triangulation $\mathcal{T}(\mathbb{P})$ such that no point in $\mathbb{P}$ is inside the circum-hypersphere of any simplex

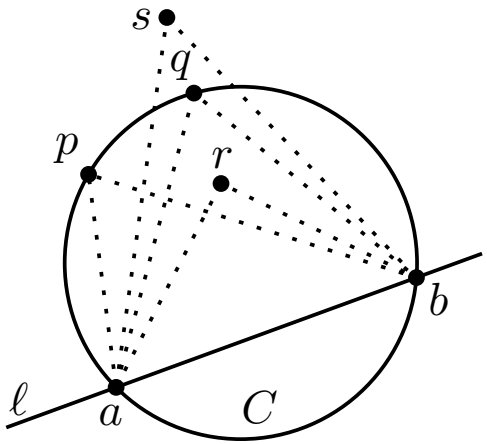

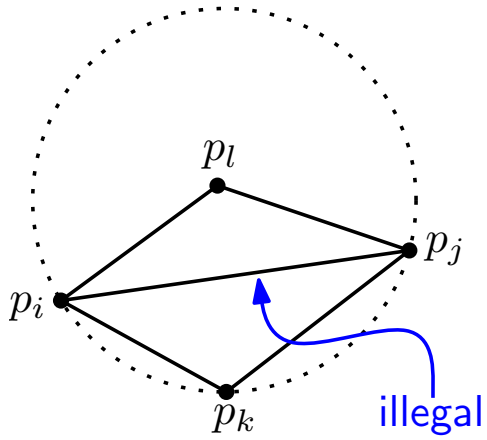

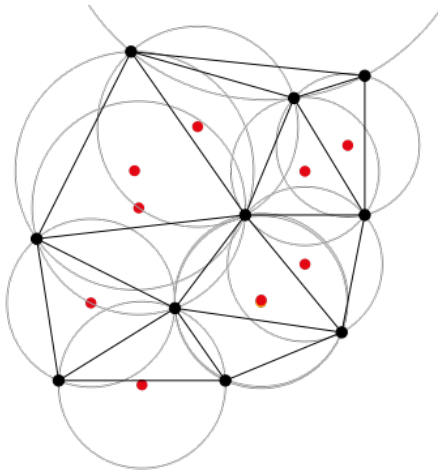

Properties of Delaunay triangulation

- Maximize the minimal angles
- The Delaunay triangulation contains at most $\mathcal{O}(n^{\lceil d/2 \rceil})$ simplexes
- The union of all simplexes in the triangulation is the convex hull of the points

Algorithms for Delaunay Triangulation

Empty circle (sphere) condition

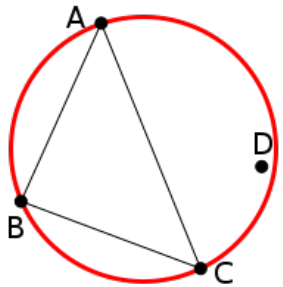

$$\Longleftrightarrow \quad \begin{vmatrix} A_1 & A_2 & A_1^2+A_2^2 & 1 \\ B_1 & B_2 & B_1^2+B_2^2 & 1 \\ C_1 & C_2 & C_1^2+C_2^2 & 1 \\ D_1 & D_2 & D_1^2+D_2^2 & 1 \end{vmatrix} > 0$$

Lawson's flip algorithm

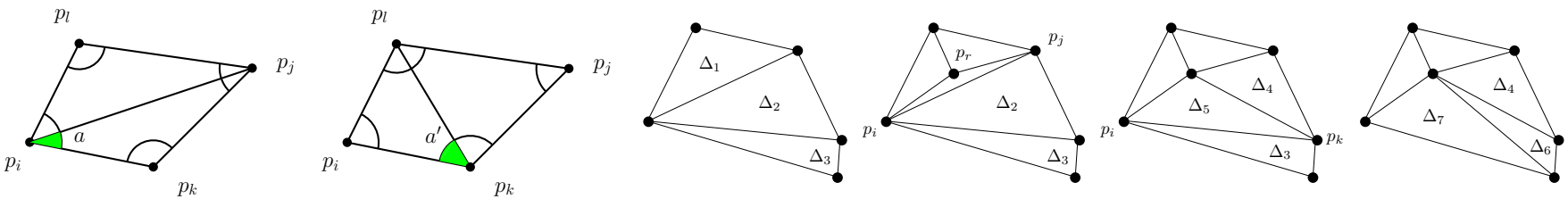

- Lawson flip algorithm terminates in finite steps
- Provides a constructive proof for the existence of Delaunay triangulation
- Sequential algorithms: [Su, Drysdale 1996]
  - Incremental algorithms
  - Divide-and-conquer algorithms
  - Fortune's sweepline algorithms
  - Convex hull based algorithms: lift-and-project

Voronoi Diagram

Voronoi Diagram

- Voronoi cell (of p_k) $= \{x \in \mathbb{R}^d \ : \ \|x - p_k\| \leq \|x - p_j\|, \ \forall\, j \neq k\}$
- An edge of Voronoi diagram is equidistant to the two nearest sites
- Dual graph of the Delaunay triangulation

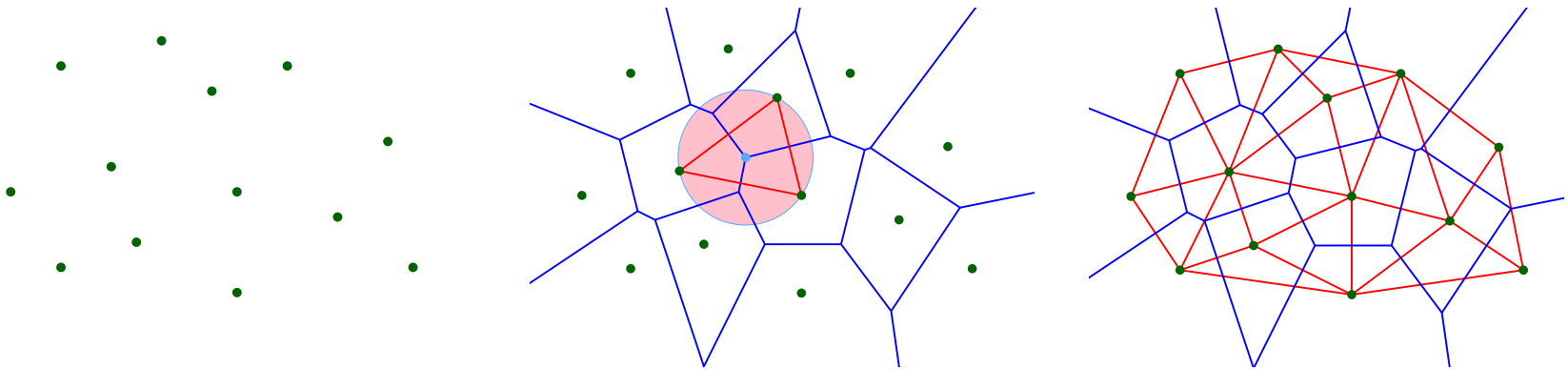

Generating Voronoi diagram

- Bowyer-Watson algorithm via Delaunay triangulation: $\mathcal{O}(n \log n)$ to $\mathcal{O}(n^2)$
- Fortune's algorithm: $\mathcal{O}(n \log n)$
- Lloyd's algorithm and k-means clustering

Dynamic demo of Voronoi diagram. https://bl.ocks.org/mbostock/4060366

Adaptive Mesh Refinement

Red-green refinement, longest edge bisection, and newest vertex bisection

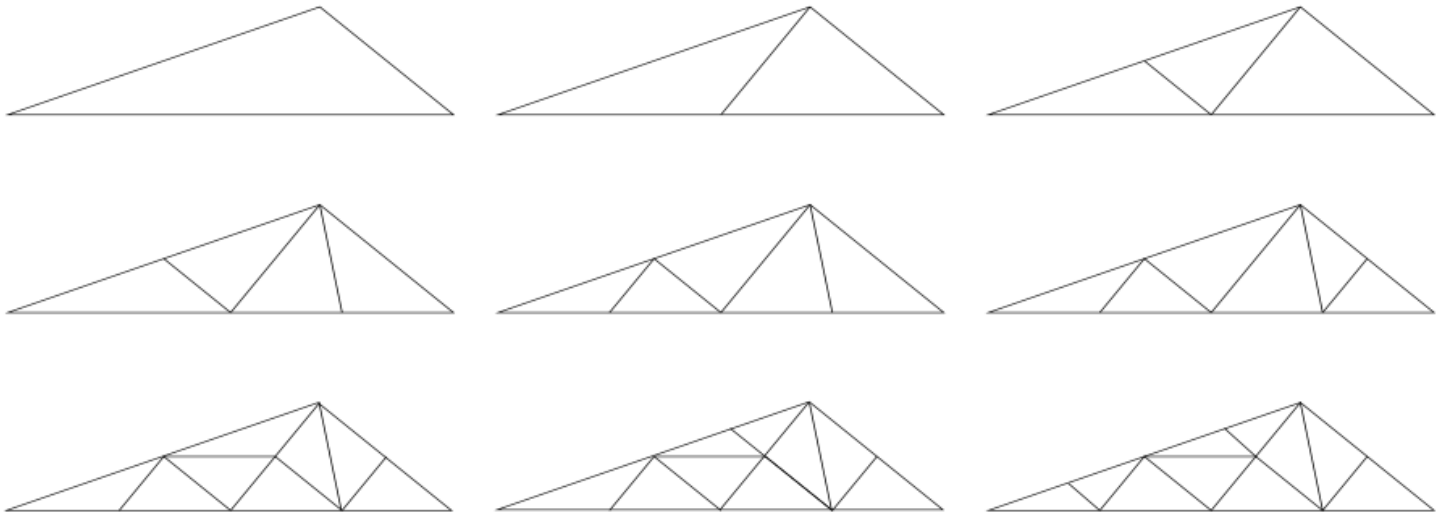

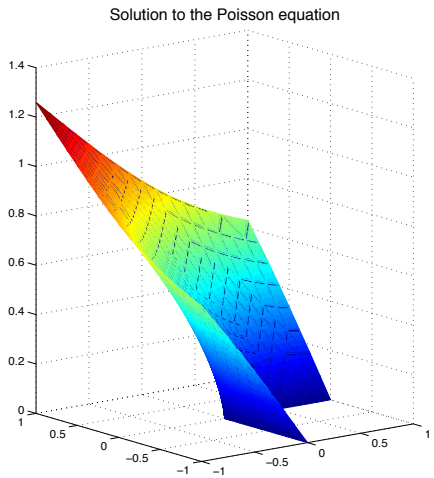

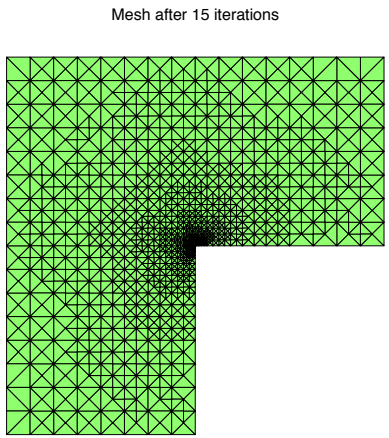

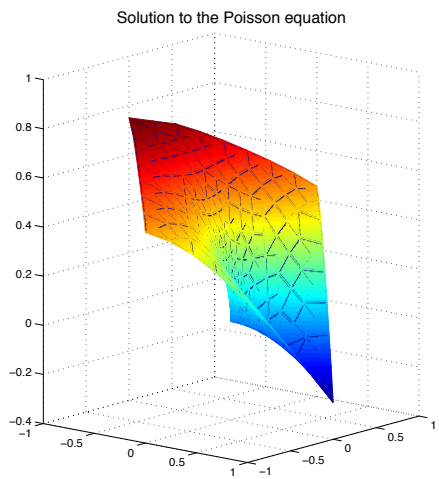

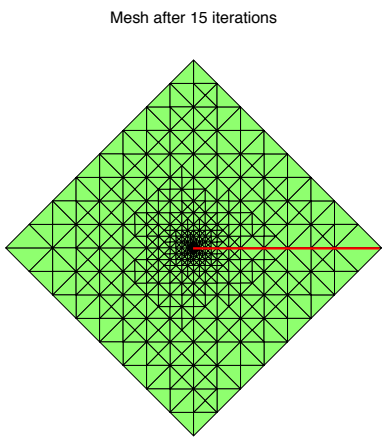

[Chen, Z. 2010]

Adaptive Mesh and Nonlinear Approximation

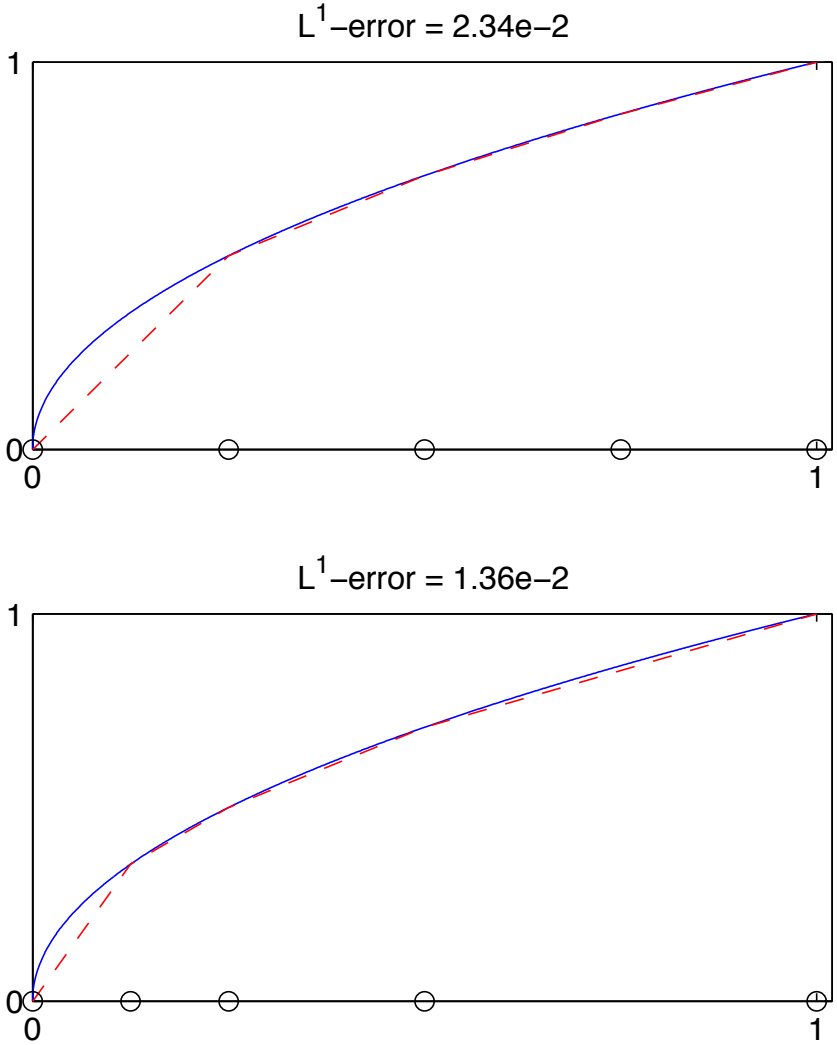

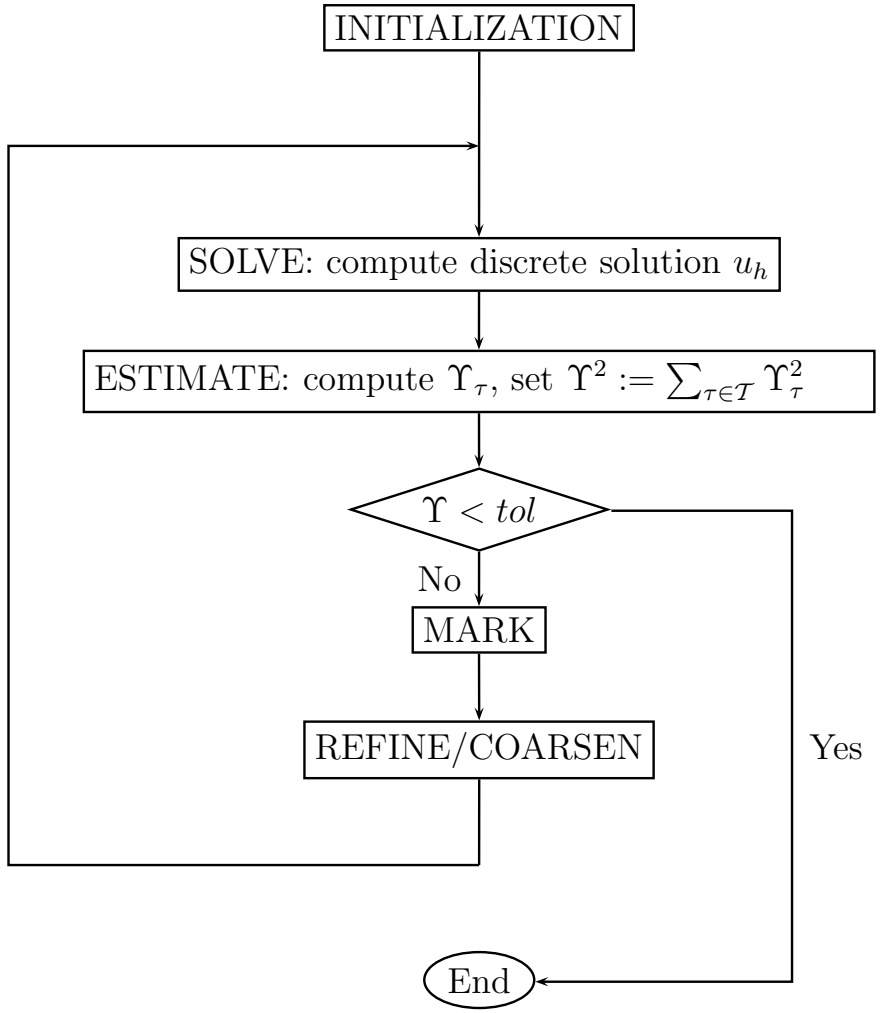

Approximate $f(x) = x^{1/2}$. Left: Solution and error; Right: Adaptive algorithm.

Future Work

- 3D pre-processing code for MHM $\Longrightarrow$ 3D simulation
- Multiscale modeling, method, and analysis for DFM
- Energy-stable, mass-conservative, and positivity-preserving schemes
- Multiphase flow in porous media with fractures and vugs
- Geo-mechanical coupling with fluid simulation
- Non-Newtonian fluid in discrete fracture networks
- Large-scale carbonate oil reservoir simulation in parallel
- Improve model using data $\Longrightarrow$ Better simulation of hydraulic fractures

Financial Support

- CNOOC-2010-ZHKY-ZX-008
- PetroChina International Collaborative Project 12HT10500002654
- SYSU Key Research Project 2014
- Key Research Program of Frontier Sciences of CAS 2016
- PetroChina Test Projects 2017, 2019
- PetroBras Brazil–China Collaborative Project 2019
- PetroChina Key Research Program, CUP, East China 2019
- PetroChina International Collaborative Project 2020

Our Team and Collaborators

- Kunming Univ of Sci & Tech: Zheng Li
- LSEC, CAS: Chensong Zhang, Ronghong Fan, ...
- Penn State Univ: Jinchao Xu, Changhe Qiao, Hongxuan Zhang, Lian Zhang
- Sichuan Univ: Shiquan Zhang
- Tufts Univ: Xiaozhe Hu
- Xiangtan Univ: Shi Shu, Chunsheng Feng, Xiaoqiang Yue, Zhiyang Zhou, ...
- China Univ of Petroleum: Ruizhong Jiang, Wenchao Teng, ...
- CoCreative Center: David Zhu, Zhongjian Zhang, ...
- CNOOC: Xiansong Zhang, Chunyang Lin, ...
- Monix Energy: Wei Liu, Jing Wen, ...
- Houston Univ: Guan Qin, Tao Yuan
- RIPED, PetroChina: Shuhong Wu, Baohua Wang, Guanren Huan, ...
- SYSU, Guangzhou: Yuesheng Xu, Yongdong Zhang, Wenchao Guan, ...
- Univ of Campinas: Philippe Devloo, Omar Durán, Pablo Carvalho, ...

Contact me: zhangcs@lsec.cc.ac.cn, http://lsec.cc.ac.cn/~zhangcs